

E12-23-004

A Search for a Nonzero Strange Form Factor of the Proton at 2.5 (GeV/c)²

R.Beminiwattha, S.P.Wells, N.Simicevic, C. Palatchi, K.Paschke, S.Ali, X.Bai, G.Cates, R.Lindgren, N.Liyanage, V.Nelyubin, X.Zheng, B.Wojtsekhowski, S.Barcus, A.Camsonne, R.Carlini, S.Covrig Dusa, P.Degtiarenko, D.Gaskell, O.Hansen, D.Higinbotham, D.Flavy, D.Jones, M.Jones, C.Keppel, D.Meekins, R.Michaels, B.Raydo, G.Smith, H.Szumila-Vance, A.S.Tadepalli, T.Horn, E.Cisbani, E.King, J.Napolitano, P.M.King, P.A.Souder, D.Hamilton, O.Jevons, R.Montgomery, P.Markowitz, E.Brash, P.Monaghan, T.Hobbs, G.Miller, J.Lichtenstadt, T.Kolar, E.Piassetzky, G.Ron, D.Armstrong, T.Averett, S.Mayilyan, H.Mkrtchyan, A.Mkrtchyan, A.Shahinyan, V.Tadevosyan, H.Voskanyan, W.Tireman, P.Datta, E.Fuchey, A.J.R.Puckett, S.Seeds, C.Munoz-Camacho

LaTech, Indiana, UVa, JLab, CUA, INFN - Roma, Temple, Ohio, Syracuse, Glasgow, FIU, CNU, Fermilab, UWashington, Tel Aviv U, Hebrew U, W&M, AANL Yerevan, Northern Michigan, UConn, Orsay

Charge symmetry and the nucleon form factors

Charge Symmetry

$$G_E^p = \frac{2}{3} G_E^{u,p} - \frac{1}{3} G_E^{d,p}$$

$$G_E^n = \frac{2}{3} G_E^{u,n} - \frac{1}{3} G_E^{d,n}$$

Charge symmetry is assumed for the form factors, $G_E^{u,p} = G_E^{d,n}$, etc. and used to find the flavor separated form-factors, measuring $G_{E,M}^{p,n}$ to find $G_{E,M}^{u,d}$

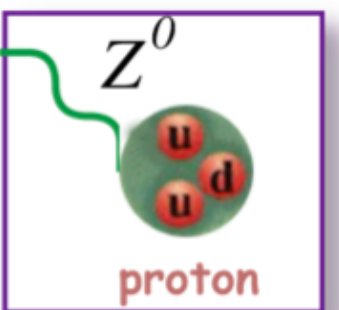
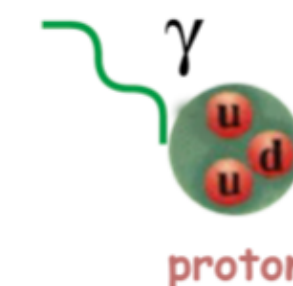
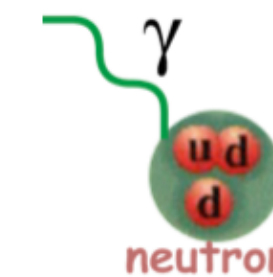
$$G_E^p = \frac{2}{3} G_E^{u,p} - \frac{1}{3} G_E^{d,p} - \frac{1}{3} G_E^s$$

$$G_E^n = \frac{2}{3} G_E^{u,n} - \frac{1}{3} G_E^{d,n} - \frac{1}{3} G_E^s$$

But this can be broken! One way is to have a non-zero strange form-factor, which breaks the "2 equations and 2 unknowns" system

The weak form factor provides a third linear combination:

$$G_E^{p,Z} = \left(1 - \frac{8}{3} \sin^2 \theta_W\right) G_E^{u,p} + \left(-1 + \frac{4}{3} \sin^2 \theta_W\right) G_E^{d,p} + \left(-1 + \frac{4}{3} \sin^2 \theta_W\right) G_E^s$$



A strange quark form factor would be indistinguishable from a broken charge symmetry in u,d flavors

$$\delta G_E^u \equiv G_E^{u,p} - G_E^{d,n}$$

$$\delta G_E^d \equiv G_E^{d,p} - G_E^{u,n}$$

So, more generally: this experiment tests the assumption of charge symmetry which is crucial to the flavor decomposition of the form factors

Parity Violating Electron Scattering

Elastic e-p scattering with longitudinally polarized beam and unpolarized target:

Weak and EM amplitudes interfere:

$$\sigma = |\mathcal{M}_\gamma + \mathcal{M}_Z|^2$$

$$A_{PV} = \frac{\sigma_R - \sigma_L}{\sigma_R + \sigma_L} \sim \frac{\begin{array}{c} \text{---} \gamma \text{---} \\ \text{---} Z^0 \text{---} \end{array}}{\left| \begin{array}{c} \text{---} \gamma \text{---} \end{array} \right|^2} \approx \frac{|\mathcal{M}_Z|}{|\mathcal{M}_\gamma|}$$

Expressing A_{PV} for e-p scattering, with proton and neutron EM form-factors plus strange form factors:

$$A_{PV} = -\frac{G_F Q^2}{4\pi\alpha\sqrt{2}} \cdot \left[(1 - 4\sin^2\theta_W) - \frac{\epsilon G_E^p G_E^n + \tau G_M^p G_M^n}{\epsilon(G_E^p)^2 + \tau(G_M^p)^2} - \frac{\epsilon G_E^p G_E^s + \tau G_M^p G_M^s}{\epsilon(G_E^p)^2 + \tau(G_M^p)^2} + \epsilon'(1 - 4\sin^2\theta_W) \frac{G_M^p G_A^{Zp}}{\epsilon(G_E^p)^2 + \tau(G_M^p)^2} \right]$$

If sFF contribution is zero, $A_{PV} = 150$ ppm at $\theta = 15.5^\circ$, $Q^2 = 2.5$ GeV²

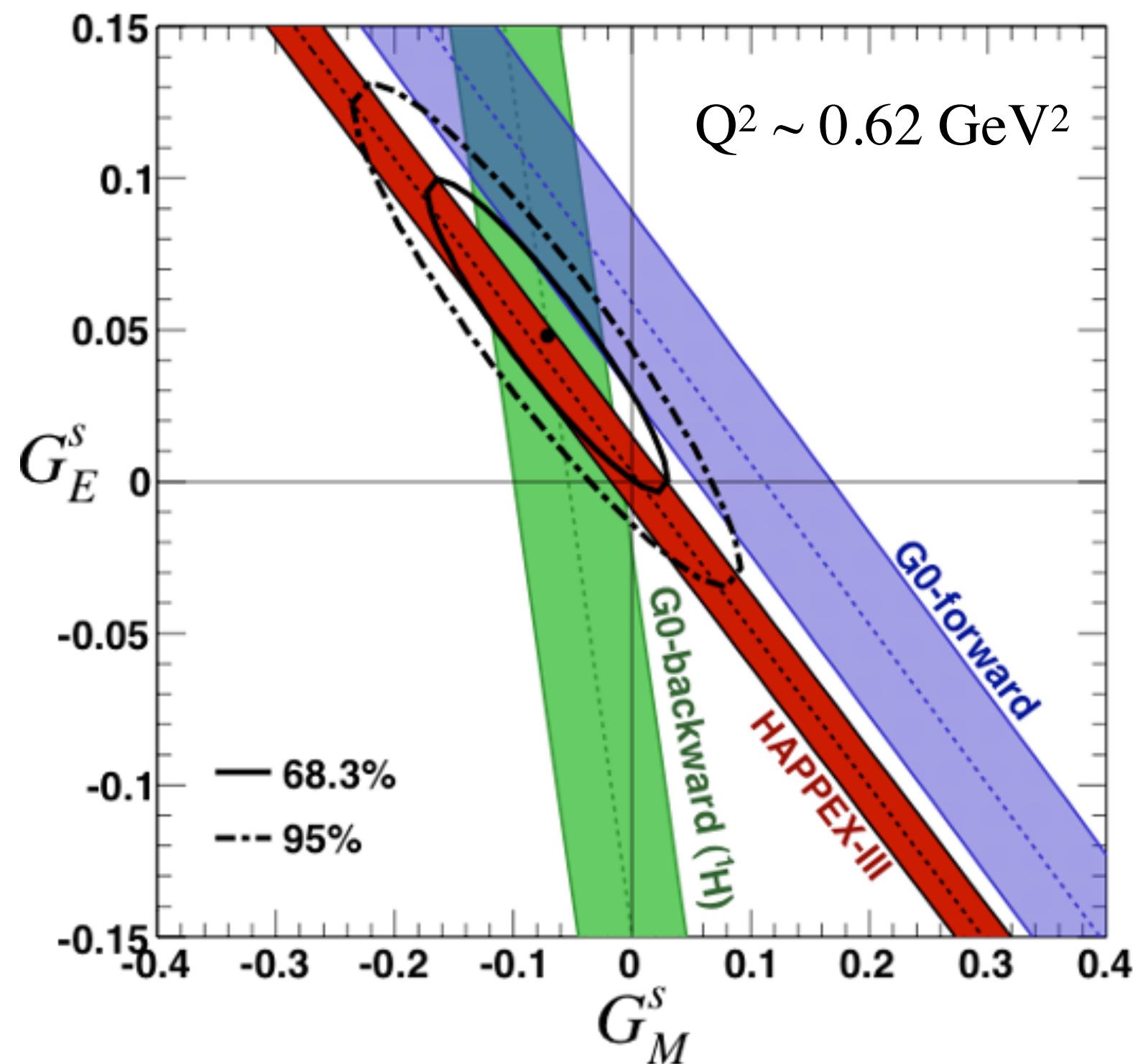
$$A_{PV} = (-226 \text{ ppm}) * \left[\underbrace{0.075}_{Q_w} + \underbrace{0.542}_{EMFF} - 6.43 * \left(\underbrace{G_M^s}_{\text{strange form-factors}} + 0.32 \underbrace{G_E^s}_{\text{axial}} \right) + 0.038 \right]$$

Proton strange form factors via parity violating elastic electron scattering

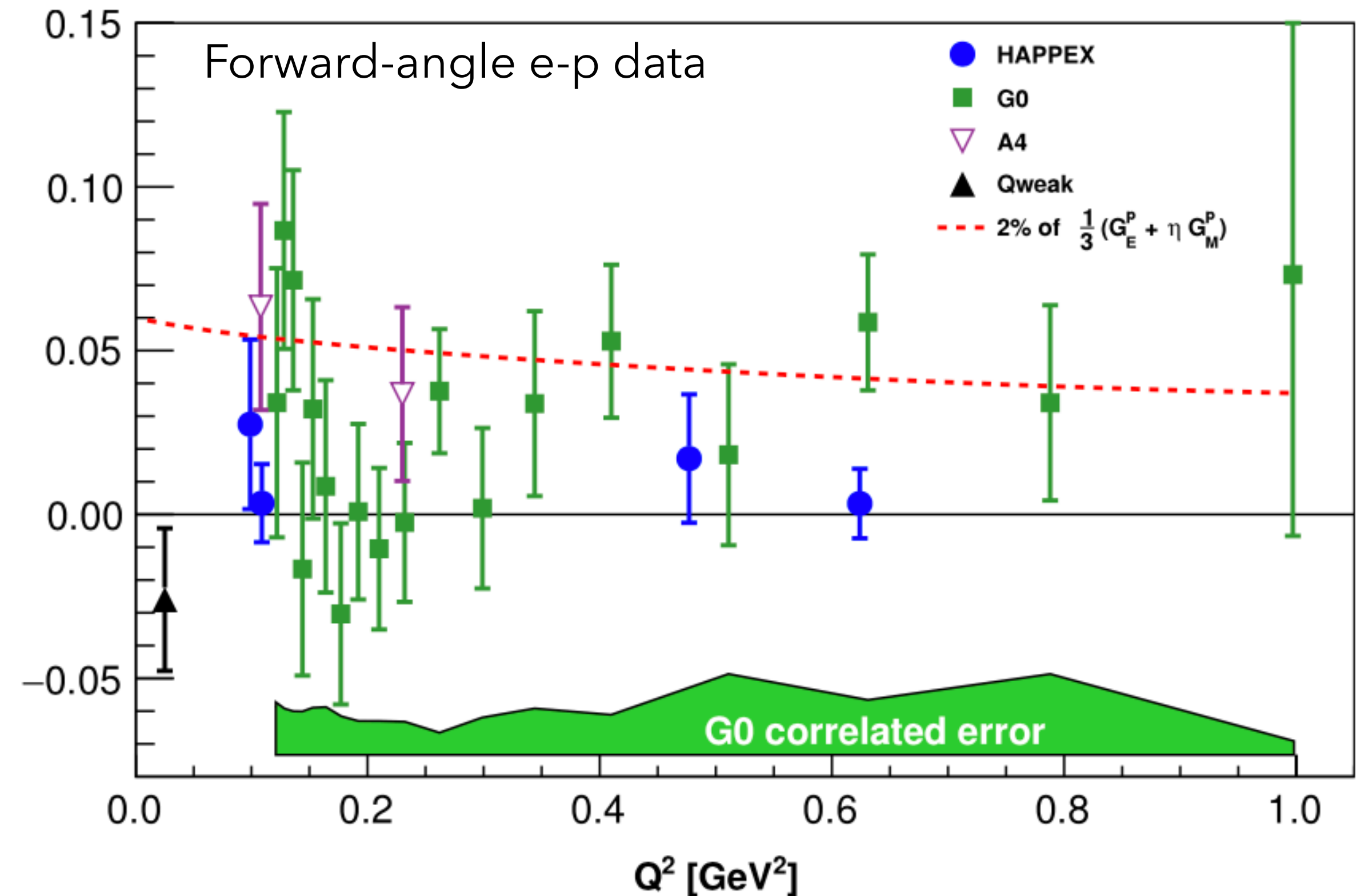
This technique was used to hunt for indications of strange quark contributions in the nucleon, particularly in the *static* (i.e. $Q^2 \rightarrow 0$) properties: a strange charge radius or strange magnetic moment

Strange form factors are measured to be consistent with zero at low Q^2 and small at $<2\%$ of G_E^p, G_E^n

but do not rule out non-zero values at higher Q^2 ,
especially for the magnetic form factor which is highly suppressed at low Q^2

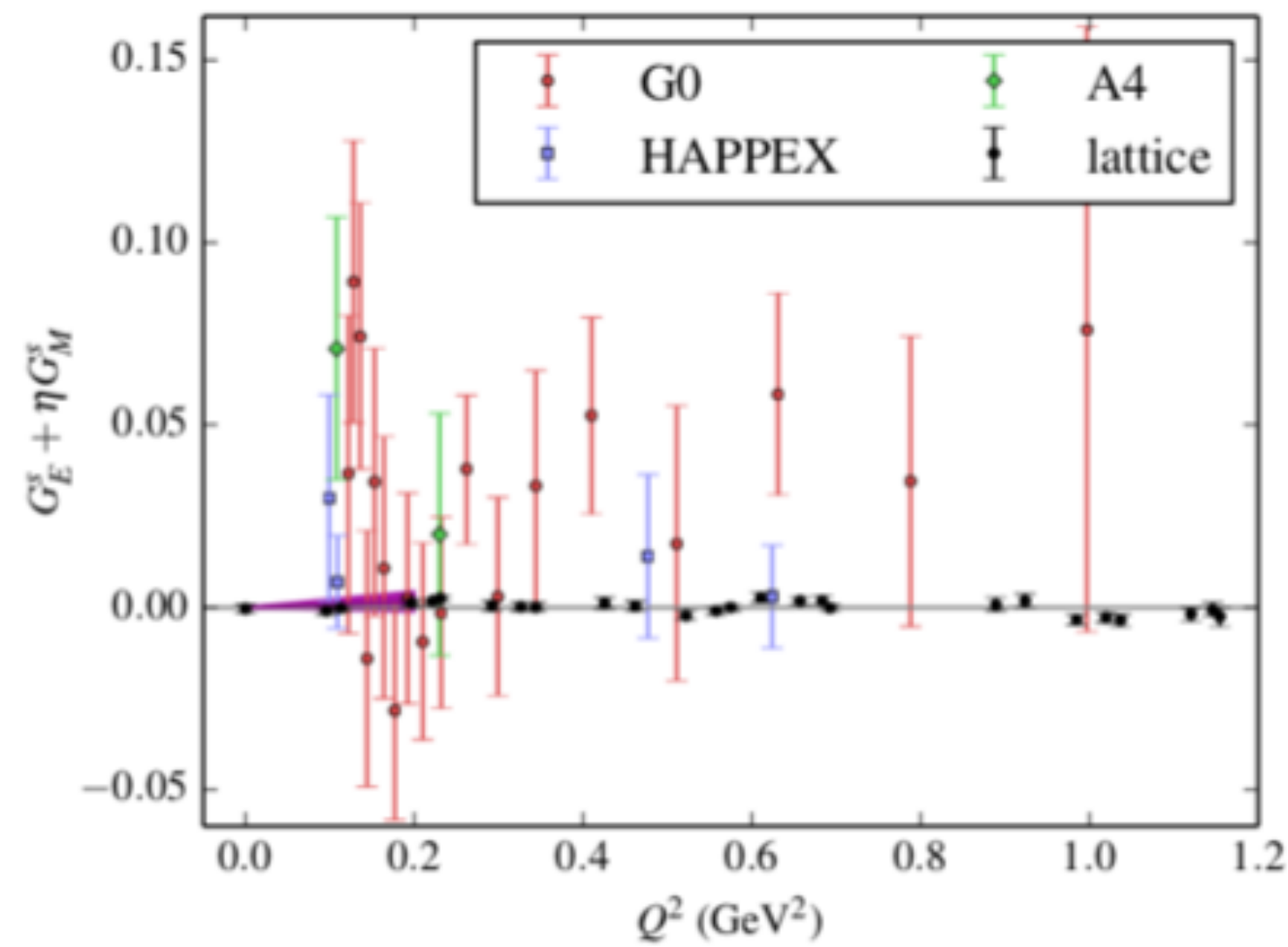


$$G_E^s + \frac{\tau G_M^p G_M^s}{G_E^p}$$



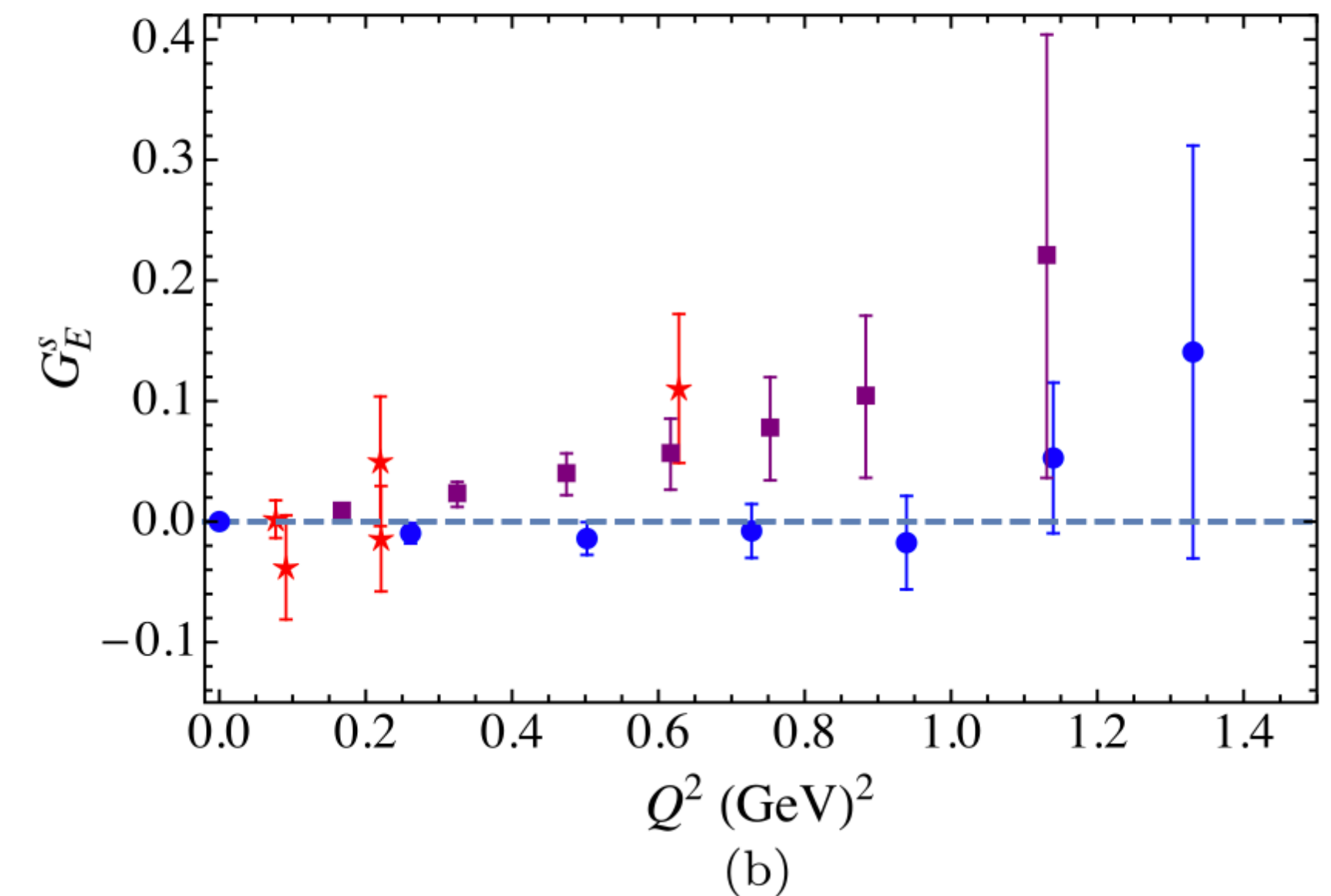
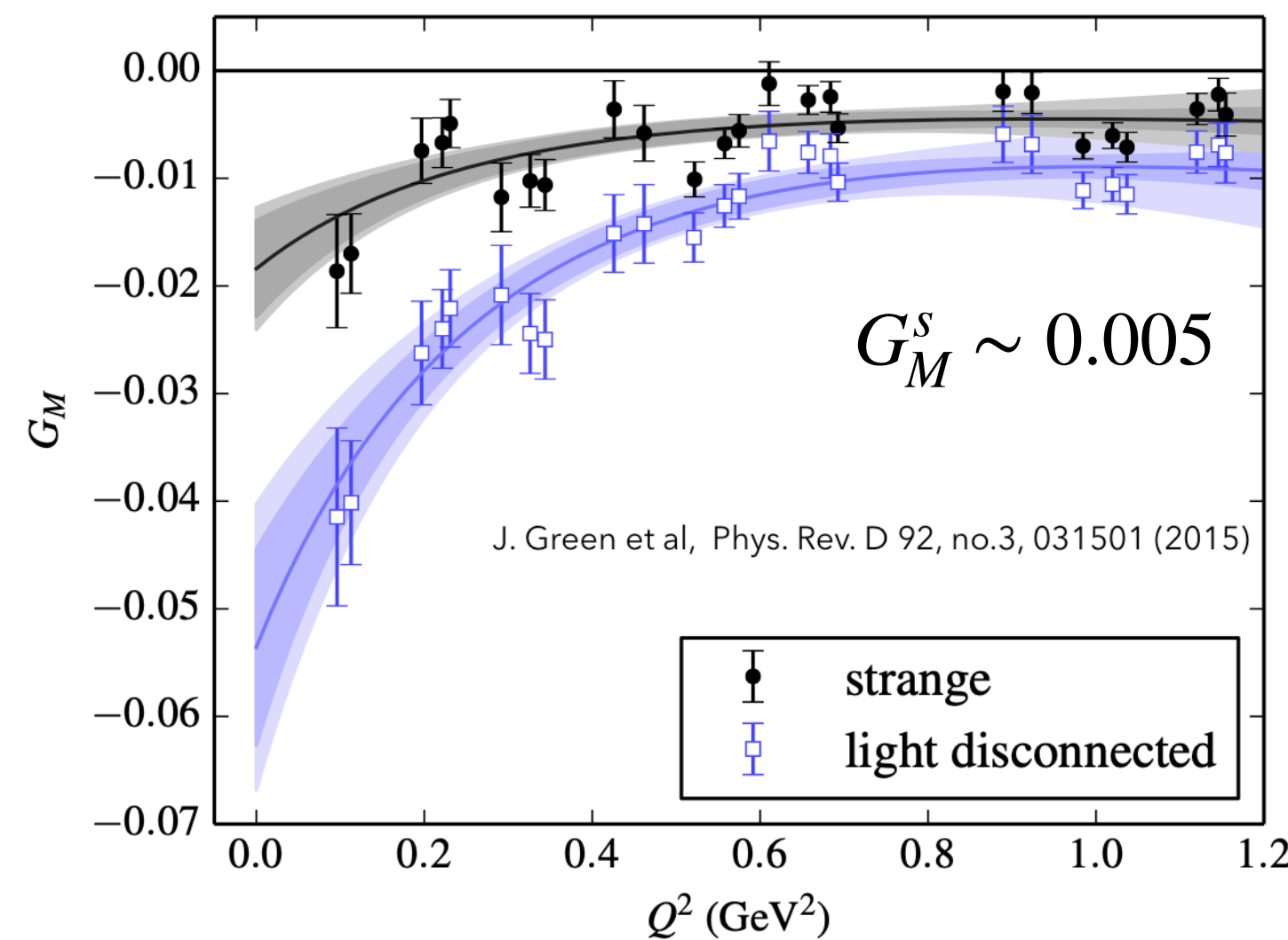
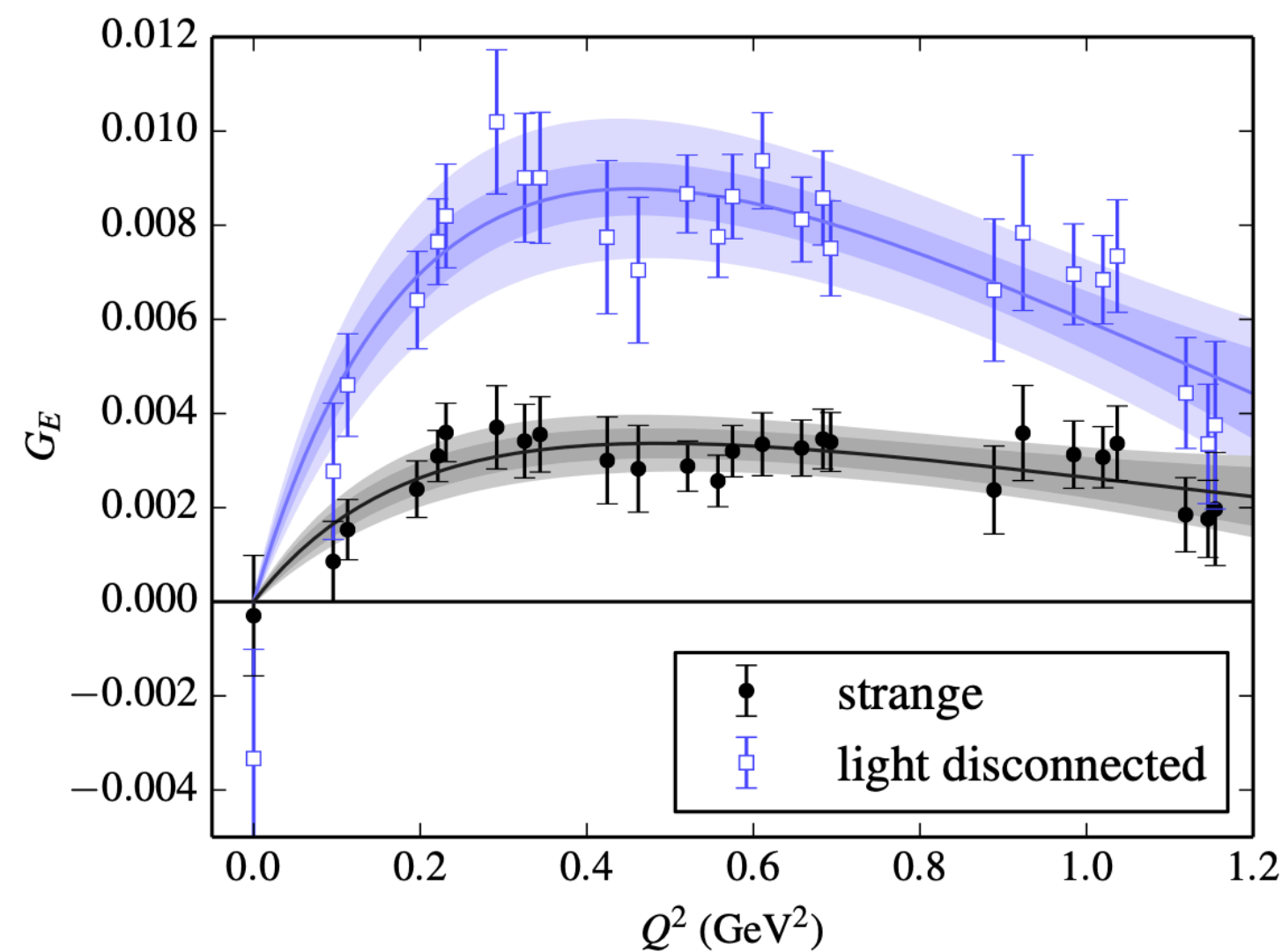
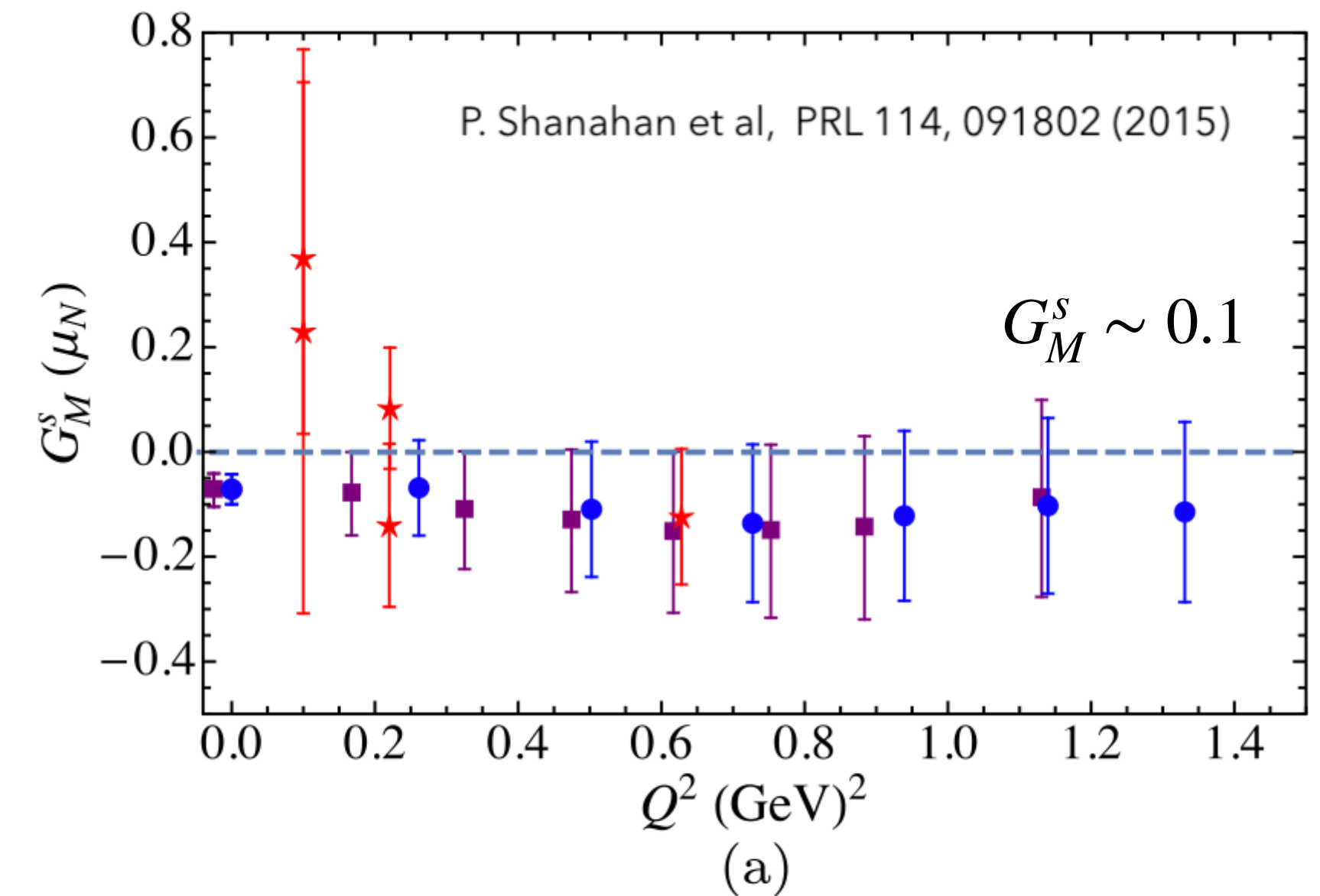
Strange form-factors on the lattice

J.Green et al, 2015



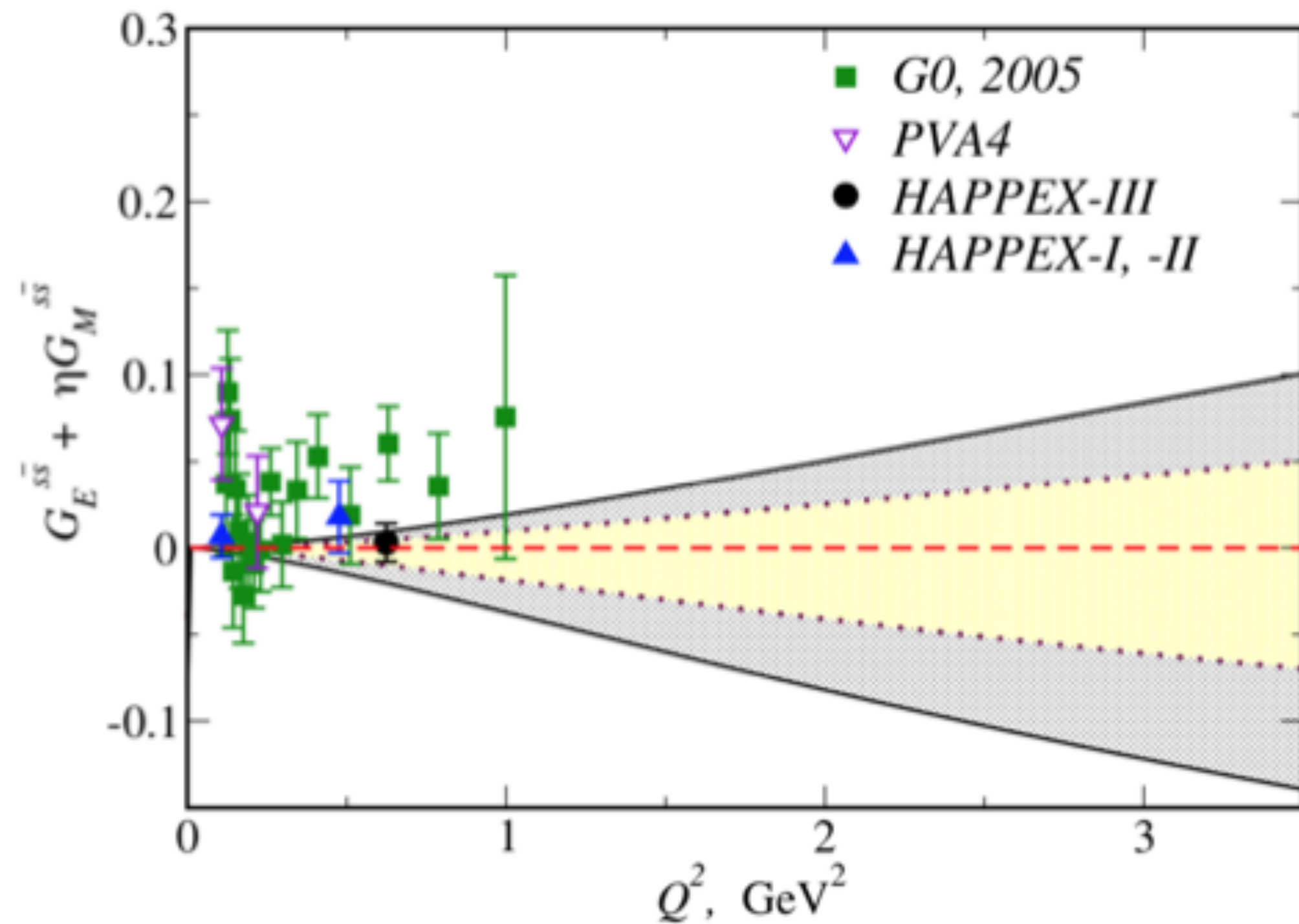
Some lattice calculations predict central values which are small, 10x below the limit of low Q^2 studies.

But they do not apparently fall with Q^2 . These values would be significant contributions at high Q^2 , and visible in the planned experiment



Strange form-factor predictions

T.Hobbs & J.Miller, 2018



Follows work from *Phys.Rev.C* 91 (2015) 3, 035205
(LFWF to tie DIS and elastic measurements in a simple model)

Tim Hobbs and Jerry Miller both joined the proposal

Conclusion: sFF small (but non-zero) at low Q^2 , but quite reasonable within constraints from data to think that they may grow relatively large at larger Q^2

To set the scale of the data constraints:
the width of the uncertainty at $Q^2 = 2.5 \text{ GeV}^2$ is roughly the size of the dipole form-factor parameterization G_D

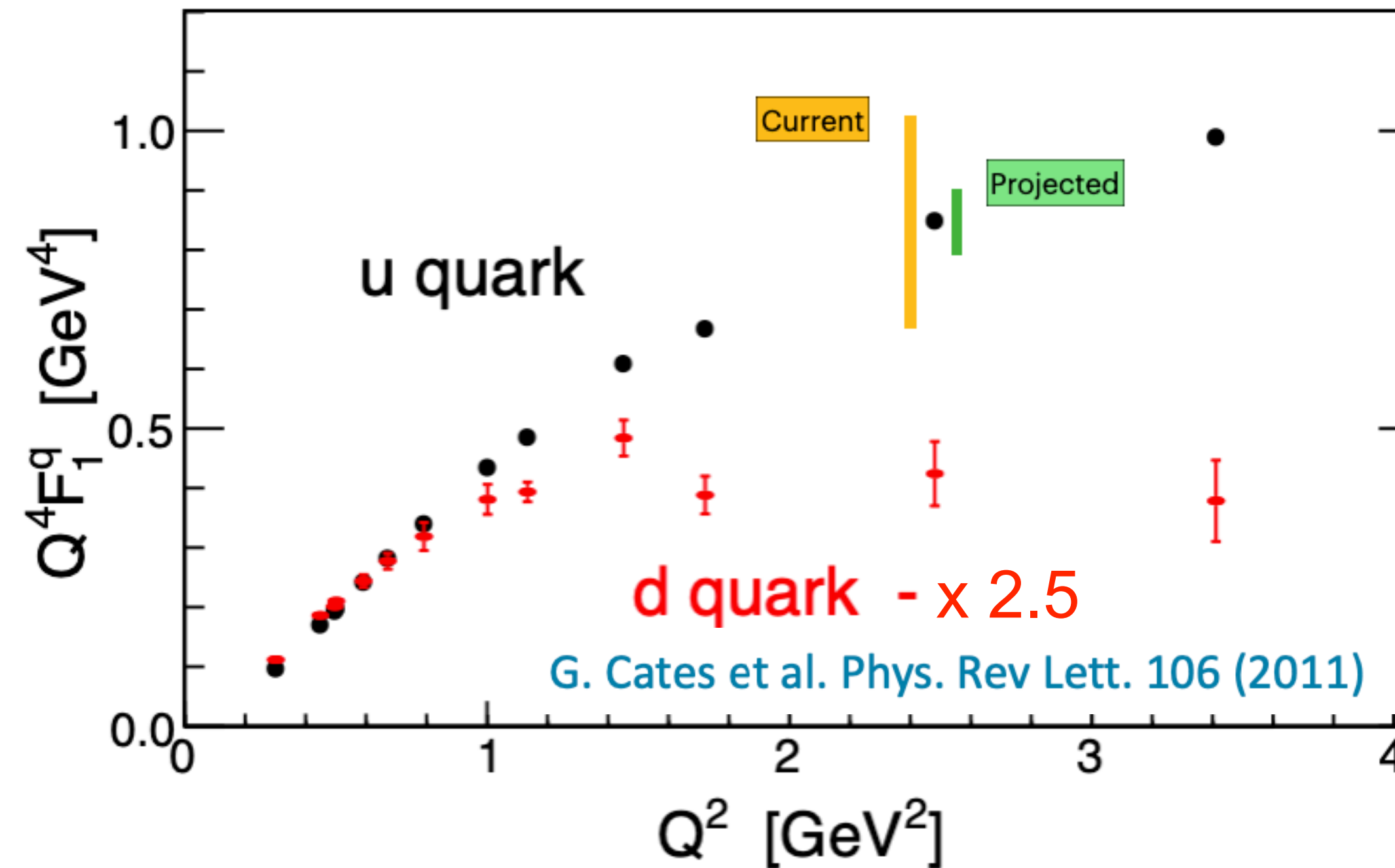
$G_s/G_D \sim 1$ is not excluded

Such a large SFF could be quite visible in a
proton PV measurement

$$\delta A_{PV} \sim \pm 22 \text{ ppm}, \sim \pm 15\% \text{ of } A_{PV}^{ns}$$

Q^2 dependence of Q^4F_1

Assuming $\delta G_{E,M}^s \sim G_D$



- Flavor separated form factors are a crucial piece of information for GPDs / nuclear femtography.
- So far, these have relied on poorly tested assumptions of strange quark contributions.
- Experimentally not ruled out (at level of yellow band) and lattice calculations do not rule out significant contributions (at level of 1x-2x the green band)

A measurement is needed

The planned measurement

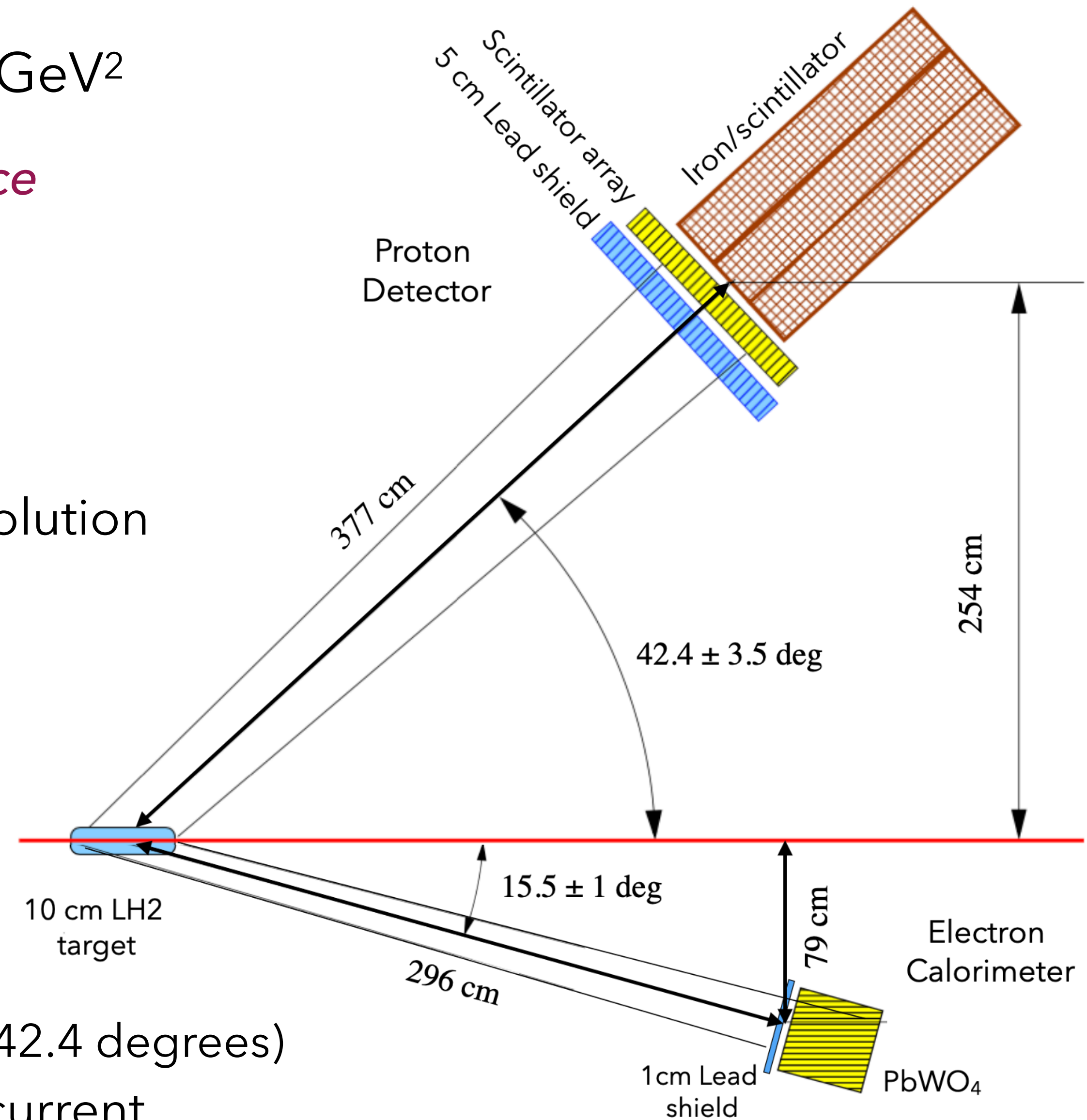
Aim for $Q^2 = 2.5 \text{ GeV}^2$

Identify elastic kinematics with electron-proton coincidence

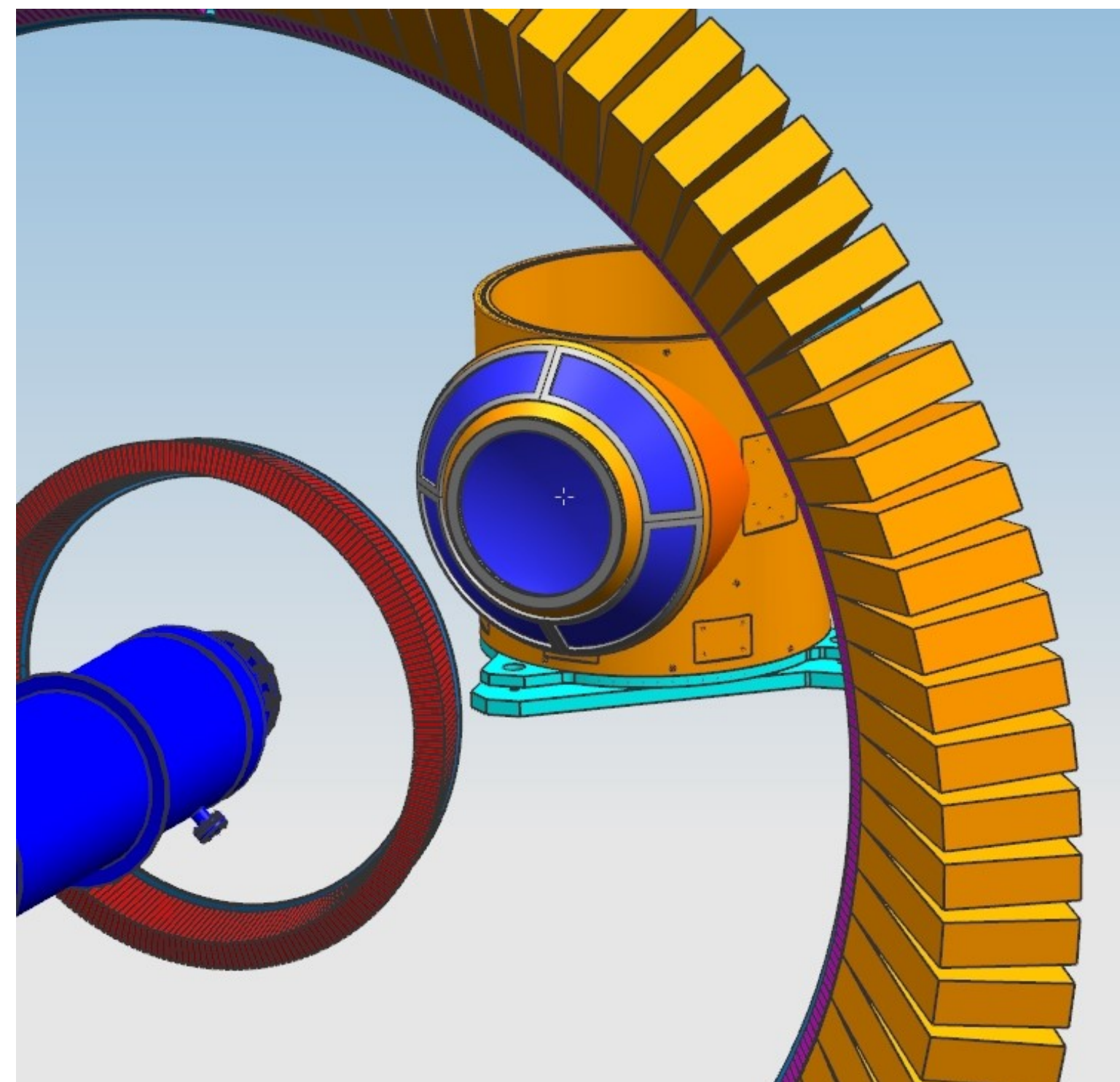
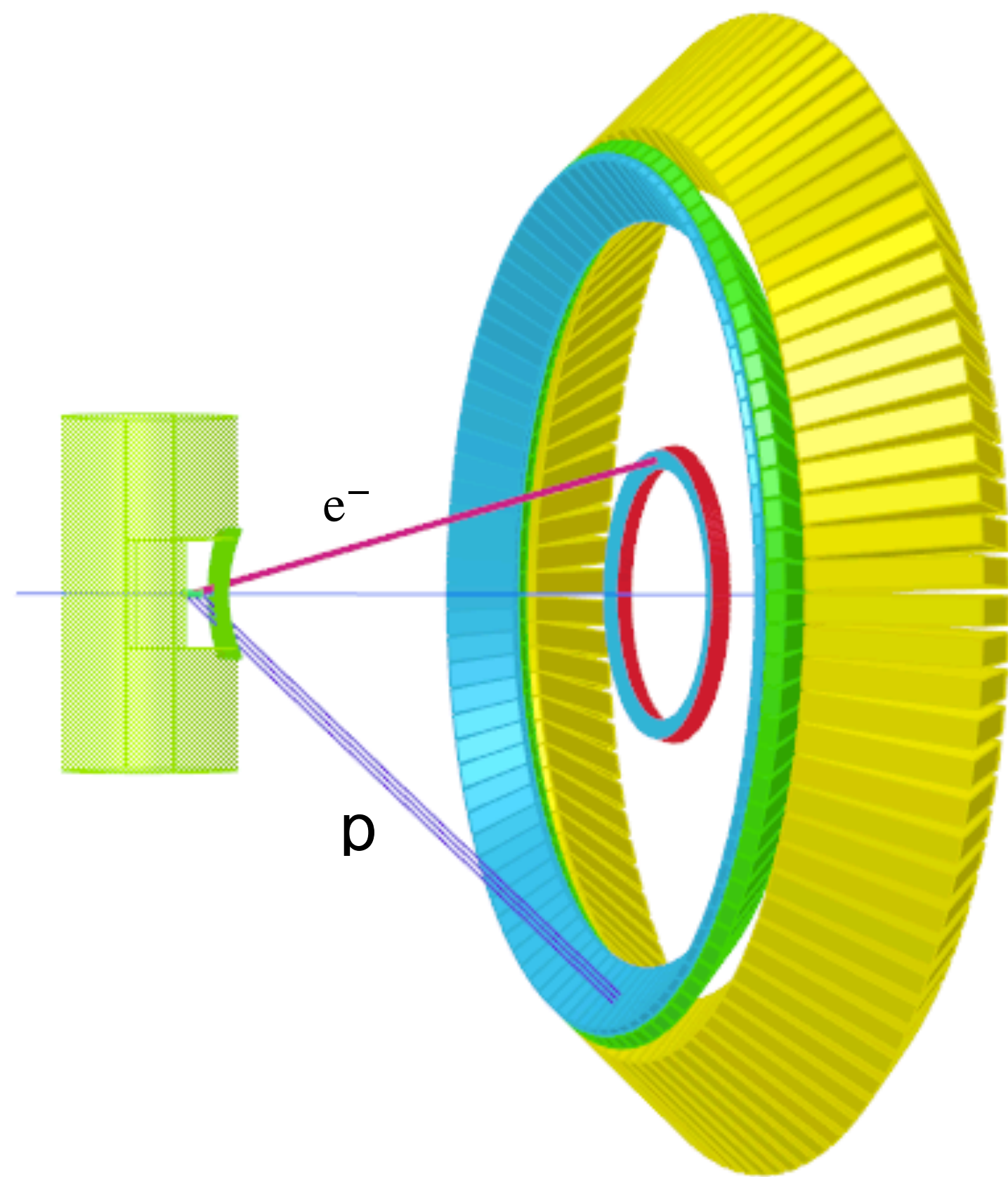
- Angular e-p correlation
- High resolution calorimeter for electron arm
- Calorimeter for proton arm
- Trigger on calorimeter coincidence (time, geometry)
- Scintillator array on proton arm, to improve position resolution

High luminosity and acceptance at optimized kinematics

- Full azimuthal coverage, $\sim 42 \text{ msr}$
- 6.6 GeV beam energy (electron at 15.5 degrees, proton at 42.4 degrees)
- $\mathcal{L} = 1.7 \times 10^{38} \text{ cm}^{-2}/\text{s}$, 10 cm LH₂ target and 65 μA beam current
- APV = 150 ppm, 4% precision goal, so 3×10^{10} elastic scattering events



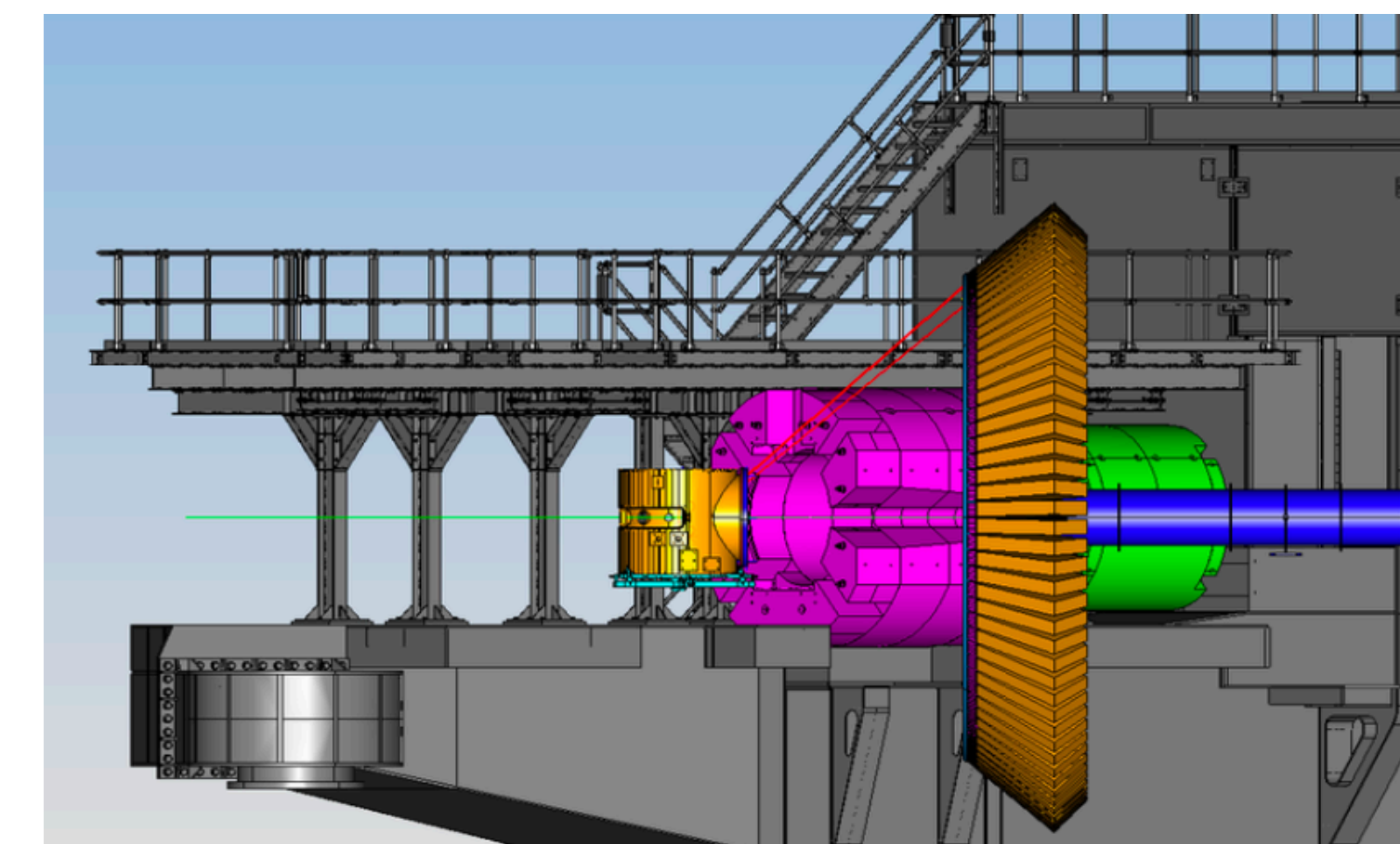
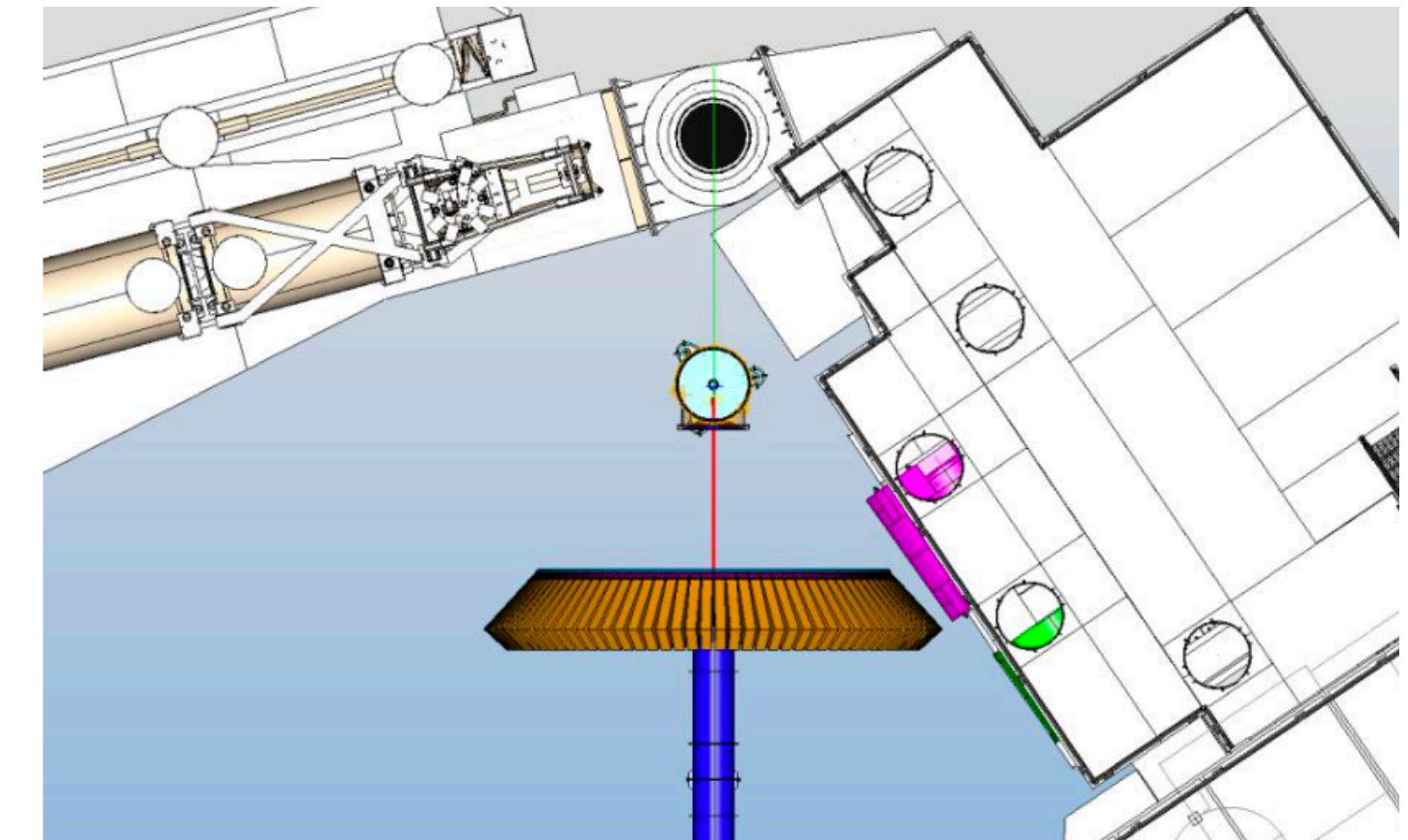
Experimental concept



Preliminary design of scattering chamber

He bag will reduce backgrounds between target chamber and exit beampipe

This fits in Hall C (but it's tight)



Detector System

HCAL - hadron calorimeter

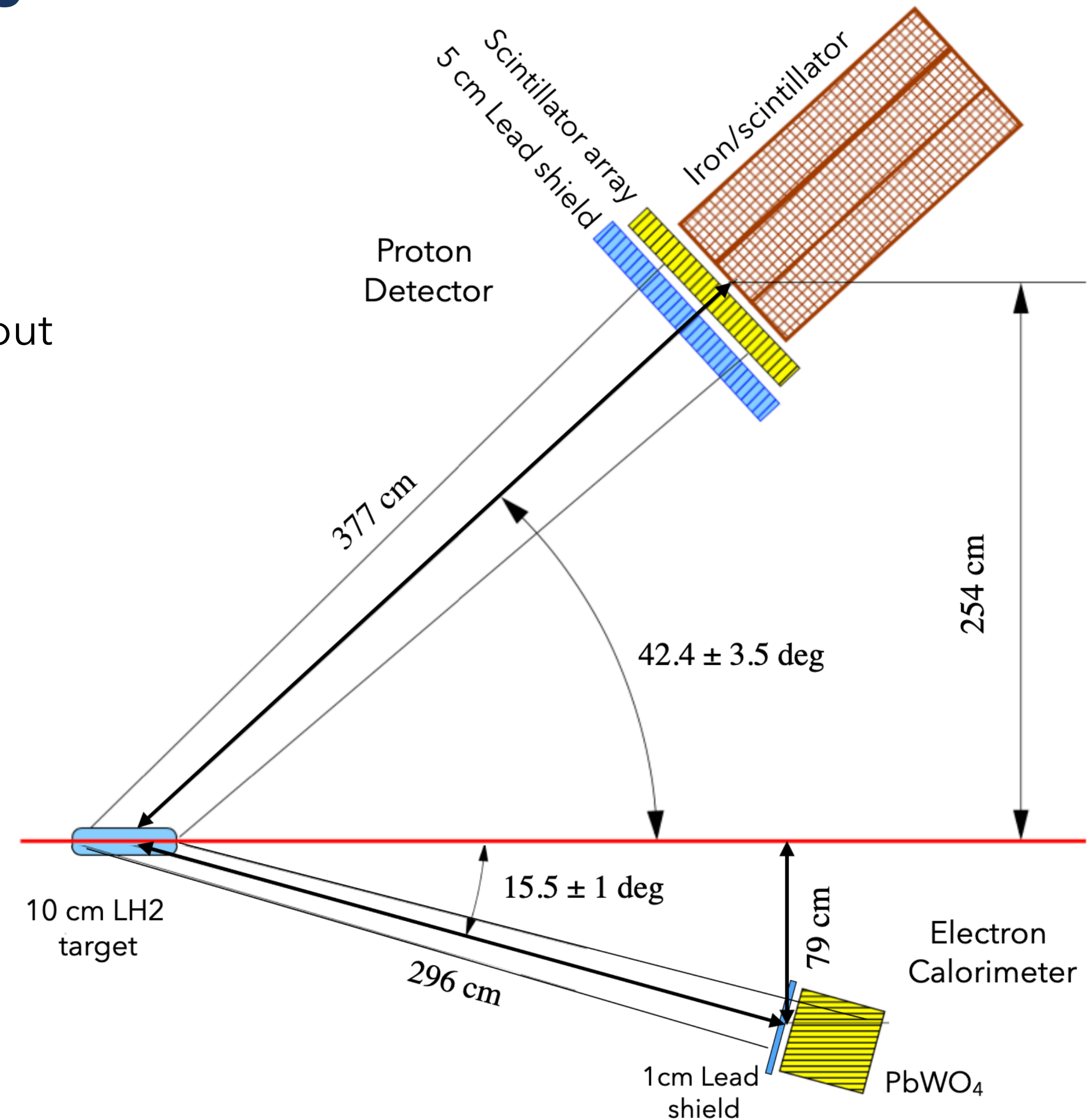
- Detector elements from the SBS HCAL (or similar option)
- 288 blocks, each $15.5 \times 15.5 \times 100 \text{ cm}^3$
- iron/scintillator sandwich with wavelength shifting fiber readout

ECAL - electron calorimeter

- Detector elements from the NPS calorimeter
- 1200 blocks, each $2 \times 2 \times 20 \text{ cm}^3$
- PbWO_4 scintillator

Scintillator array

- New fabrication for this experiment
- Used for position resolution in front of HCAL
- 7200 plastic scintillators, each $3 \times 3 \times 10 \text{ cm}^3$
- Wavelength shifting fiber to MA-PMT

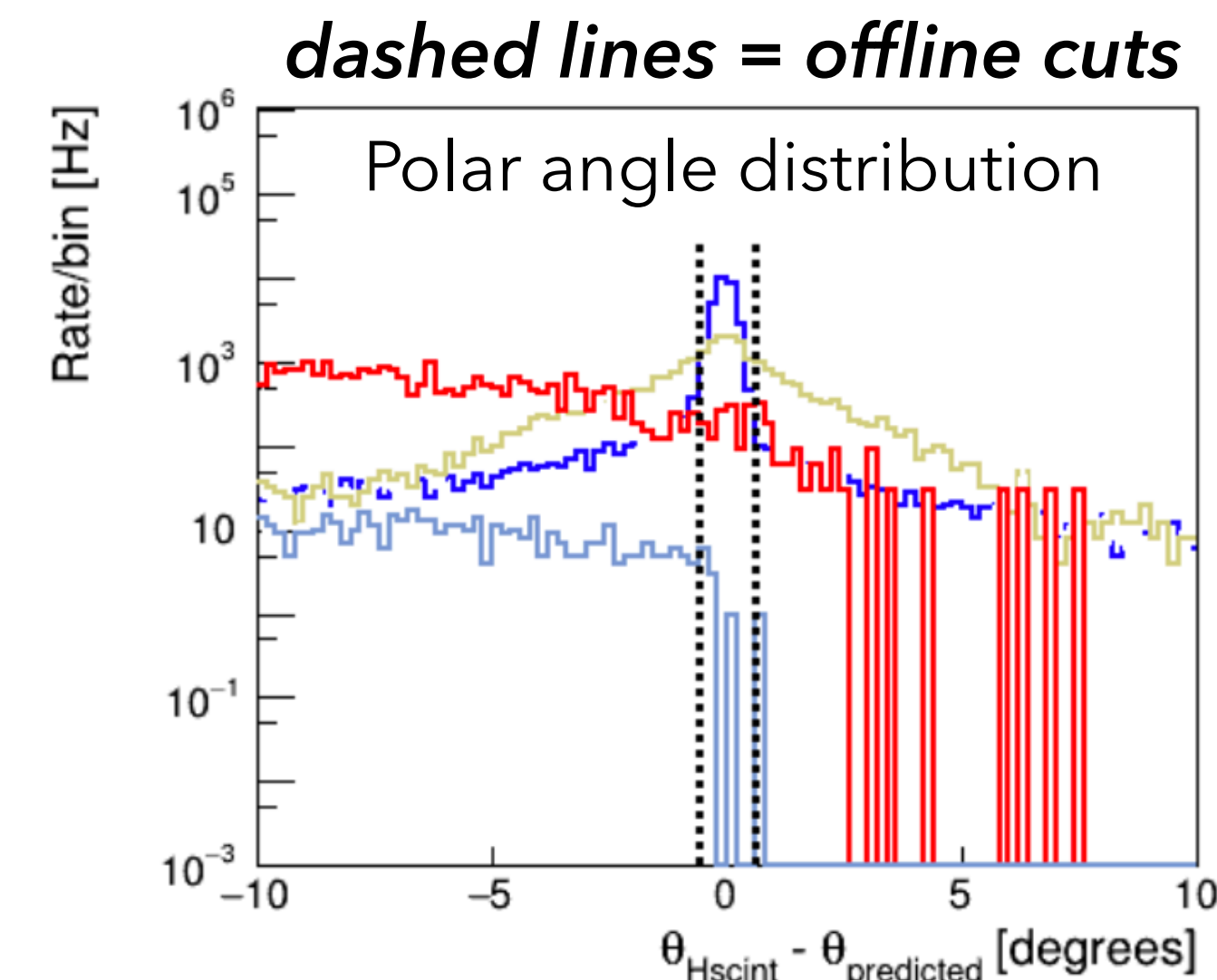
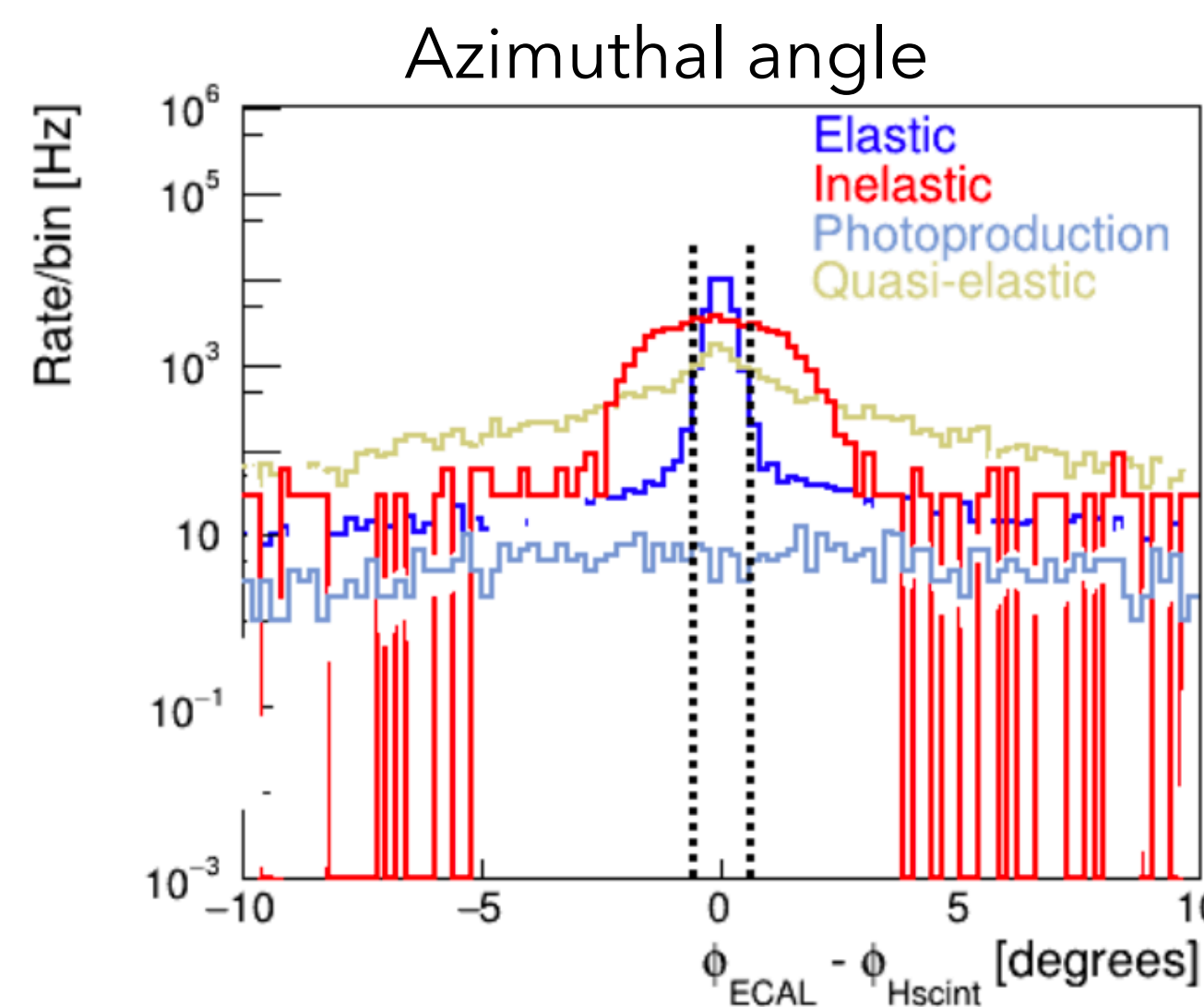
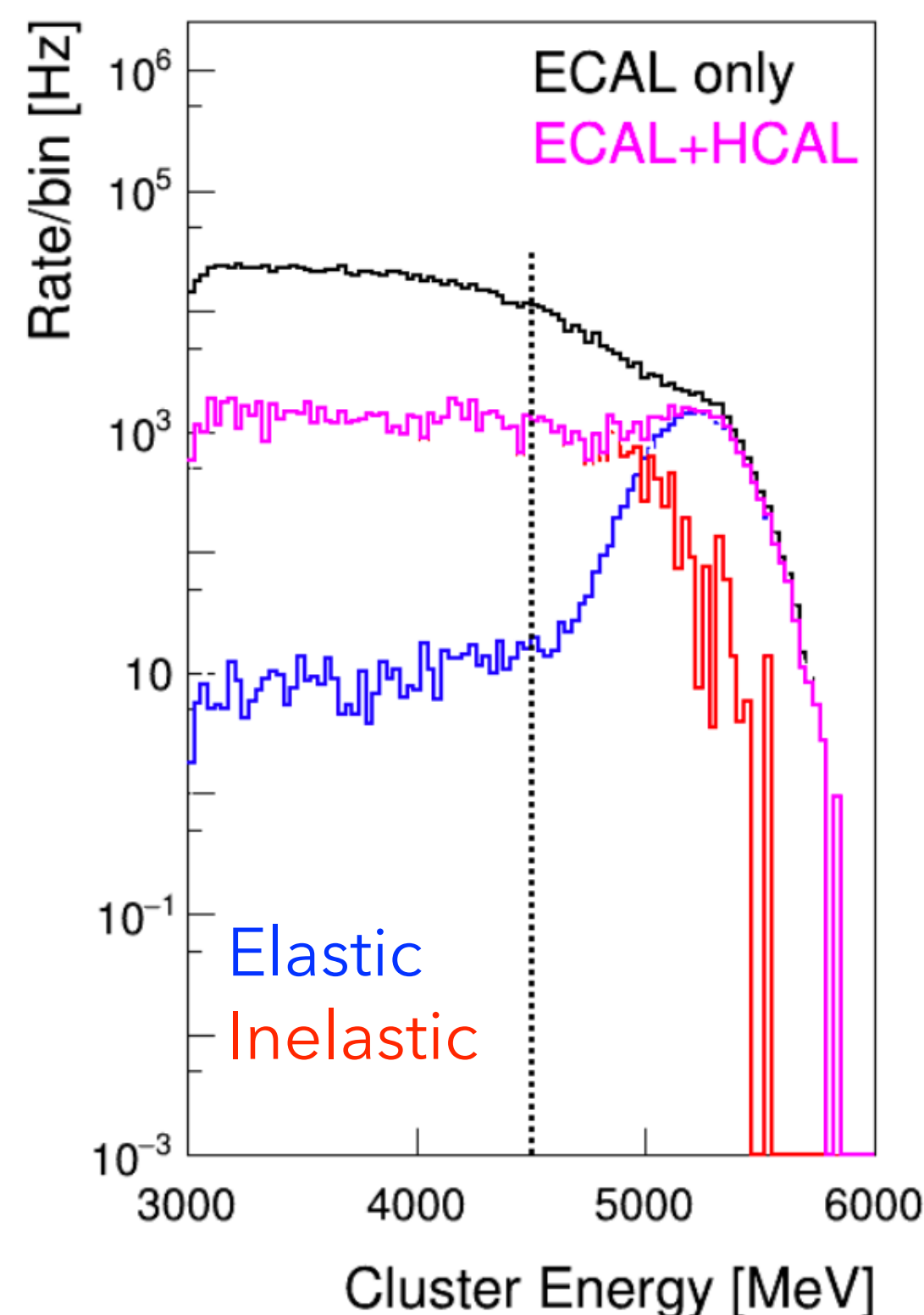


Trigger: calorimeters, with geometric coincidence

Trigger: Loose cuts on ECAL and e-p coincidence provides high efficiency with manageable data rate

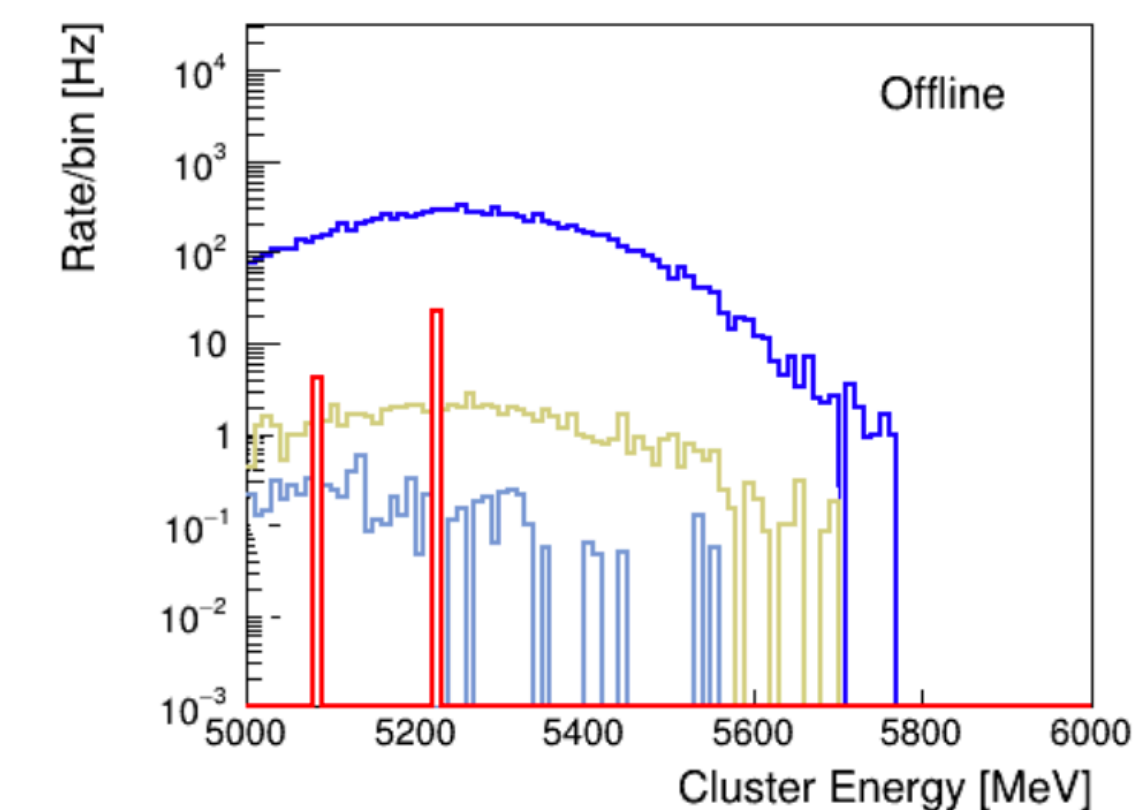
Offline: tighten geometric cut with pixel hodoscope and ECAL cluster center

Exclude inelastic background to $\sim 0.2\%$



Fraction of total by event type	Offline
---------------------------------	---------

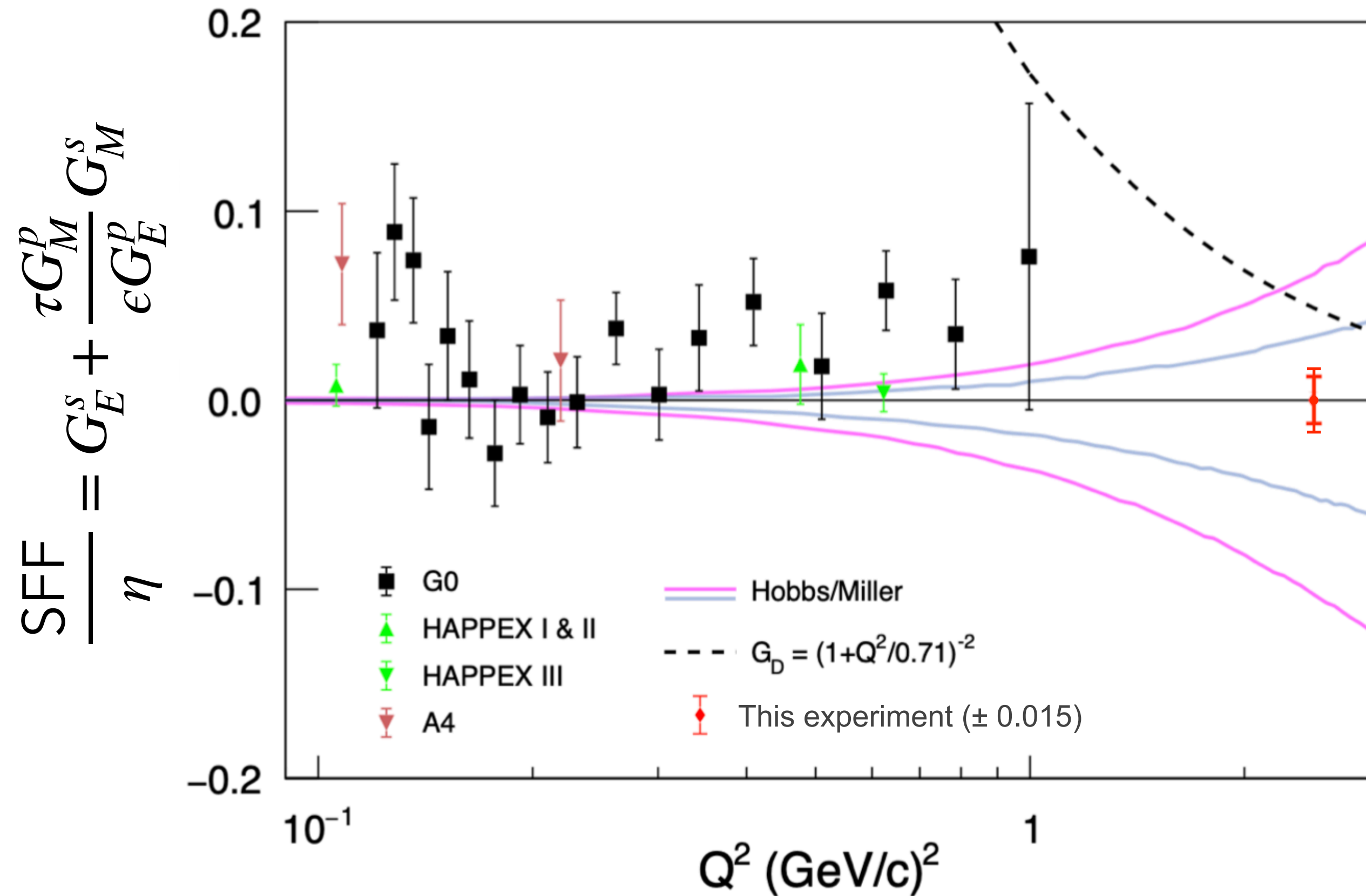
Elastic scattering	0.989
Inelastic (pion electro-production)	0.002
Quasi-elastic scattering (target windows)	0.008
π^0 photo-production	0.001



- ECAL + HCAL in coincidence
- 35 kHz total rate, $\sim 50\%$ signal
- $\sim 45\%$ inelastic (π production)

"sideband" analyses of non-elastic-geometry events can verify simulation

Projected result



The proposed error bar reaches the range of lattice predictions and is much smaller than the range of existing empirical bounds

The proposed measurement is especially sensitive to G_M^s

$$\text{If } G_M^s = 0, \quad \delta G_E^s \sim 0.015, \quad (\text{about } 34\% \text{ of } G_D)$$

$$\text{If } G_E^s = 0, \quad \delta G_M^s \sim 0.005, \quad (\text{about } 11\% \text{ of } G_D)$$

$$A_{PV} = 150 \text{ ppm (if no strange FF)}$$

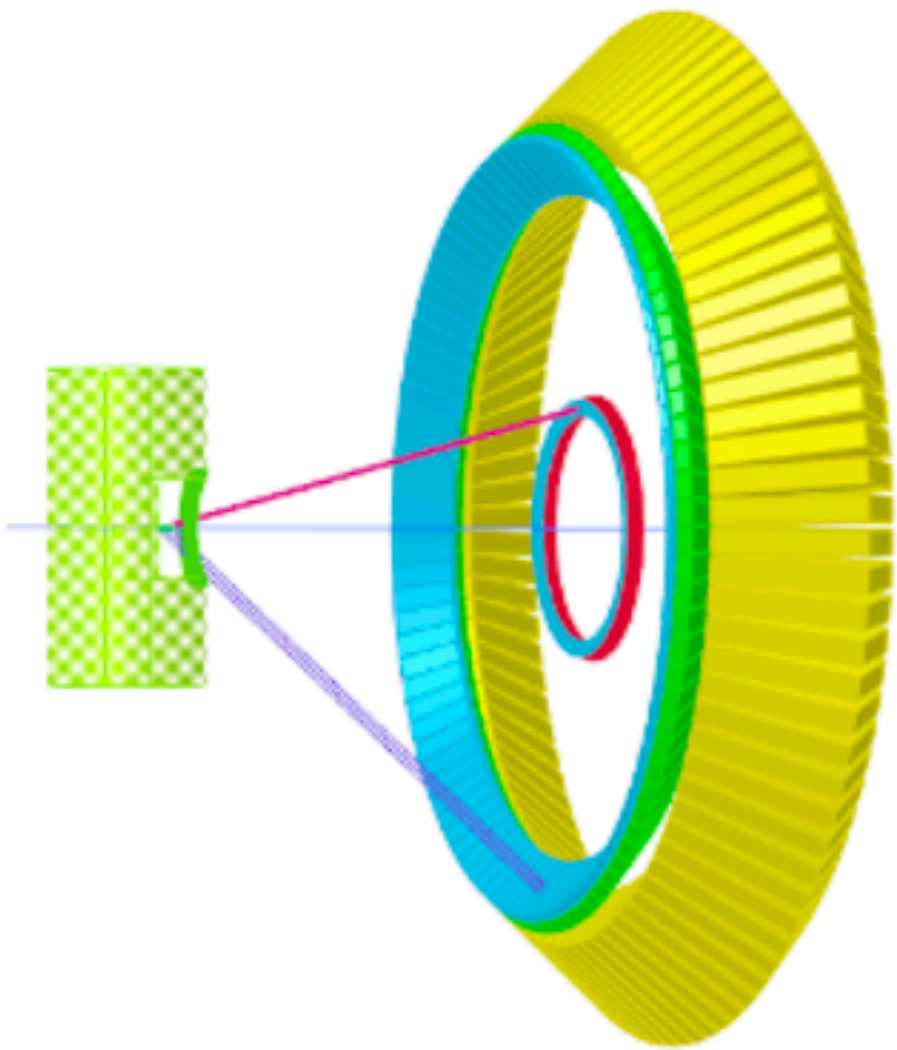
$$\delta A_{PV} = \pm 6.2 \text{ (stat)} \pm 3.3 \text{ (syst)} \quad (\delta A/A = \pm 4\% \pm 2\%)$$

$$\delta (G_E^s + 3.1G_M^s) = \pm 0.013 \text{ (stat)} \pm 0.007 \text{ (syst)} = 0.015 \text{ (total)}$$

Next Step - Test Performance of Detector Concept

Plan for beam test with detector prototype

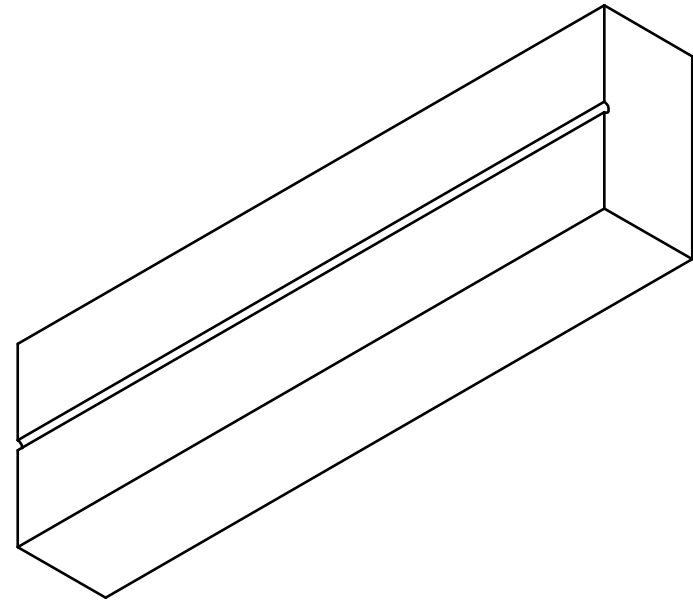
- The primary goal is to find the detector rates and responses to the protons, tagged by electron detection in the SHMS.
- Position the SHMS to 15.5° to detect electrons in coincidence with a prototype proton detector at 42.4°
- SHMS will replace the electron arm, identifying electrons for coincidence measurement
- Match this acceptance to a small proton calorimeter are (about 1% size of full proposed detector)
 - pixel array of 32 small scintillators with MA-PMT readout with 6 SBS HCAL blocks
 - Lead shield also required
- Use SMHS DAQ
- 50uA on 15cm Hydrogen target at 6.6 GeV, about 2kHz rate into detector
- Test elastic identification and background rate



electron angle 15.5°
proton angle 42.4°

Requires: detector prototype construction, detector stand, simulation for run planning, and beam time

Pixel Detector Prototyping



LaTech purchased scintillators, to be glued with WLS fibers for prototype



Initial prototype assembly, performance tested with cosmic rays

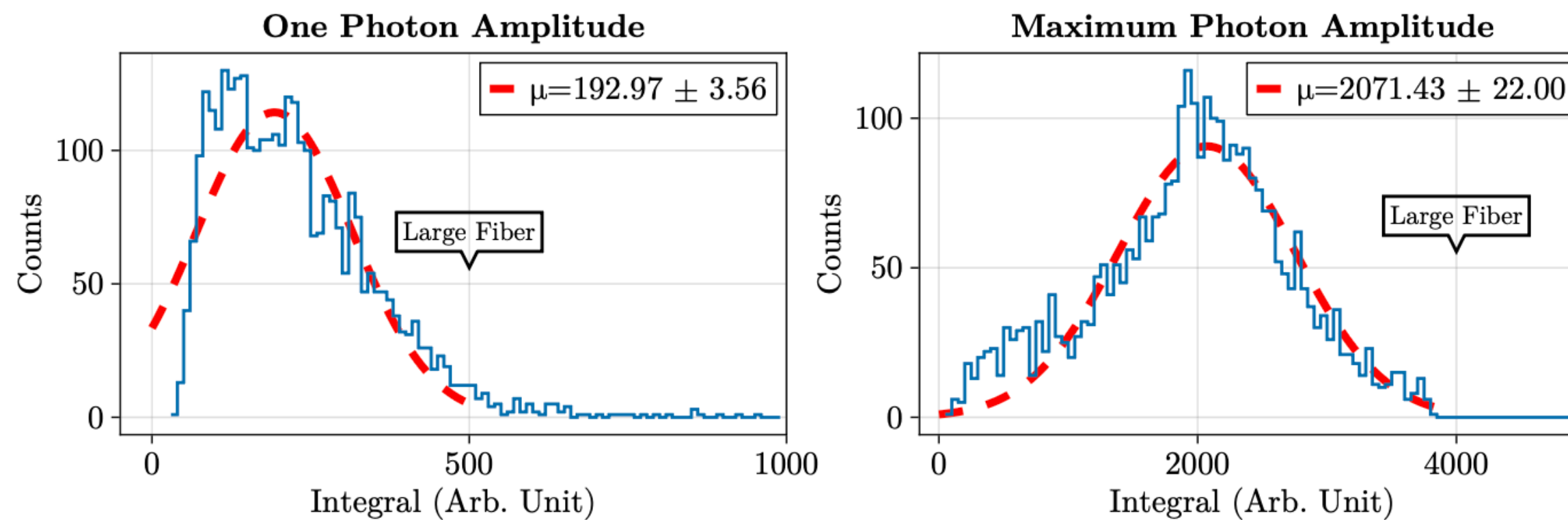


Table 1: The mean photon amplitude

Run No.	Fiber Size	Minimum	Maximum
104	Large	192.97 ± 4.25	2071.43 ± 22.00
110	Small	192.66 ± 3.32	2200.77 ± 45.32

Assembly technique has been demonstrated and first few modules are assembled

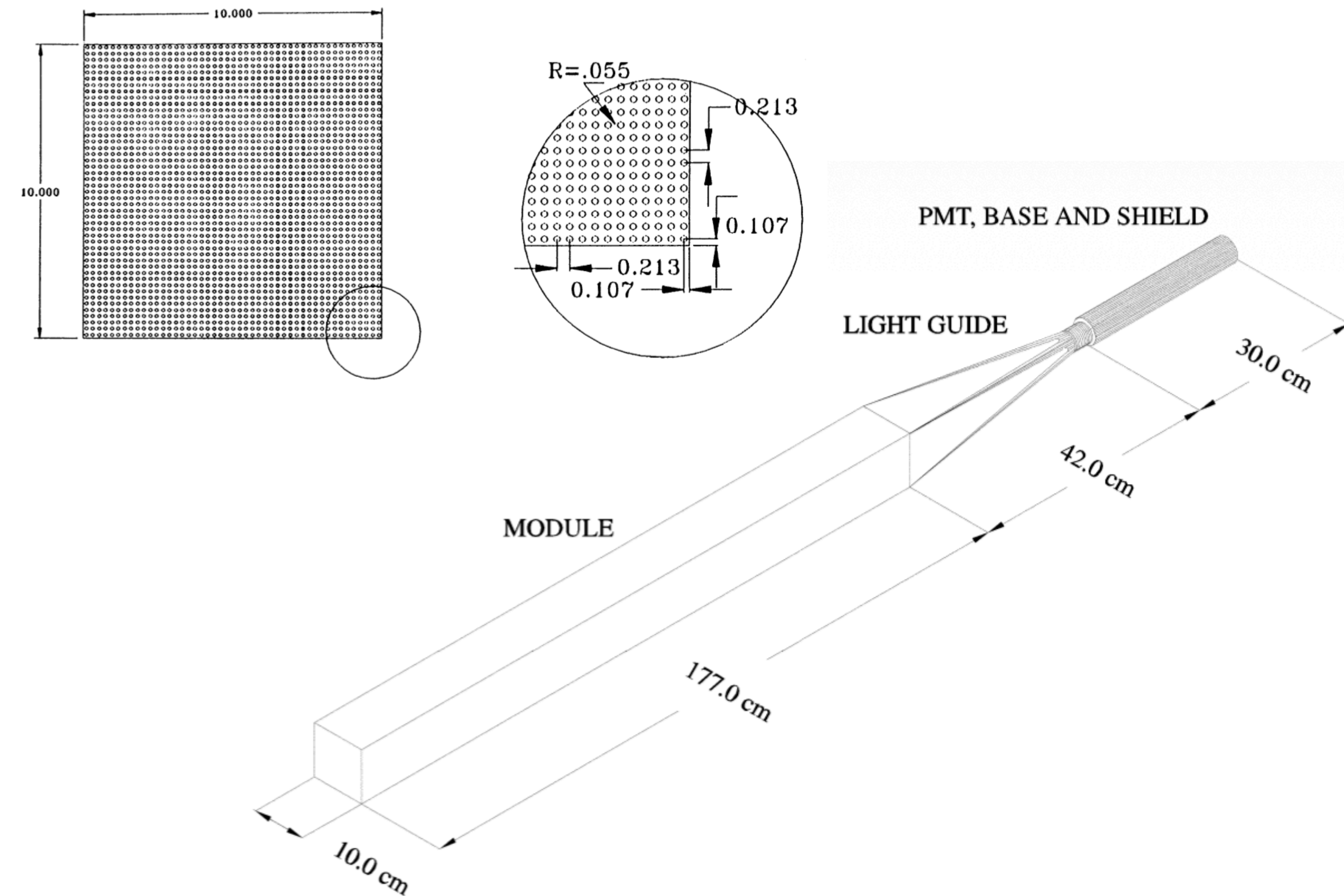
Scintillator and fibers for the rest of the prototype pixel detector are ready for assembly and testing

Alternative HCAL modules

E864 calorimeter -

- 700+ modules
- spaghetti calorimeter
- 10cm x10cmx177cm lead + scintillating fiber

- improve HCAL energy and geometric resolution
- Avoids polarized iron in detector for small asymmetry measurement (thought to be non-issue)
- be much heavier than the HCAL solution



Simulation Studies

GEANT4 framework implemented by David Hamilton

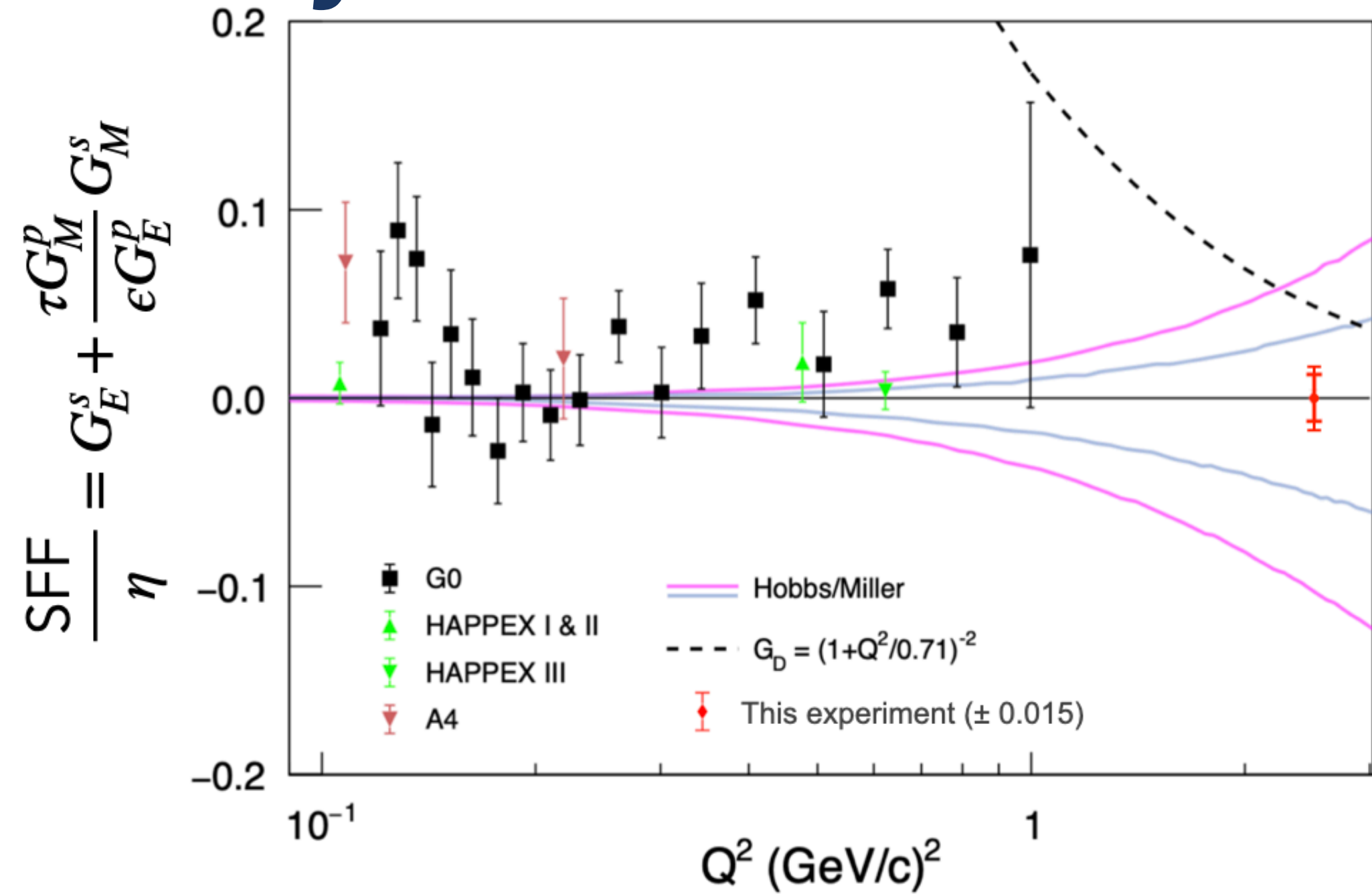
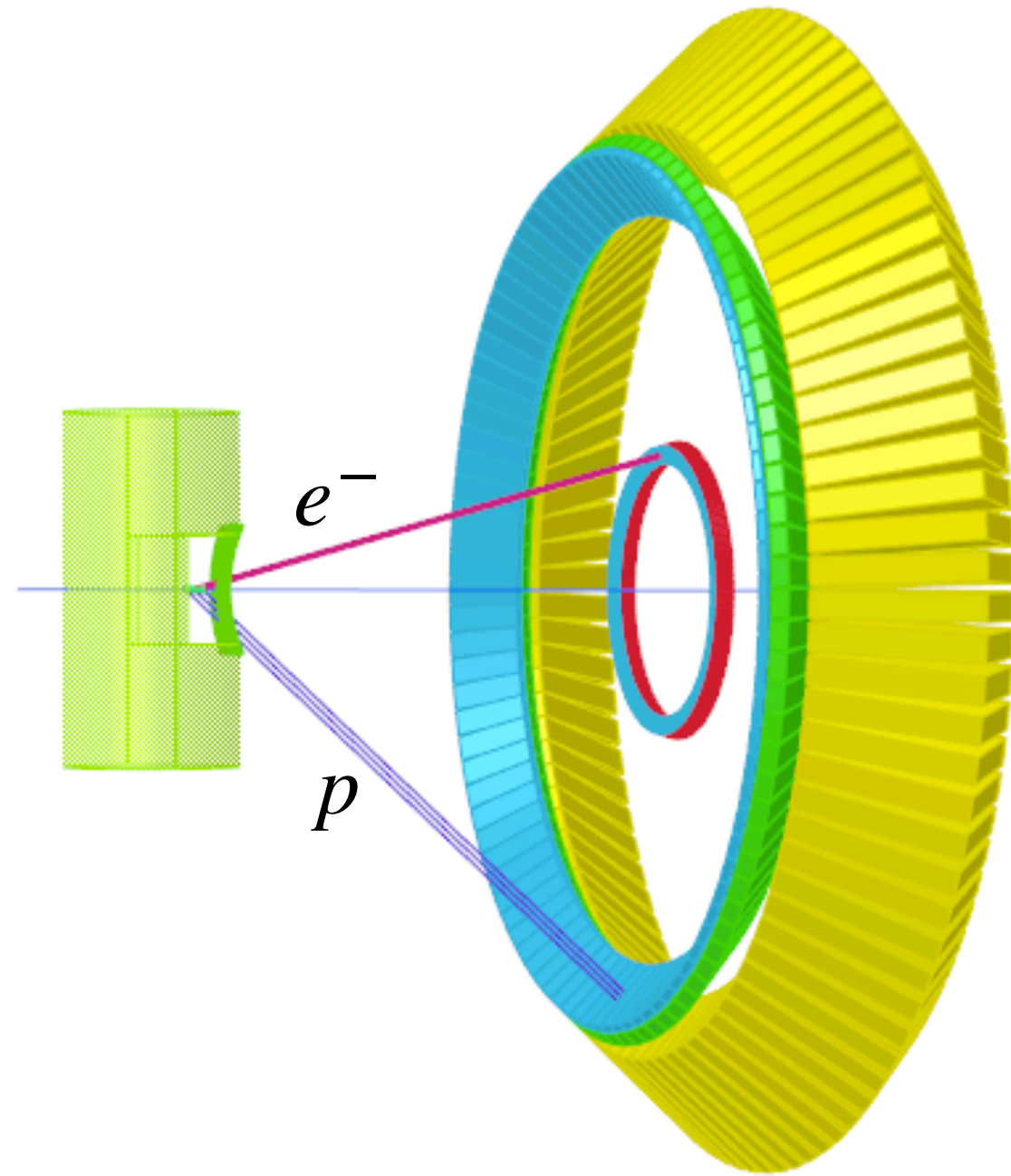
For Beamtest:

- Estimate acceptance (given solid angle coverage, and intermediate material)
- Estimate backgrounds in HCAL
- Show that position resolution (and required alignment) possible to distinguish elastic vs inelastic.

Experimental Design:

- Refine background cuts to optimize signal and background suppression
- Develop estimates for “sideband” analysis
- Test alternative geometries for scattering chamber, helium bag, support frame for background and resolution
- optimize lead shield thickness
- examine effect of alternative HCAL modules

Summary

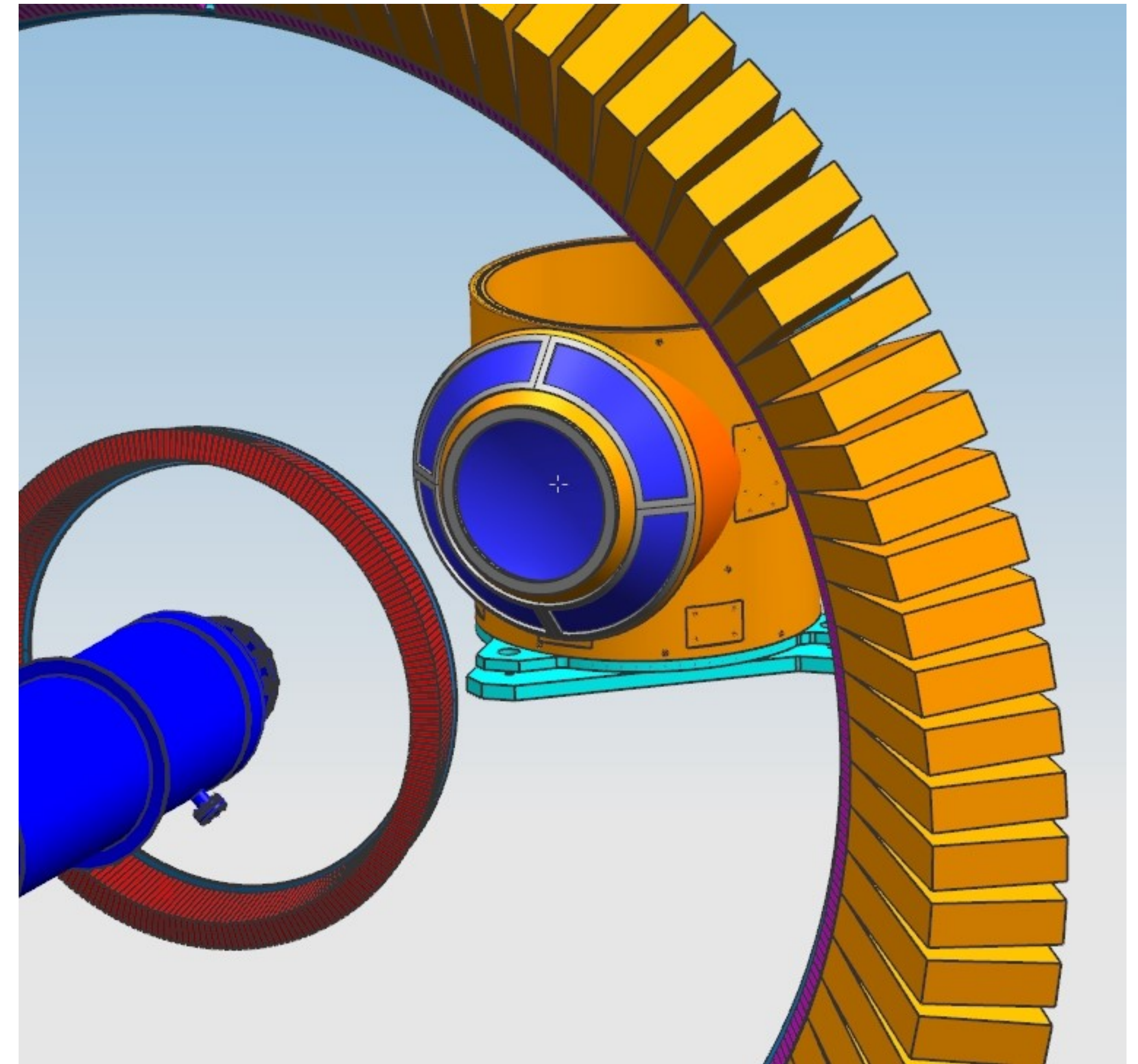
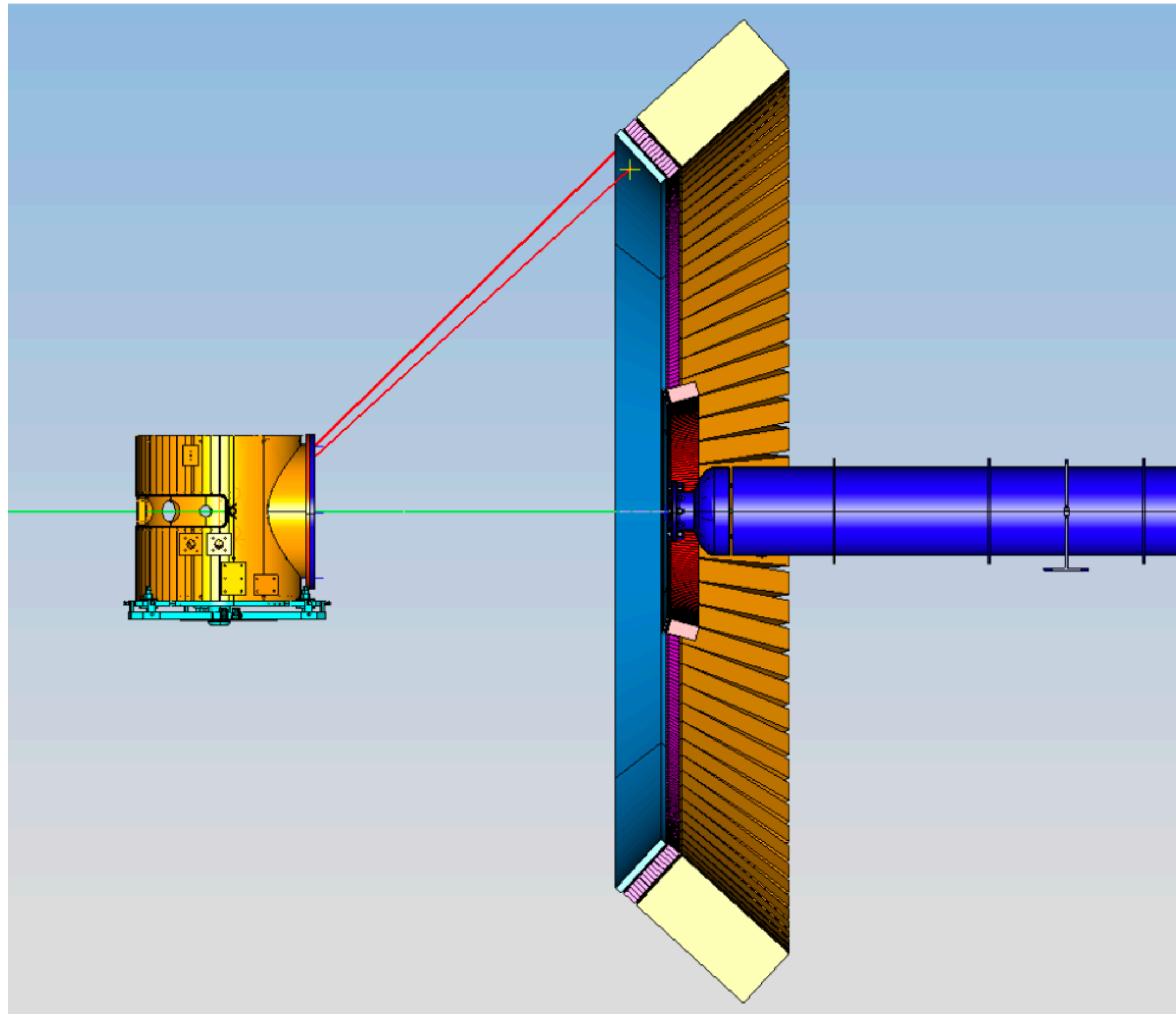


- 10+ years after the last sFF searches were performed, a new experiment is now planned for much higher Q^2 , motivated by interest in flavor decomposition of electromagnetic form factors
- Projected accuracy at $\sim 11\%$ of the dipole value allows high sensitivity search for non-zero strange form factor.
- The proposed error bar is in the range possibly suggested by lattice predictions, and significantly smaller than the uncertainty range in the extrapolation from previous strange form-factor data
- PAC approved, still needs funding and development. Much work to be done, collaborators welcome!

backup slides

Scattering chamber

Cylindrical scattering chamber with large Al window to pass 15° electrons and 45° protons
Design uses a cone with "ribs", plus an inverted hemisphere center, windows could be as thin as 0.5mm



Requires air gap - will use He bag (not shown) to transport beam, so open air gap is only ~ 50 cm

Calorimeters reusing components

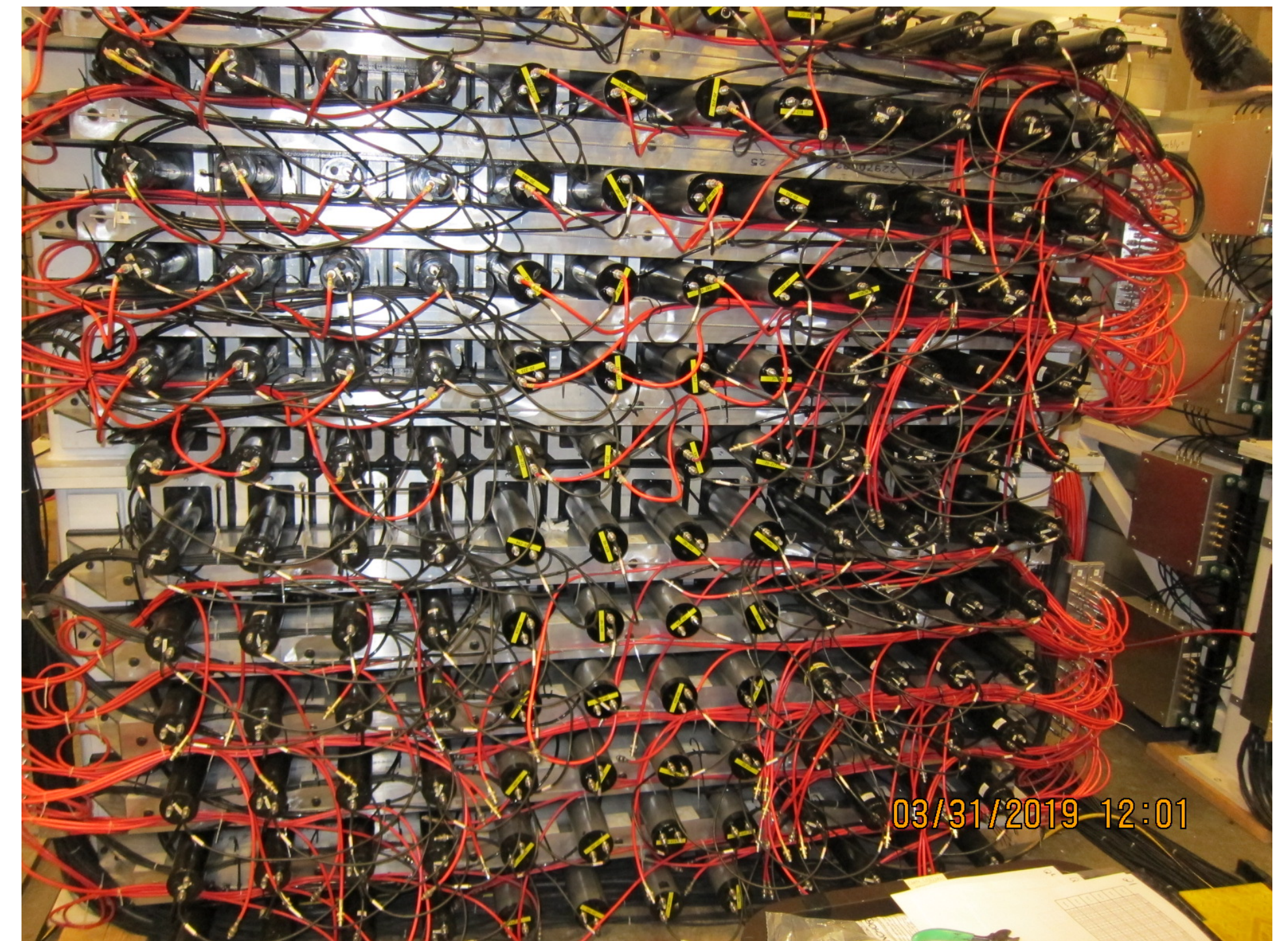
NPS electromagnetic calorimeter

- 1080 PBWO₄ scintillators, PMTs + bases
- will run in future NPS experiment



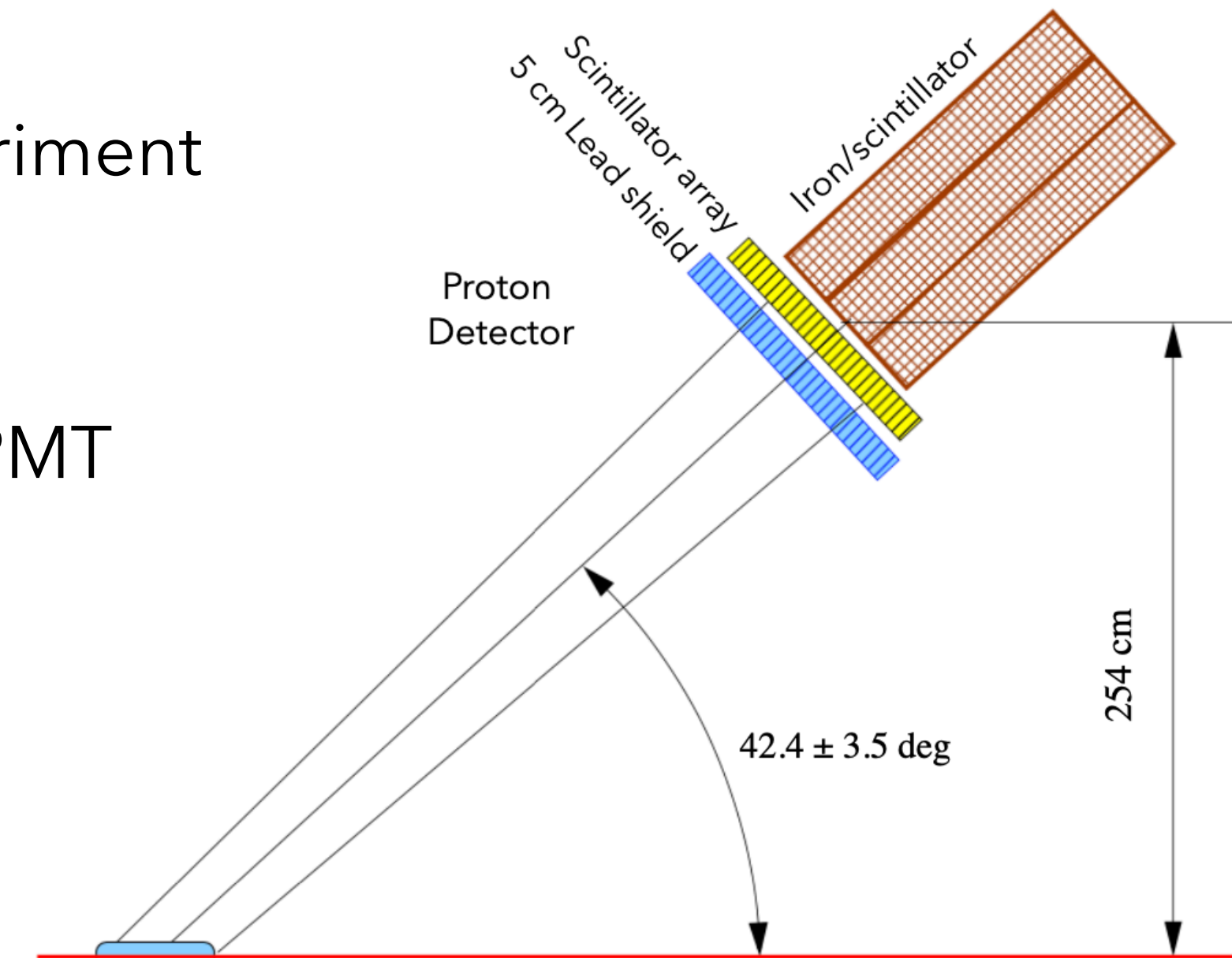
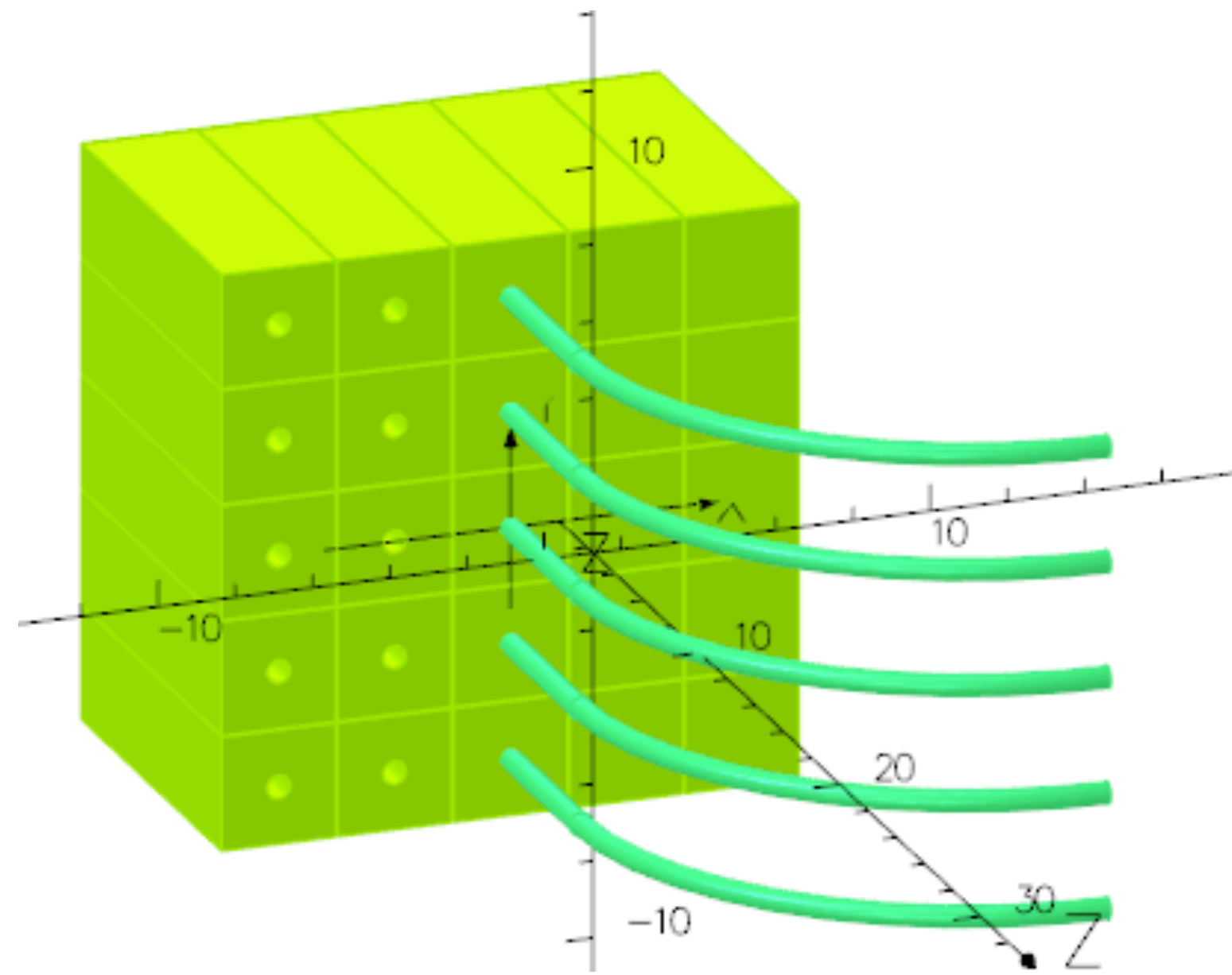
SBS hadronic calorimeter

- 288 iron/scintillator detectors, PMTs + bases
- Already in use with SBS



Scintillator Array

- New detector, must be built for this experiment
- Extruded plastic scintillator block
- Readout with wavelength-shifting fiber
- Each fiber read by pixel on multi-anode PMT
- 7200 blocks, each $3 \times 3 \times 10 \text{ cm}^3$



Design matches scintillator array built for GEP

- 2400 elements, $0.5 \times 4 \times 50 \text{ cm}^3$
- Already built, will run next year

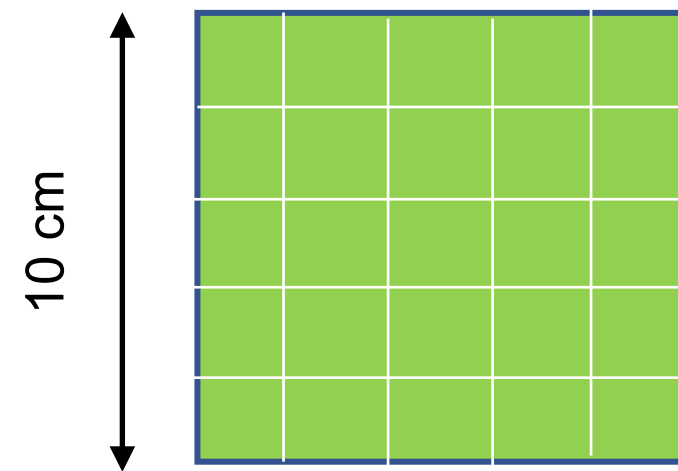


Triggering

Grouping into “subsystems” for energy threshold and coincidence triggering of event record

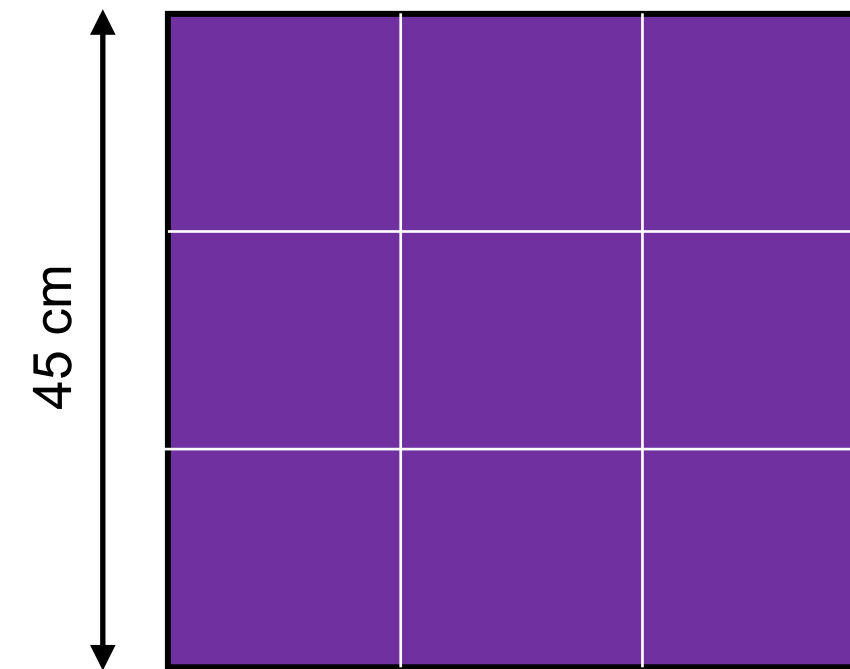
- each polar column of detectors, overlapping with neighbors
- sum amplitude with conservative coincidence timing window
- compare to conservative energy threshold
- trigger when complementary (ECAL and HCAL) subsystems are both above threshold

Electron subsystems



- 1200 PbWO_4 crystals
- $2 \times 2 \times 20 \text{ cm}^3$
- 5x5 grouping for subsystem
- 240 overlapping subsystems

Proton subsystems

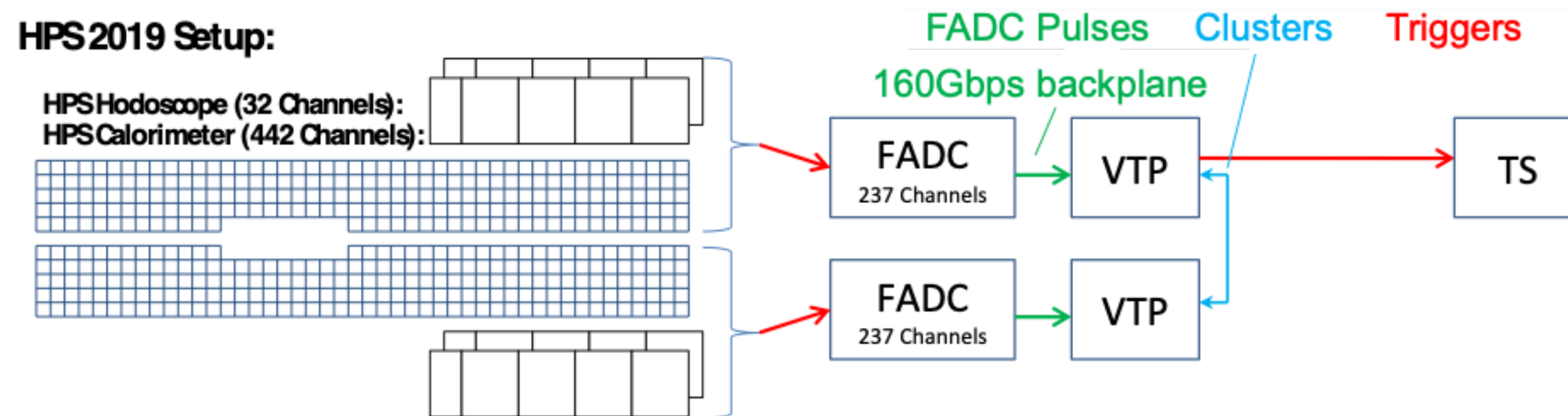


- 288 iron/scintillators
- $15.5 \times 15.5 \times 100 \text{ cm}^3$
- 3x3 grouping for subsystem
- 96 overlapping subsystems

Fast Counting DAQ

Readout for fast counting is now very common challenge and enabled by new, and now common, technologies. In particular, SOLID will face this challenge in measurement of PV-DIS, and this experiment will be an important testing ground for precise asymmetry measurements.

Concept very similar to the HPS DAQ, used in 2019 or NPS DAQ:



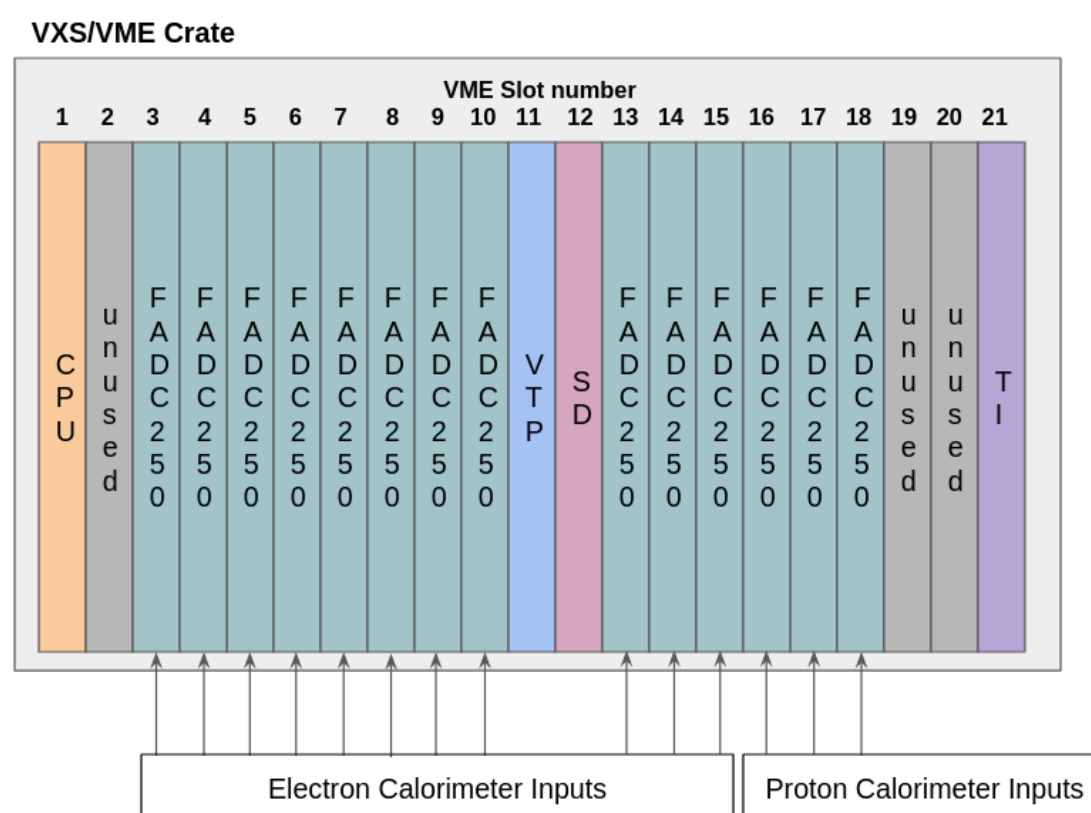
JLab FADC250 for HCAL and ECAL readout

Provides the pulse information for a fast, "deadtime-less" trigger



VTP (VXS Trigger Processor)

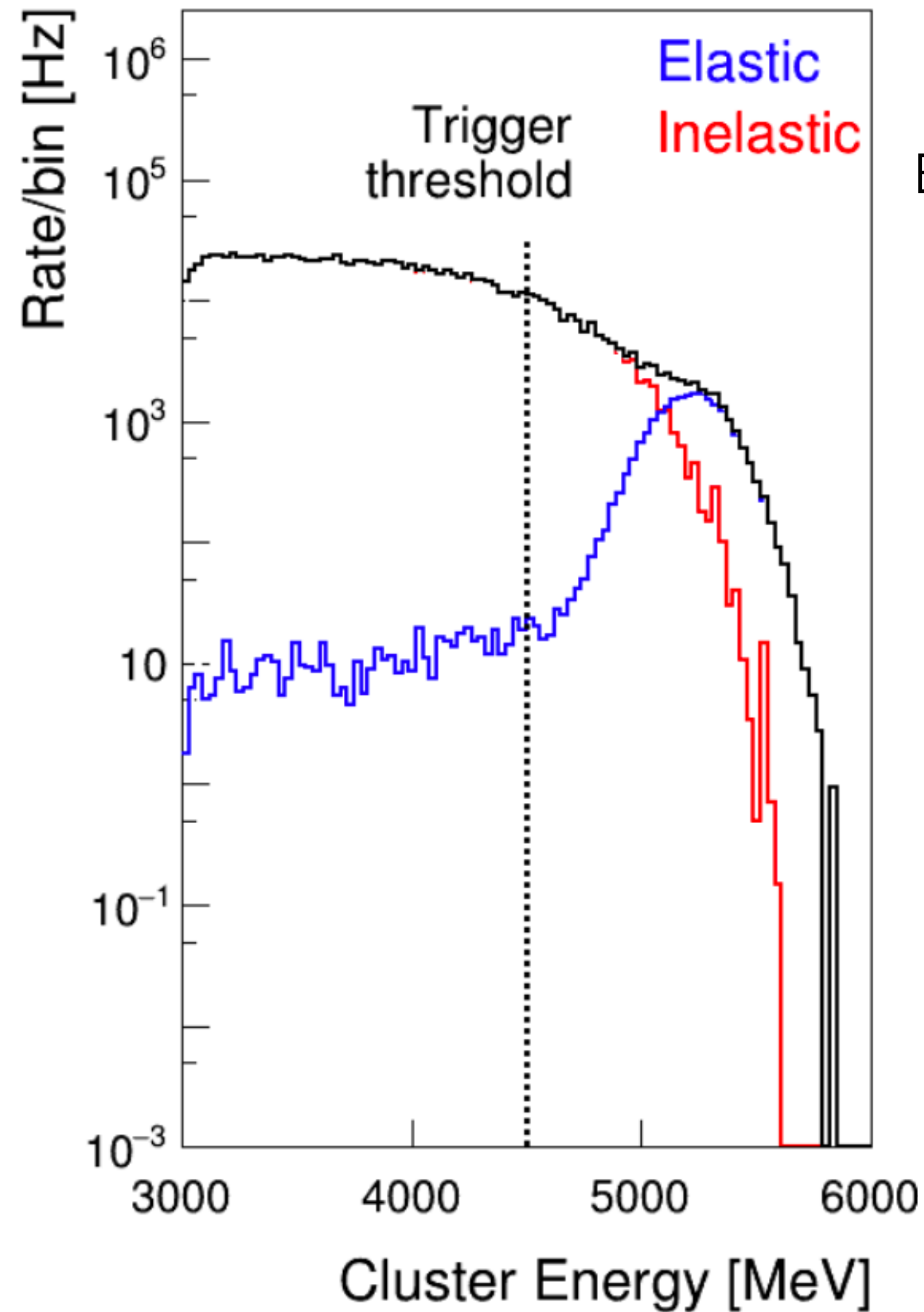
Clusters in time, sums over subsystems, finds ECAL+HCAL coincidence



One VXS crate will handle one sixth of ECAL + HCAL, also provide external trigger for ScintArray pipeline TDC readout

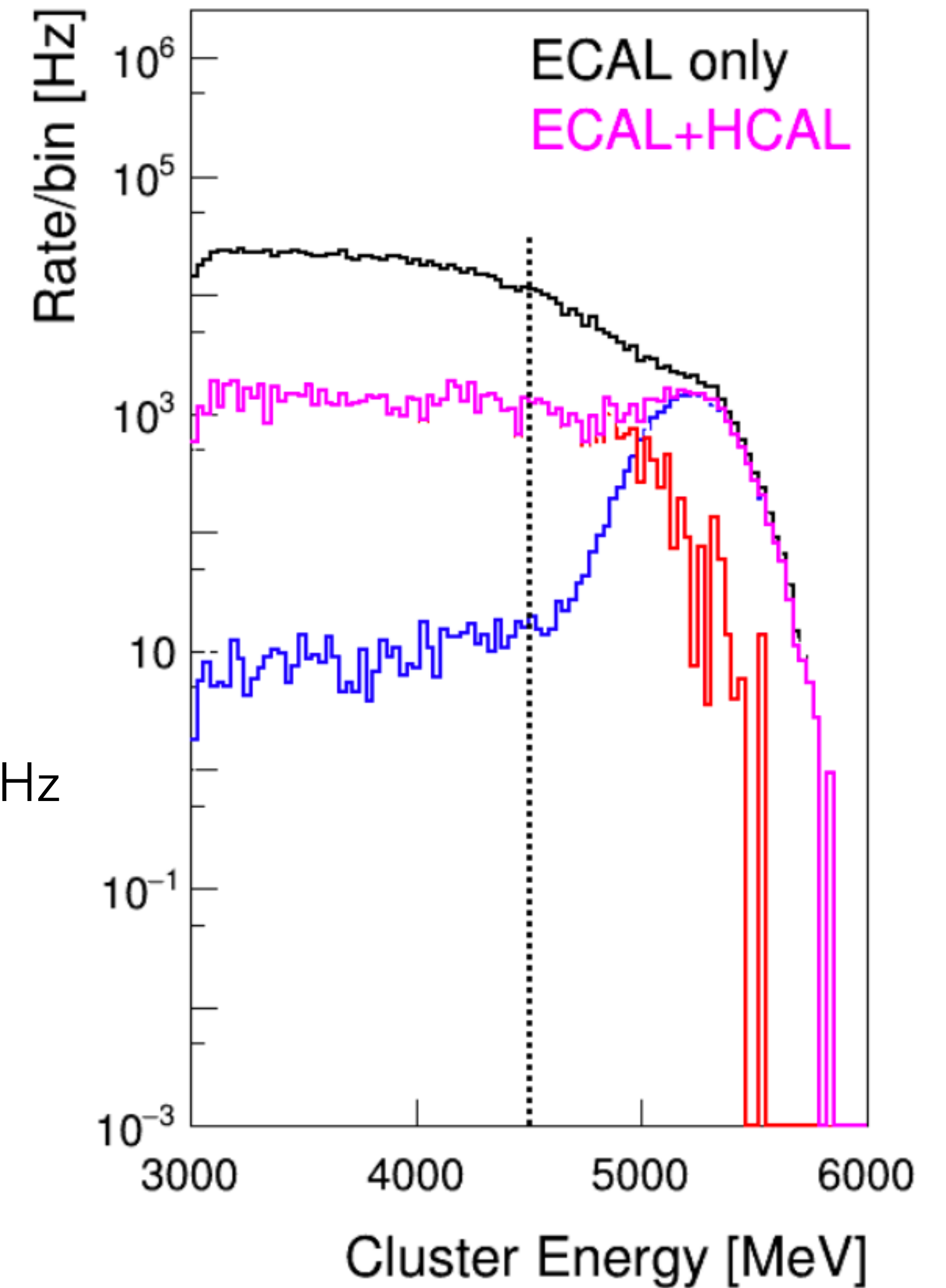
Expect ~50kHz total, ~250 Mb/s data rate, distributed over 6 separate crates

ECAL cluster rates



ECAL > 4.5 GeV : 153 kHz

ECAL > 4.5 GeV
&
HCAL > 50 MeV : 35 kHz



Rates and Precision

Beam and target: 60 μA on 10 cm LH_2 \Rightarrow luminosity is $1.6 \times 10^{38} \text{ cm}^{-2}/\text{s}$

Trigger (online)

- Elastic coincidence 18 kHz signal in full detector
- Inelastic (pion production) coincidence trigger rate ~ 16 kHz
- Accidental coincidence rate < 0.2 kHz
 - ~ 150 kHz total singles rate in ECAL > 4.5 GeV energy threshold, 200/5 unique subsystems
 - ~ 19 MHz total singles rate in HCAL > 50 MeV energy threshold, 96/3 unique subsystems
 - Temporal coincidence cut 40ns
- ~ 35 kHz total coincidence trigger rate

Offline analysis

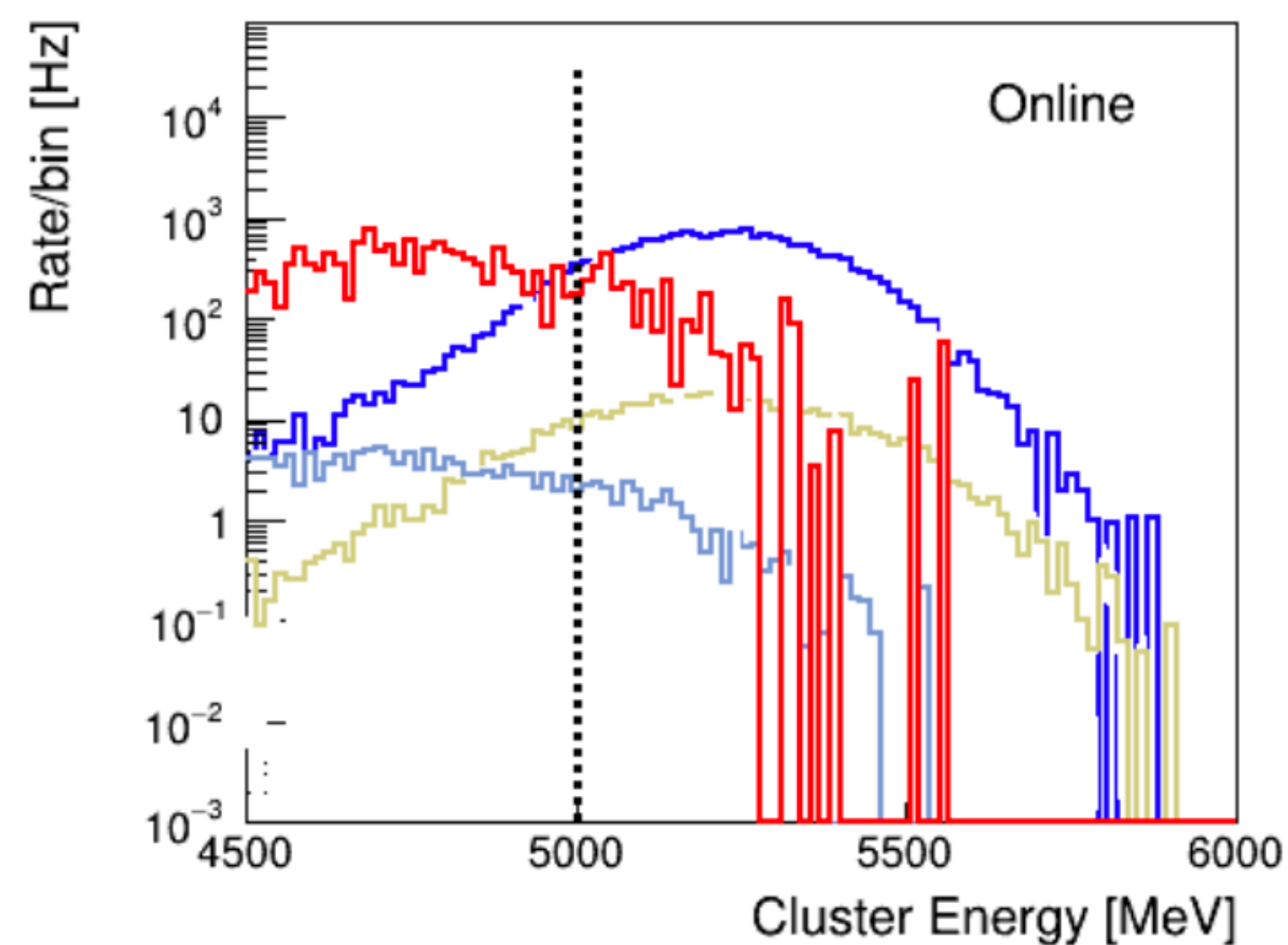
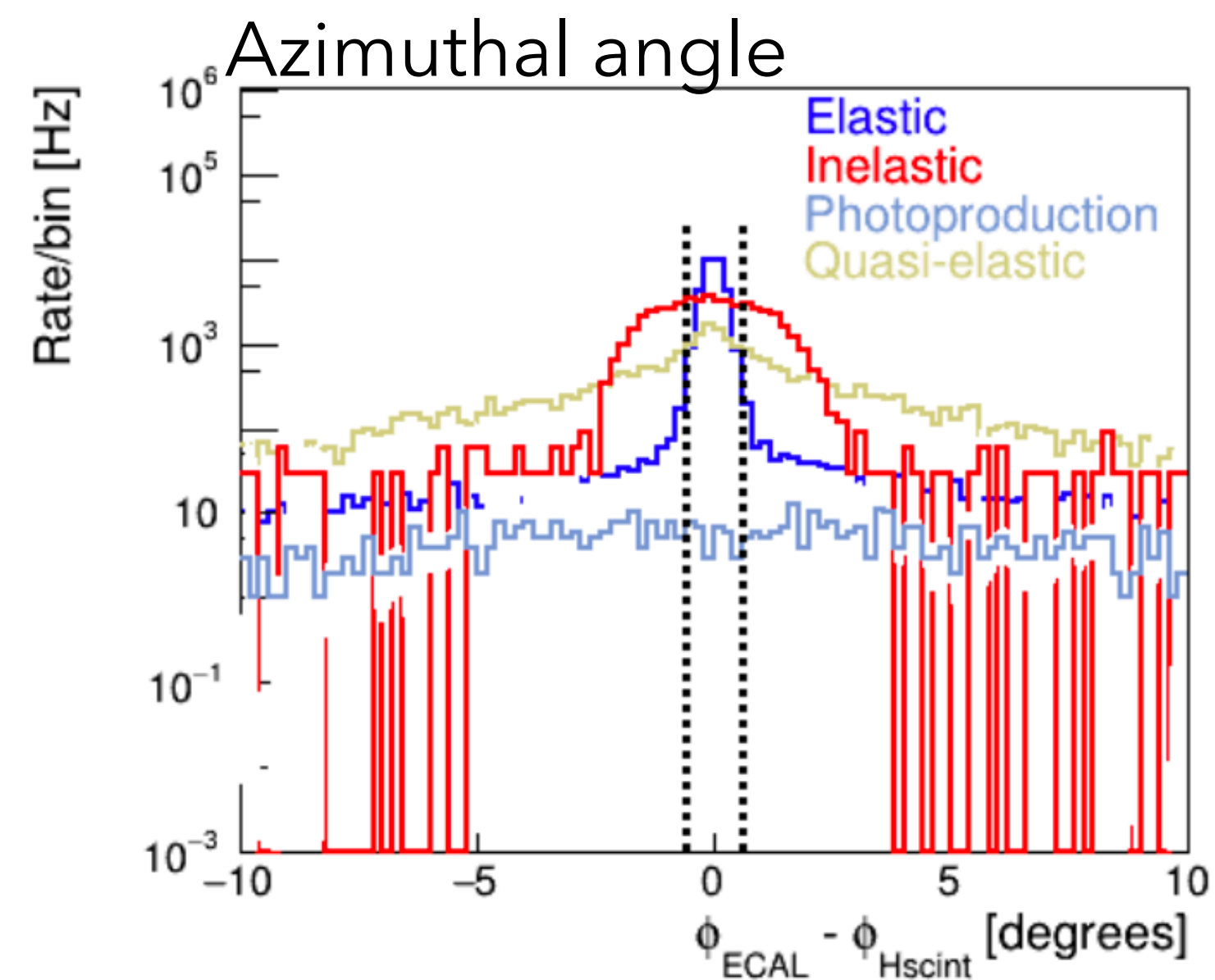
- clustering, scintillator array to improve geometric cuts, tighter acceptance and ECAL cut, 4 ns timing
- Accepted elastic signal reduced to 13 kHz - production statistics
- Inelastic (pion production) $< 0.5\%$, accidentals $< 1 \times 10^{-5}$ due to angular precision and higher E cut

Beam polarization 85%

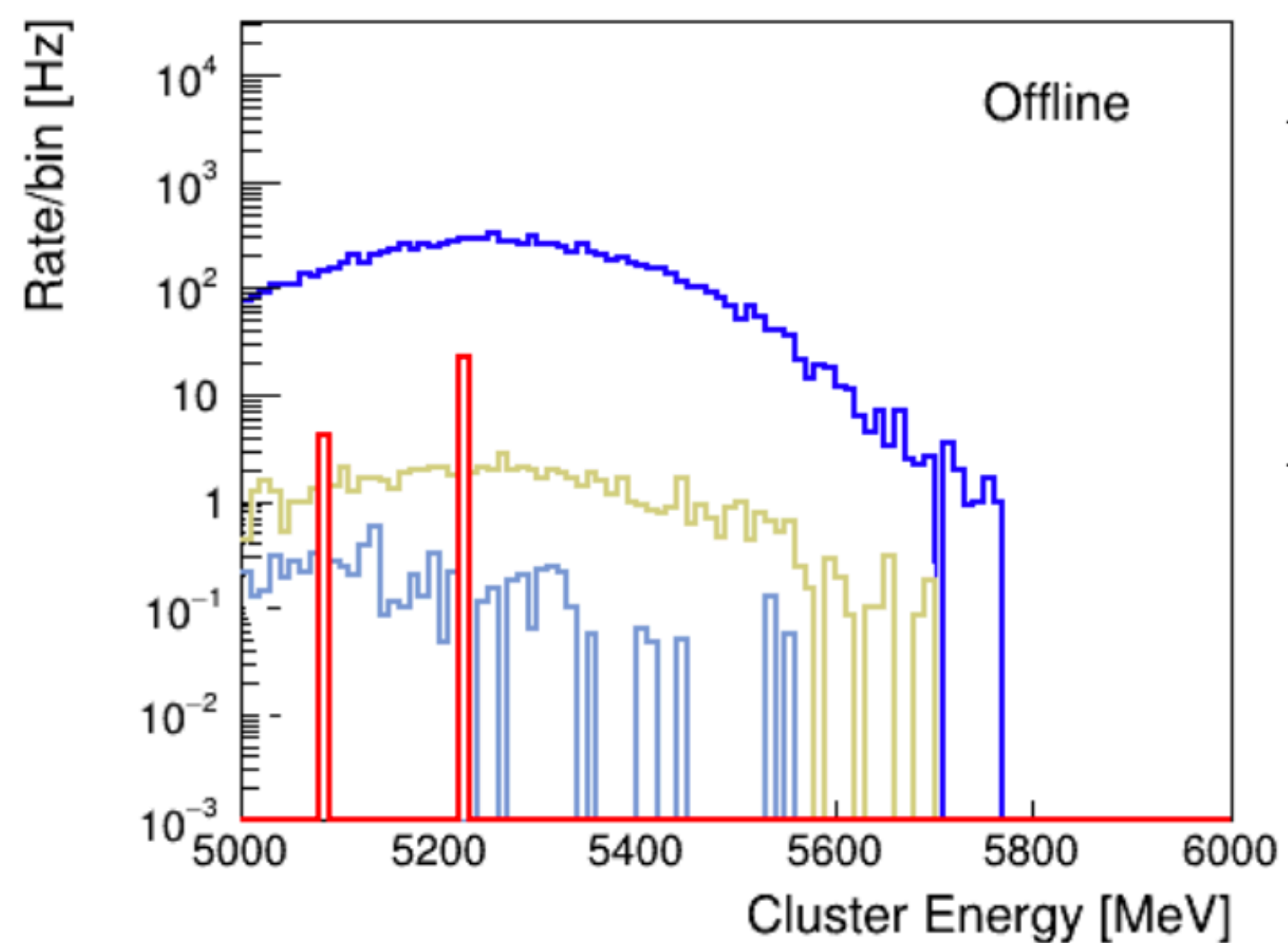
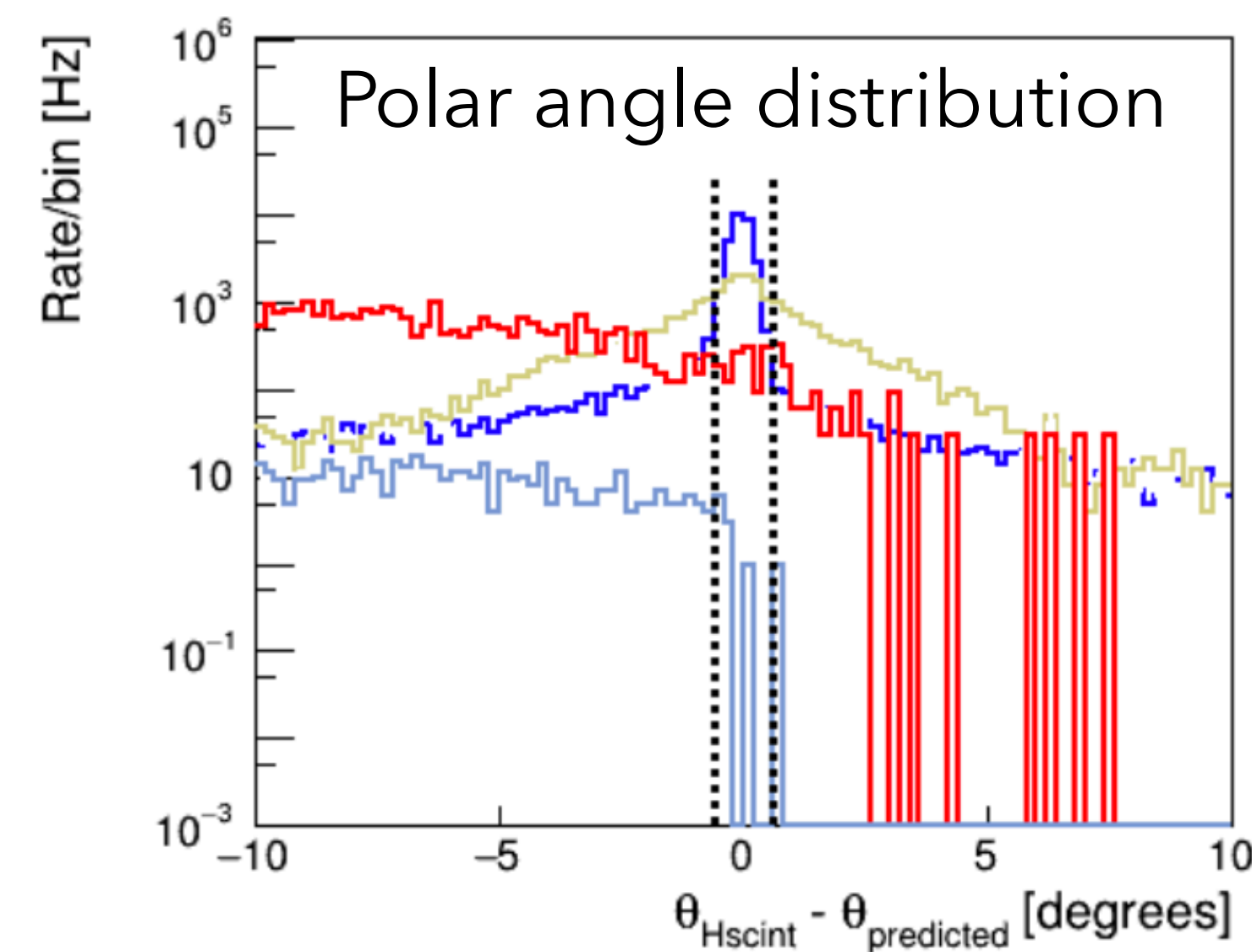
40 days production runtime \rightarrow Raw asymmetry statistical precision $\delta(A_{\text{raw}}) \sim 5$ ppm

$\rightarrow A_{\text{PV}} = -150 \pm 6.2$ ppm

Elastic event discrimination



dashed lines = offline cuts



Fraction of total by event type	Online	Offline
Elastic scattering	0.531	0.989
Inelastic (pion electro-production)	0.450	0.002
Quasi-elastic scattering (target windows)	0.015	0.008
π^0 photo-production	0.004	0.001

“sideband” analyses will help verify
QE and inelastic asymmetries

Error budget

quantity	value	contributed uncertainty
Beam polarization	$85\% \pm 1\%$	1.2%
Beam energy	$6.6 + / - 0.003 \text{ GeV}$	0.1%
Scattering angle	$15.5^\circ \pm 0.03^\circ$	0.4%
Beam intensity	$<100 \text{ nm}, <10 \text{ ppm}$	0.2%
Backgrounds	$< 0.2 \text{ ppm}$	0.2%
G_E^n / G_M^n	-0.2122 ± 0.017	0.9%
G_E^p / G_M^p	0.246 ± 0.0016	0.1%
σ_n / σ_p	0.402 ± 0.012	1.2%
$G_A^{Zp} / G_{\text{Dipole}}$	-0.15 ± 0.02	0.9%
Total systematic uncertainty:		2.2%

or 3.3 ppm

Statistical precision for A_{PV} : 6.2 ppm (4.1%)

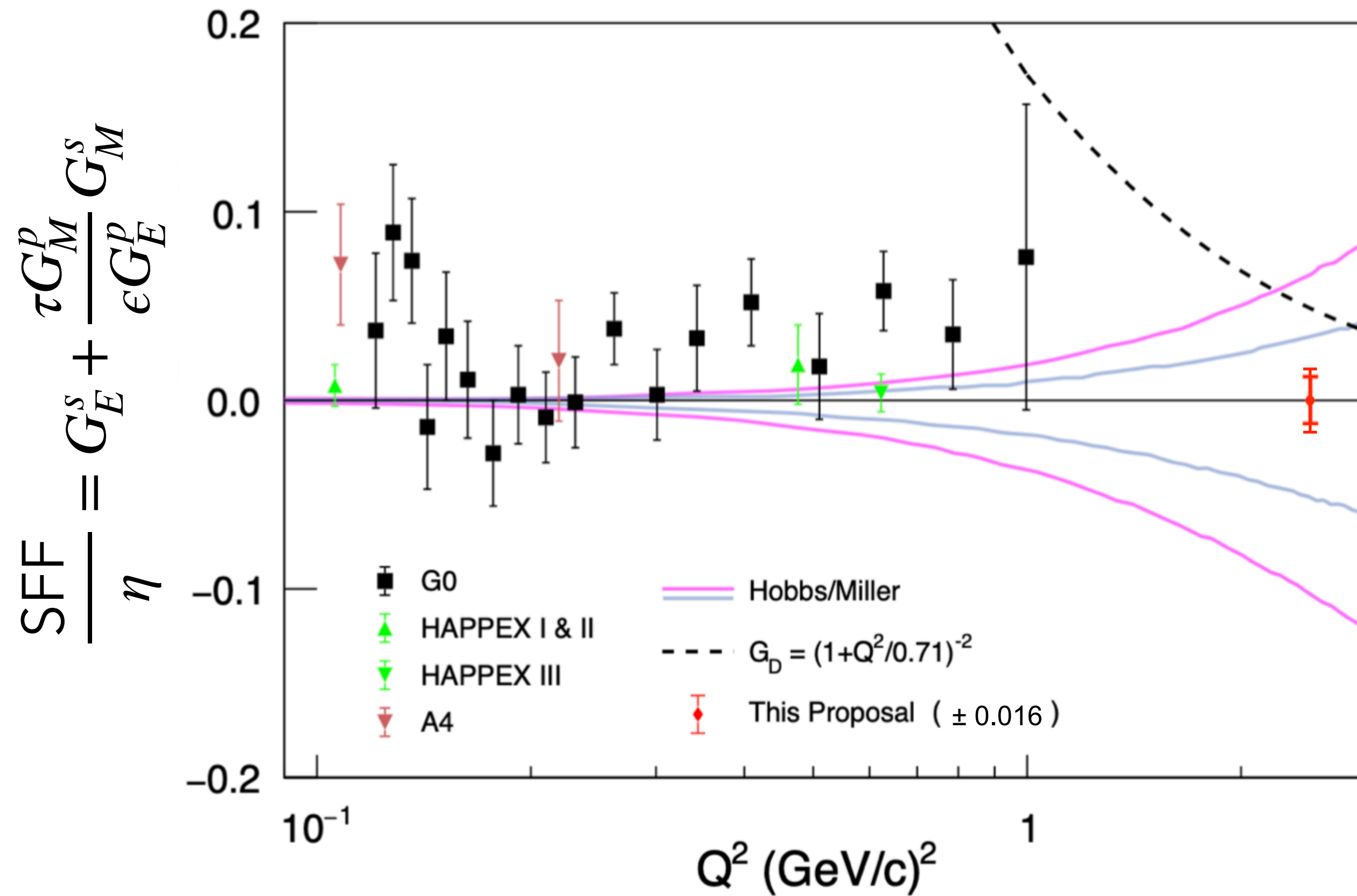
There is also an uncertainty from radiative correction, is small except for a dominant "anapole" piece.

If the anapole uncertainty is not improved, this would contribute at additional 4.1 ppm (2.7%) uncertainty

Projected result

$$\delta A_{PV} = \pm 6.2 \text{ (stat)} \pm 4.5 \text{ (syst)}$$

$$\delta (G_E^s + 3.1G_M^s) = \pm 0.013 \text{ (stat)} \pm 0.010 \text{ (syst)} = 0.016 \text{ (total)}$$



If $G_M^s = 0$, $\delta G_E^s \sim 0.016$, (about 34% of G_D)

If $G_E^s = 0$, $\delta G_M^s \sim 0.0052$, (about 11% of G_D)

The proposed measurement is especially sensitive to G_M^s

The proposed error bar reaches the range of lattice predictions, and the empirically unknown range is much larger.

Summary

Configuration #	Procedure	Beam current, μA	time, days
C1	Beam parameters	1-70	1
C2	Detector calibration	10	2/3
C3	Dummy target data	20	1/3
C4	Moller polarimetry	1-5	3
C5	A_{PV} data taking	60	40
	Total requested time		45

- 10+ years after the last sFF searches were performed, a new experiment is proposed for much higher Q^2 , motivated by interest in flavor decomposition of electromagnetic form factors
- Projected accuracy at 11% of the dipole value allows high sensitivity search for non-zero strange form factor.
- The proposed error bar is in the range possibly suggested by lattice predictions, and significantly inside the range from the simple extrapolation from previous data
- These results will be crucial to support the interpretation of the nucleon form-factors as constraints on GPDs
- We are requesting PAC approval of 45 days of beam time (65 μA on 10 cm long LH2 target).

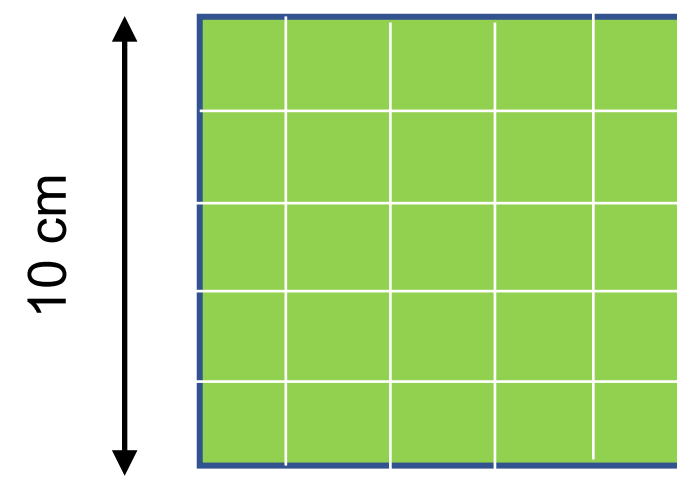
Backup slides

Triggering

Group calorimeter elements into logical “subsystems” for energy threshold and coincidence triggering

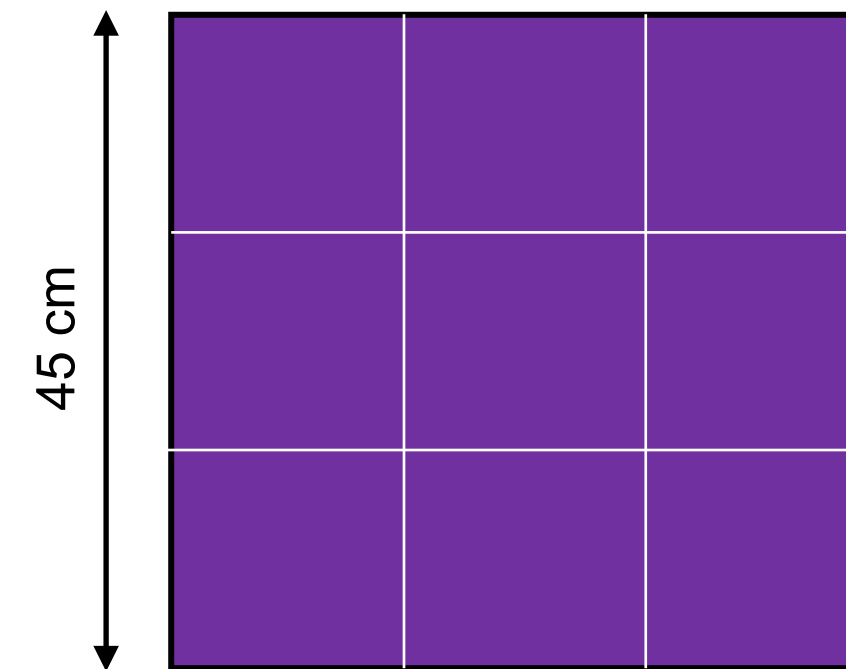
- each polar column of detectors, overlapping with neighbors
- sum amplitude with conservative coincidence timing window
- compare to conservative energy threshold
- trigger when complementary (ECAL and HCAL) subsystems are both above threshold ~ only about 35 kHz

Electron subsystems



- 1200 PbWO_4 crystals
- $2 \times 2 \times 20 \text{ cm}^3$
- 5x5 grouping for subsystem
- 240 overlapping subsystems

Proton subsystems



- 288 iron/scintillators
- $15.5 \times 15.5 \times 100 \text{ cm}^3$
- 3x3 grouping for subsystem
- 96 overlapping subsystems

Advantage: simplicity over dynamic clusterization, and fully sufficient for acceptance, resolution, and background

Scintillator TDC readout

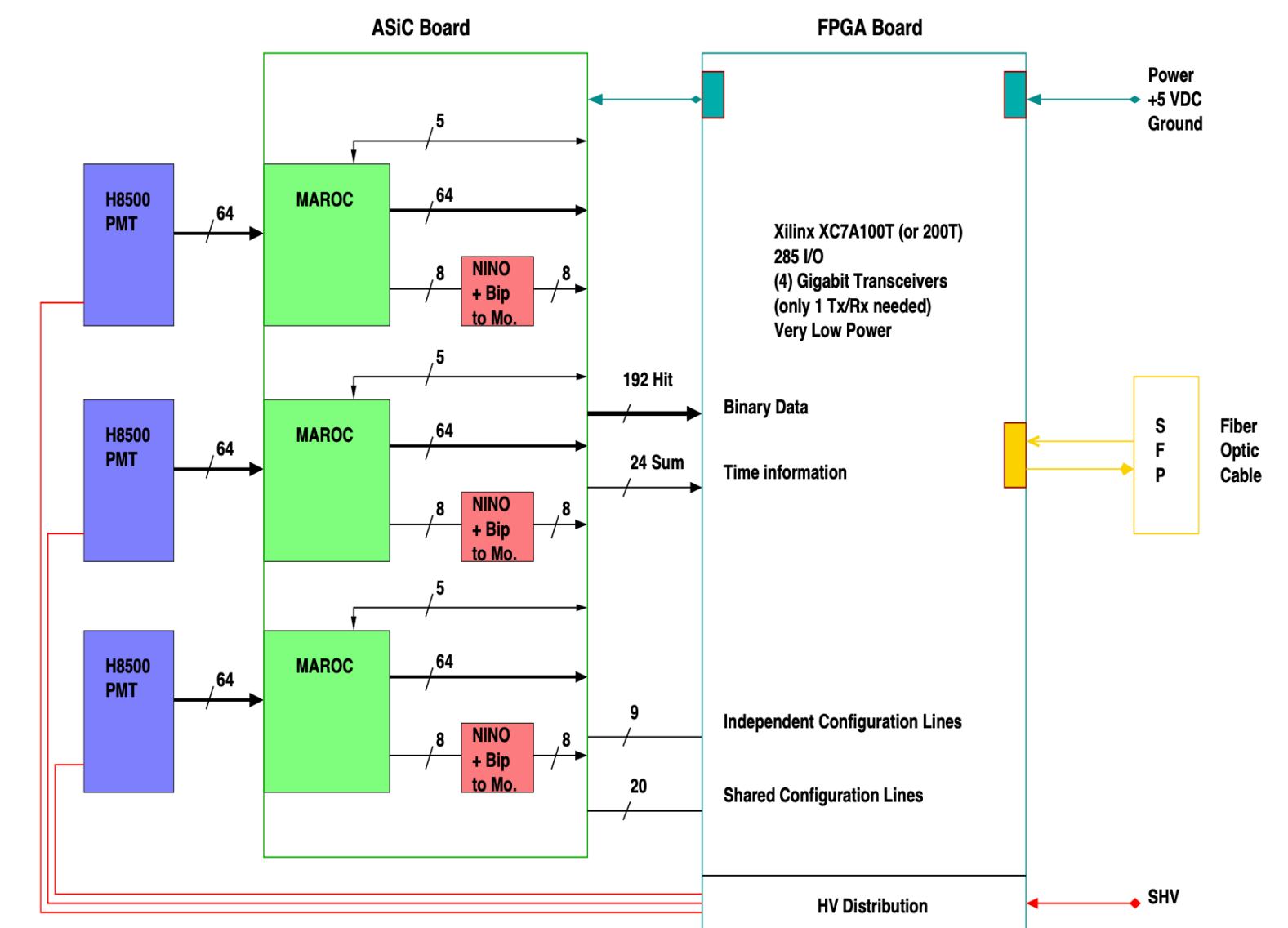
Two workable options, based on previously implements MAPMT pipeline readout

model based on CDET detector (GEP)

- NINO chip module, **VETROC** for scintillator readout.
- Need 38 boards, 3 crates.
- Pipeline event record triggered by calorimeter coincidence trigger.
- Use HCAL subsystem number to select scint elements for readout
- Record time, time-over-threshold for scint elements (**preferred**)
- 35 kHz trigger rate, 8 Bt/read, 225 elements = 65 MB/sec

model based on CLAS12 RICH

- MAROC3a FPGA readout module
- discriminated signal
- **SSP** readout board for scintillator readout.
- Need 38 front-end boards, 2 SSP, 1 crate.
- Event record triggered by calorimeter coincidence trigger.
- All elements recorded hit or not, $35\text{kHz} \times 7200 \text{ bits} = 32 \text{ MB/sec}$



Other possible discriminator boards, if availability is limited (such as SAMPA...)

Helicity-correlated Beam Asymmetries

Position differences (like angle, but angle $\sim 10x$ smaller):

$d\sigma / dQ^2$ roughly proportional to Q^{10} , so sensitivity $\delta A / \delta\theta \sim 10 \delta\theta / \theta$

Assume very large (by today's standards) position difference of 60 nm, to be compared to 79cm radius of ECAL

$$60\text{nm} / 79 \text{ cm} \sim 75 \text{ nrad} \rightarrow \frac{\delta\theta}{\theta} \sim 0.3 \text{ ppm}, \text{ or } \frac{\delta A}{A} \sim 3 \text{ ppm}, \sim 2\%.$$

Azimuthal symmetry leads to excellent cancellation, so the net effects will be very small.

Similarly, energy, assuming 60 nm in dispersive bpm ($\sim 1\text{m}$ dispersion) $\rightarrow 0.06 \text{ ppm}$, or 0.4%

Can be corrected with regression

Charge asymmetry

Using feedback, $<10\text{ppm}$ easily achievable. 1% calibration $\rightarrow 0.1 \text{ ppm}$ systematic, 0.06%

A sense of scale is important here: Qweak ($\sigma \sim 10\text{ppb}$), PREX-2 (16ppb) and CREX (100ppb) were between 60x - 600x more precise in terms of the absolute asymmetry error bar, they were all much more sensitive to beam asymmetries (by factors of 4x-100x), and they all successfully kept the total beam correction uncertainty to be small compared to their statistical error.

With regard to the challenges of HCBA, this proposal is far inside the envelope of the tools we have used many times here at JLab.

Anapole Moment

In the context of a very large discrepancy from SAMPLE, the anapole radiative correction was investigated as a possible cause

$$\tilde{G}_A^e(Q^2) = \left[\tau_3 g_A (1 + R_A^{(T=1)}) + \frac{3F - D}{2} R_A^{(T=0)} + (1 + R_A^{(0)}) \Delta s \right] G_A^D(Q^2)$$

The 1-quark and many-quark corrections to the axial charges in the \overline{MS} renormalization scheme.

	$R_A^{(T=1)}$	$R_A^{(T=0)}$	$R_A^{(0)}$
1-quark	-0.172	-0.253	-0.551
Many-quark	-0.086(0.34)	0.014(0.19)	-
Total	-0.258(0.34)	-0.239(0.20)	-0.551

values from Shi-Lin Zhu, S.J. Puglia, Barry R. Holstein, M.J. Ramsey-Musolf, Phys. Rev. D 62 (2000) 033008.

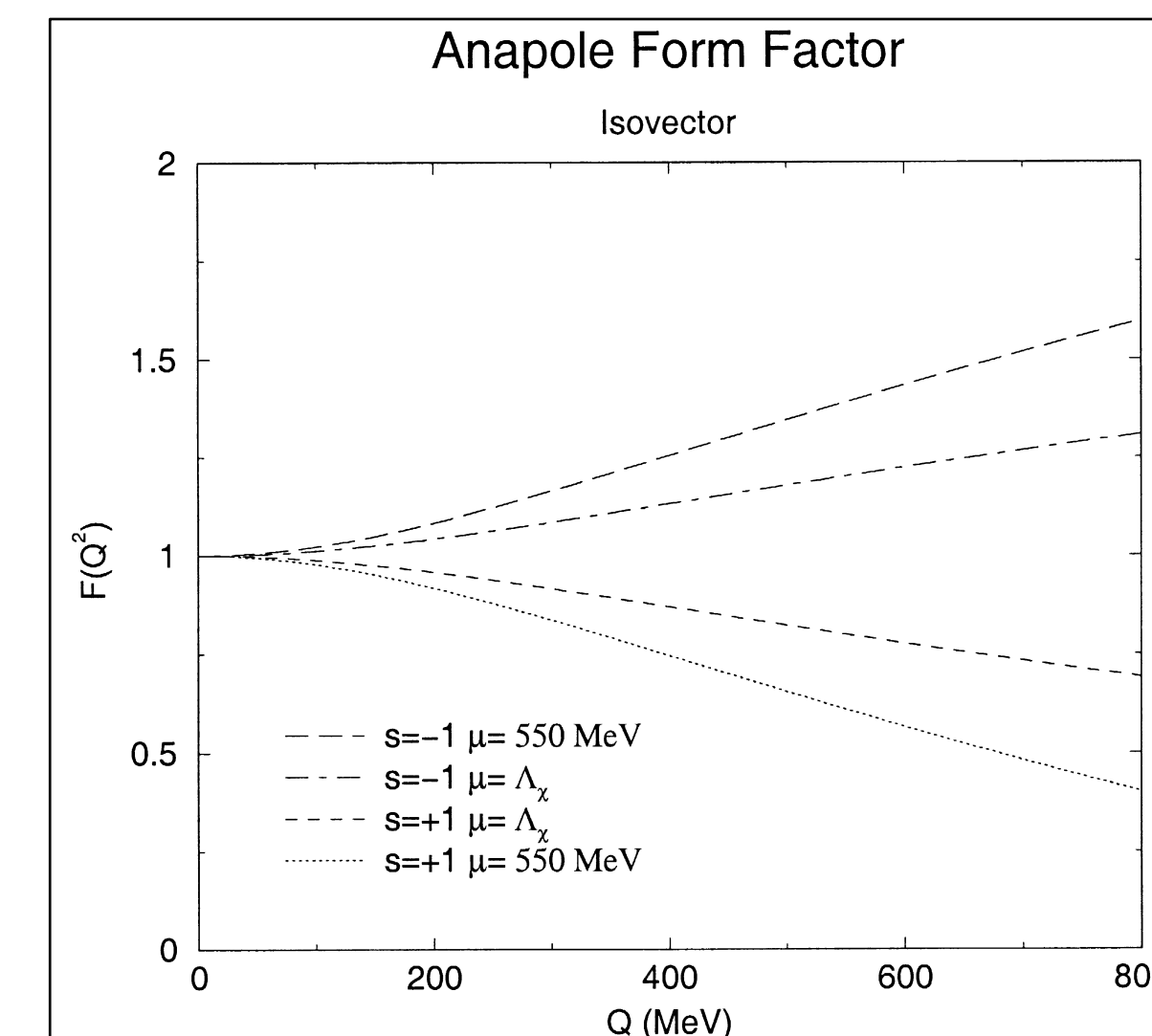
Suggests a coefficient on the axial term at $Q^2 = 0$:

$$(1 + R_A^{(T=1)}) = 0.74 \pm 0.34$$

Without improvement, this would correspond to 4.1 ppb, or 2.7% of A_{PV}

Q^2 dependence was explored at that time - suggested that it may be significant, but hasn't been evaluated since, or to high Q^2 .

(Here, I believe this $F(Q^2)$ multiplies only the many-quark $R_A^{(T=1)} = -0.086$ contribution.)



(Maekawa et al, Physics Letters B 488 2000. 167-174)

Gamma-Z Box

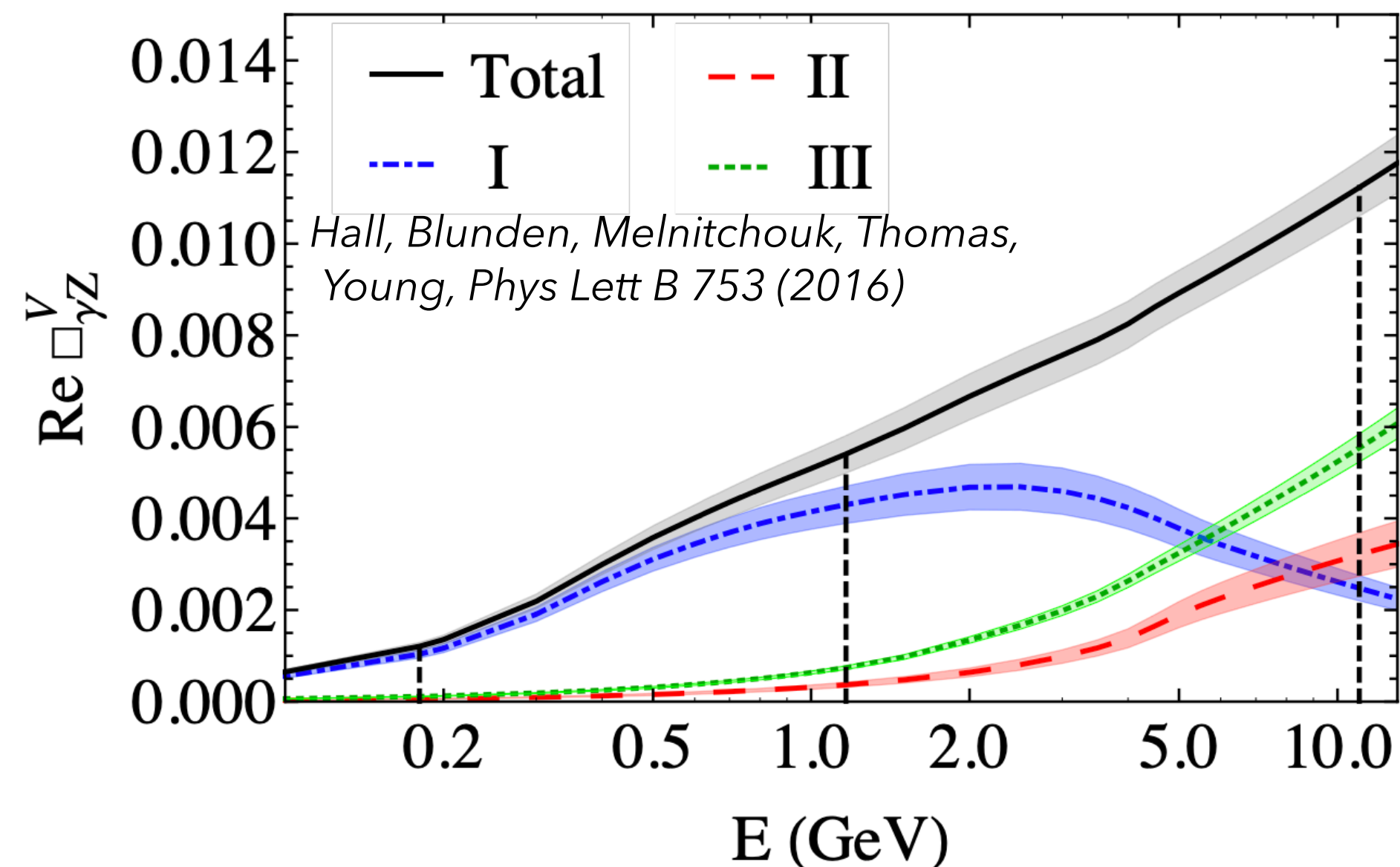
Additional radiative correction to Q_W

$$Q_W^p = (1 + \Delta\rho + \Delta_e) \left(1 - 4 \sin^2 \theta_W(0) + \Delta'_e \right) + \square_{WW} + \square_{ZZ} + \underline{\square_{\gamma Z}(0)}$$

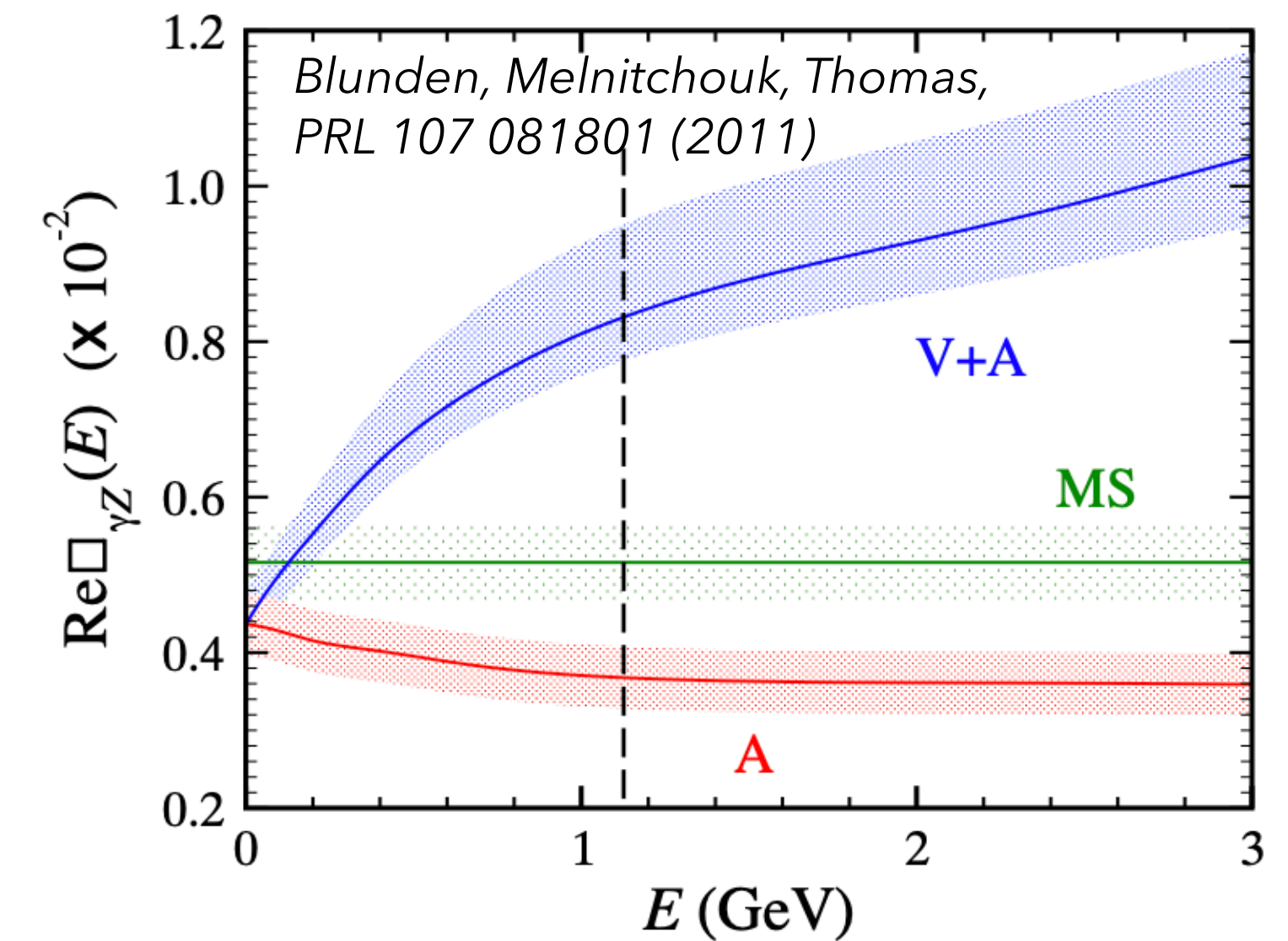
For Q_{weak} , added
~0.5% uncertainty

Here, $\square_{\gamma Z}^v(0) = 0.0095 \pm 0.0005$ and $\square_{\gamma Z}^a(0) = -0.0036 \pm 0.0004$
which together is about 1.33 ± 0.14 ppm ($0.9 \pm 0.1\%$)

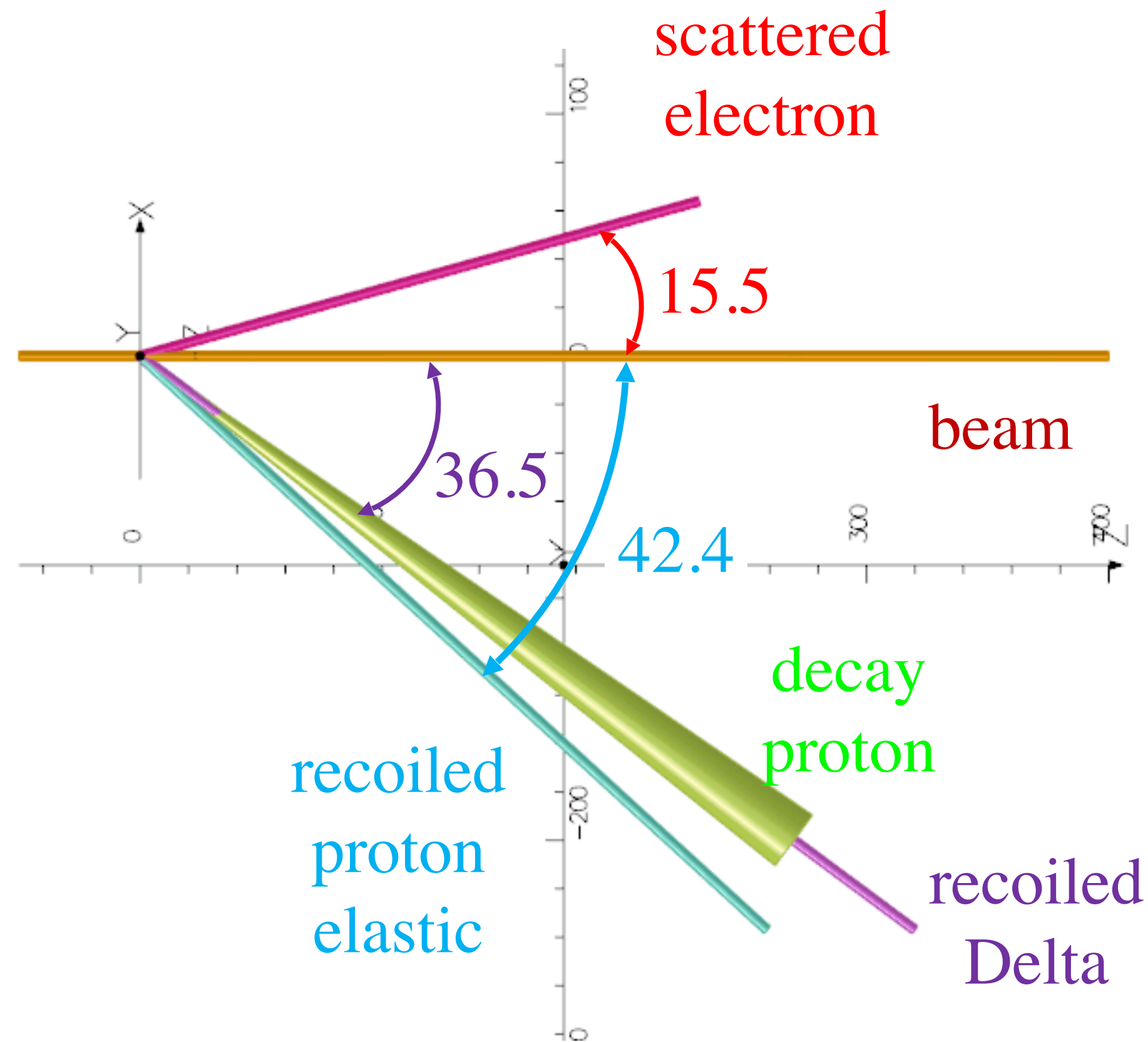
Caveat: this calculation is for forward direction.
Off-forward expected to be greatly reduced
(but this is also model dependent).



Axial piece smaller, didn't receive as much recent attention/update, seems stable with energy



Pion electro-production contribution



Pion production rate
above offline ECAL threshold ~ 3 kHz

Angular separation:

6° (at Δ peak)

2.8° (at π threshold)

Angular resolution $\sim 0.6^\circ$ (polar)

Proton cone around Δ recoil, projected to polar angle:

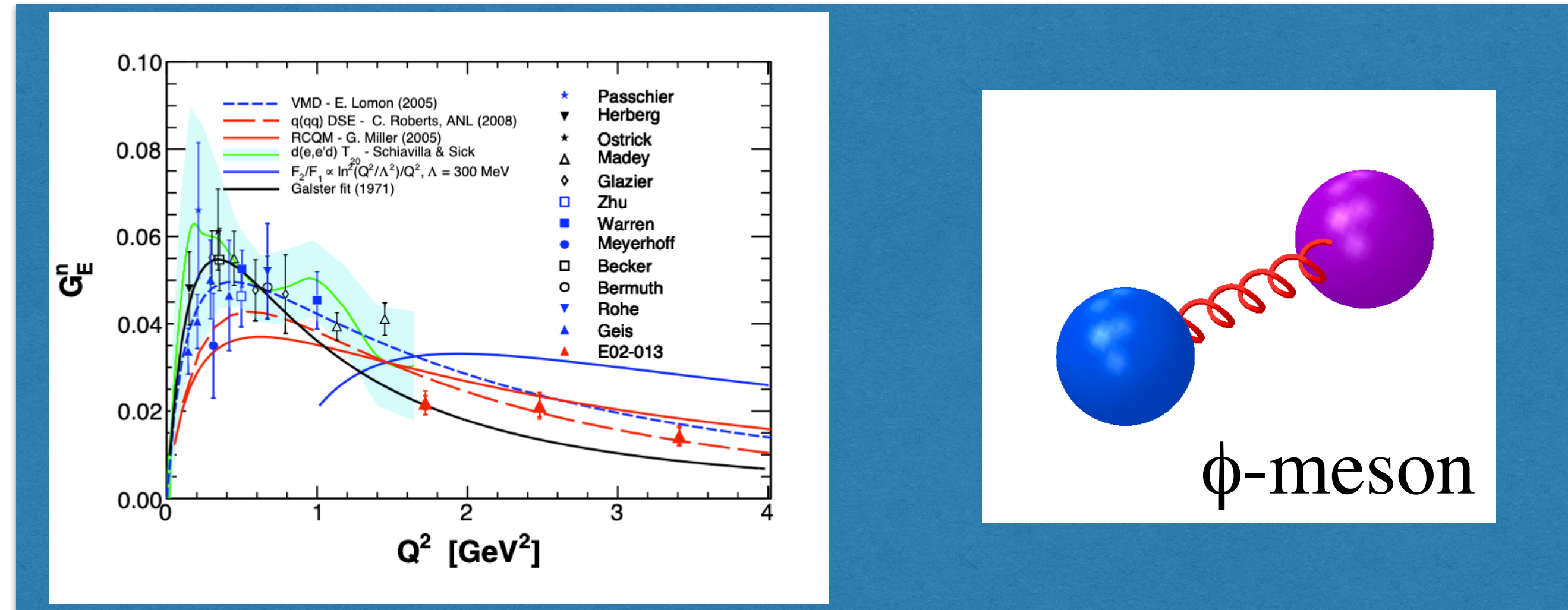
RMS = 2° (so, 2.5σ separation for Δ)

Fraction to elastic rate $< 0.3\%$

Background events from Al

- assumed 5 mils target cell windows, ~5% nucleon
- Fermi energy smears quasi-elastic scattering distribution, about 80x suppression
- B/S < 0.1%
- a dummy target will be used to check accepted rate

Why search at high Q^2 ?



PARAMETER β IN $\phi \rightarrow \pi^0 e^+ e^-$ DECAY

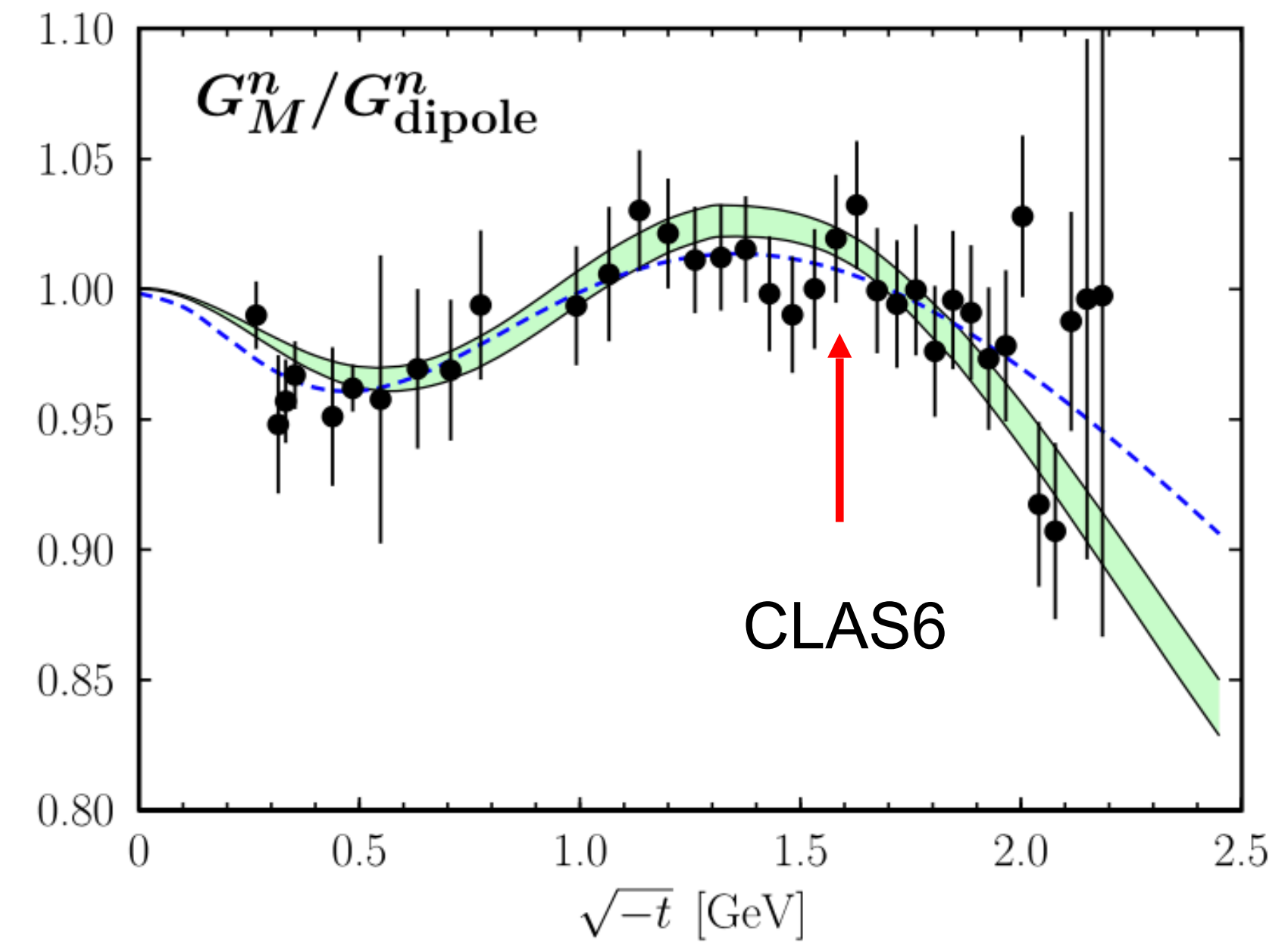
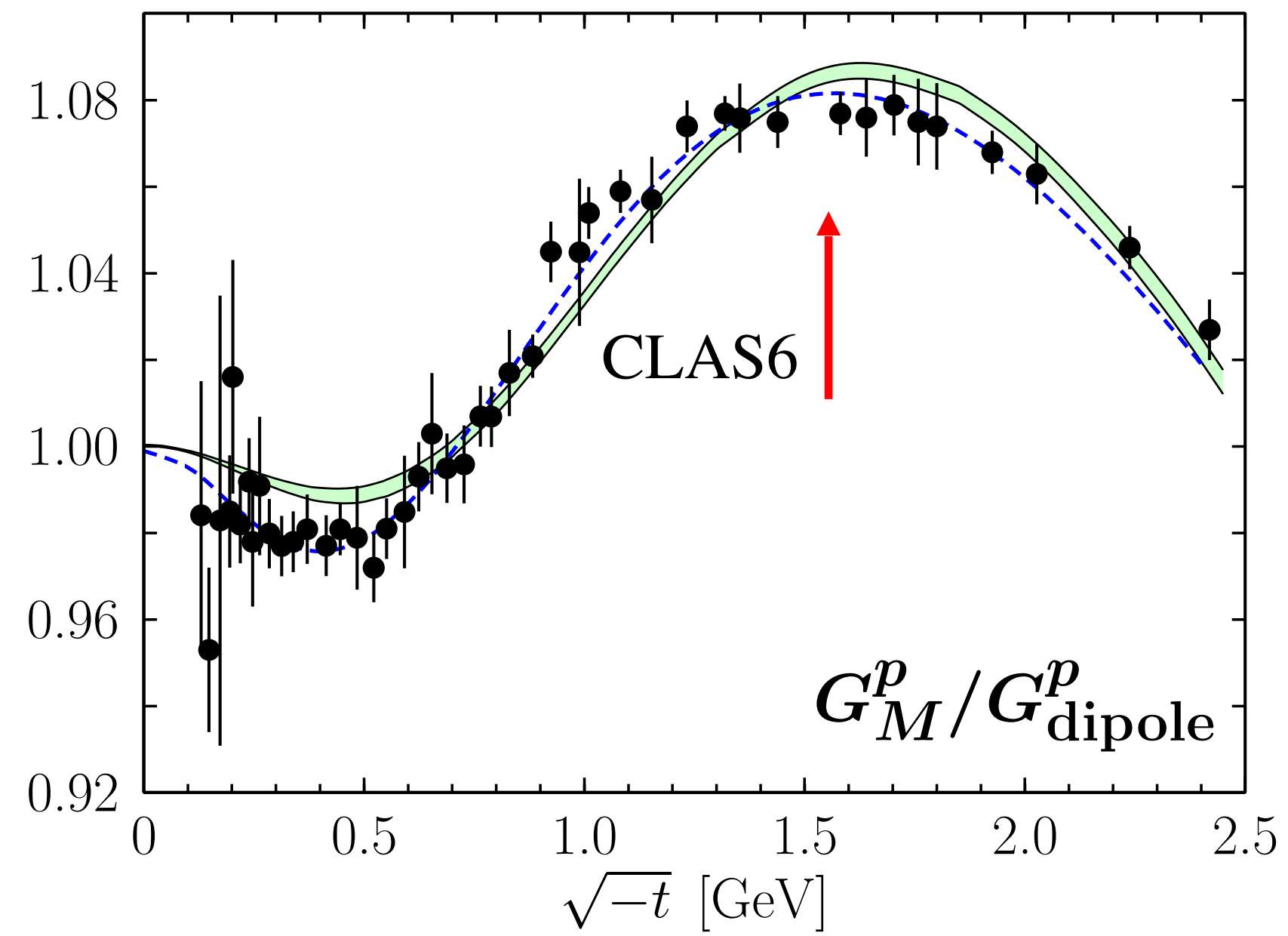
VALUE (GeV^{-2})	EVTS	DOCUMENT ID	TECN	COMMENT
2.02 ± 0.11	9.5k	¹ ANASTASI	16B KLOE	$1.02 e^+ e^- \rightarrow \pi^0 e^+ e^-$

This combined phi-pi radius ~ 0.69 fm
 with a pi-0 radius of ~ 0.64 fm and
 a ϕ -meson radius of ~ 0.26 fm

EMFF accuracy at $Q^2 \sim 2.5 \text{ GeV}^2$

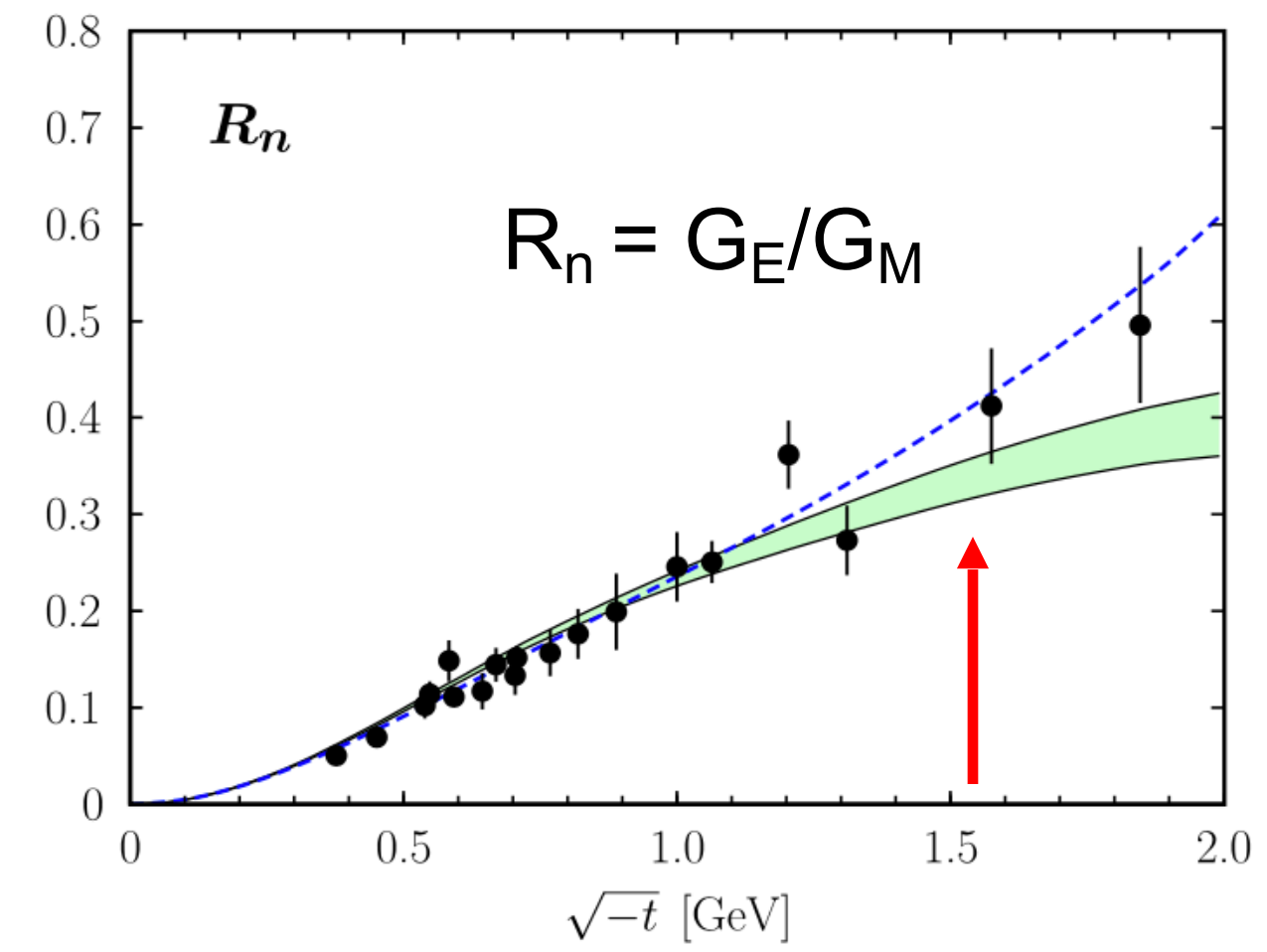
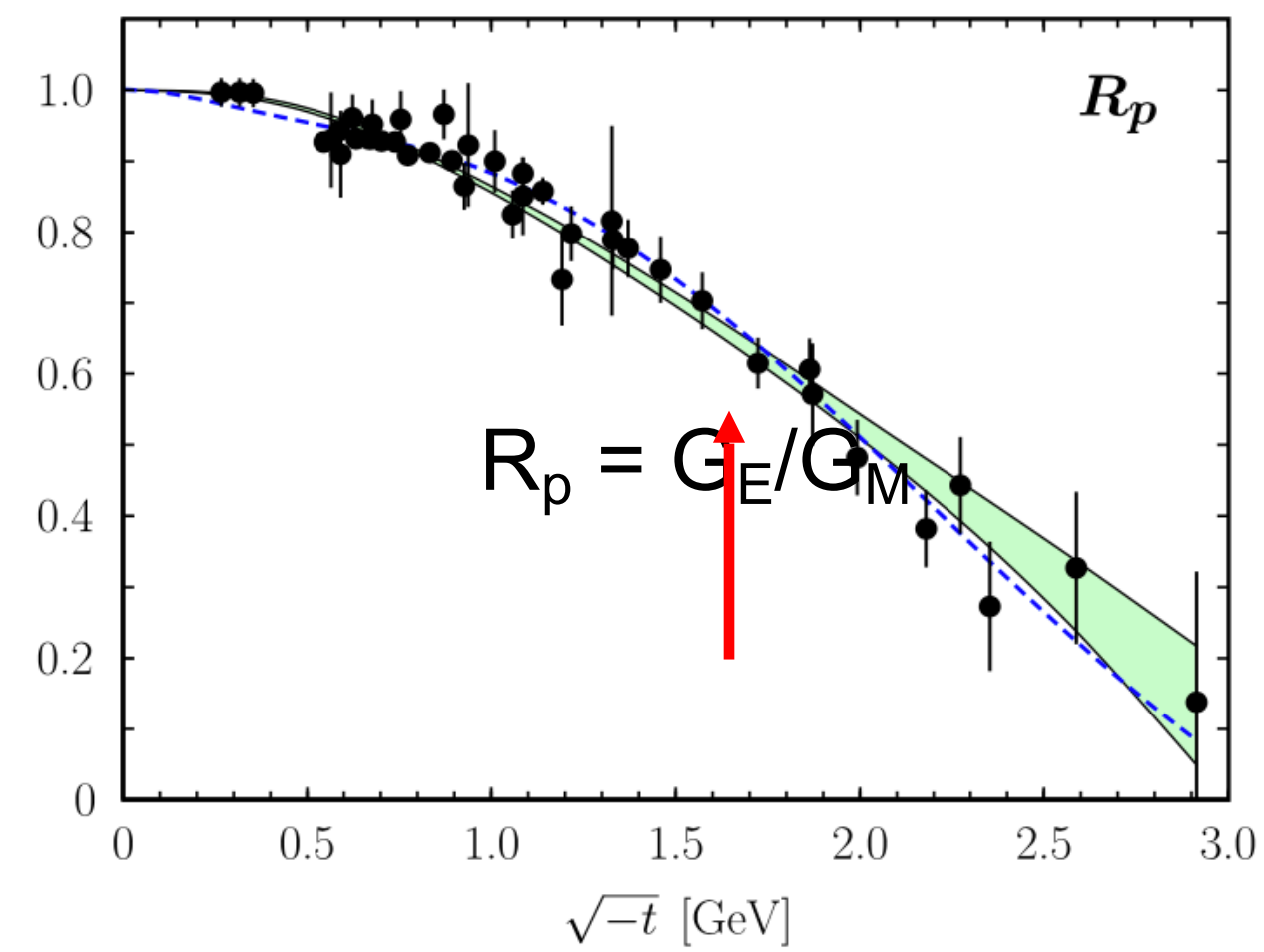
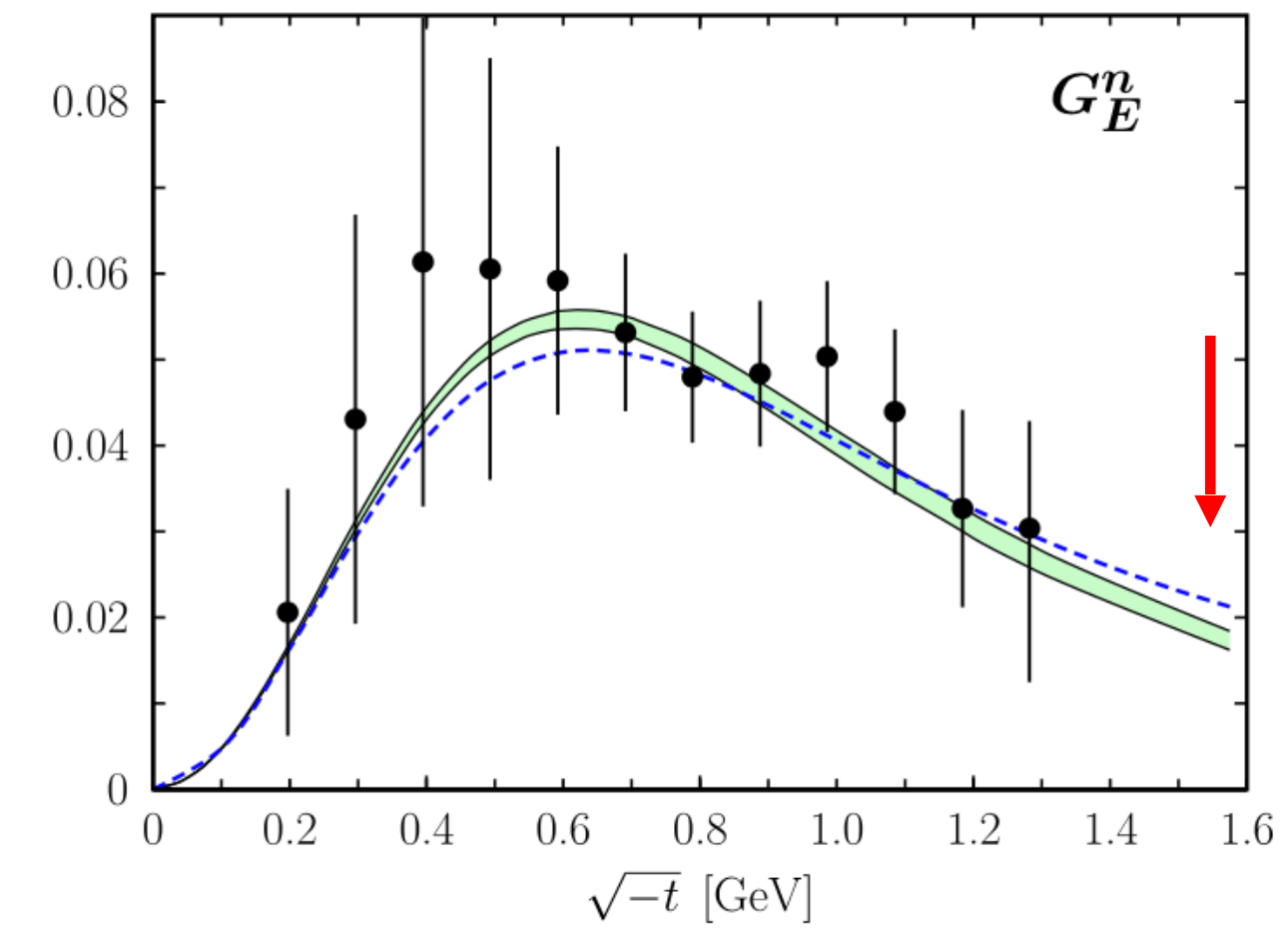
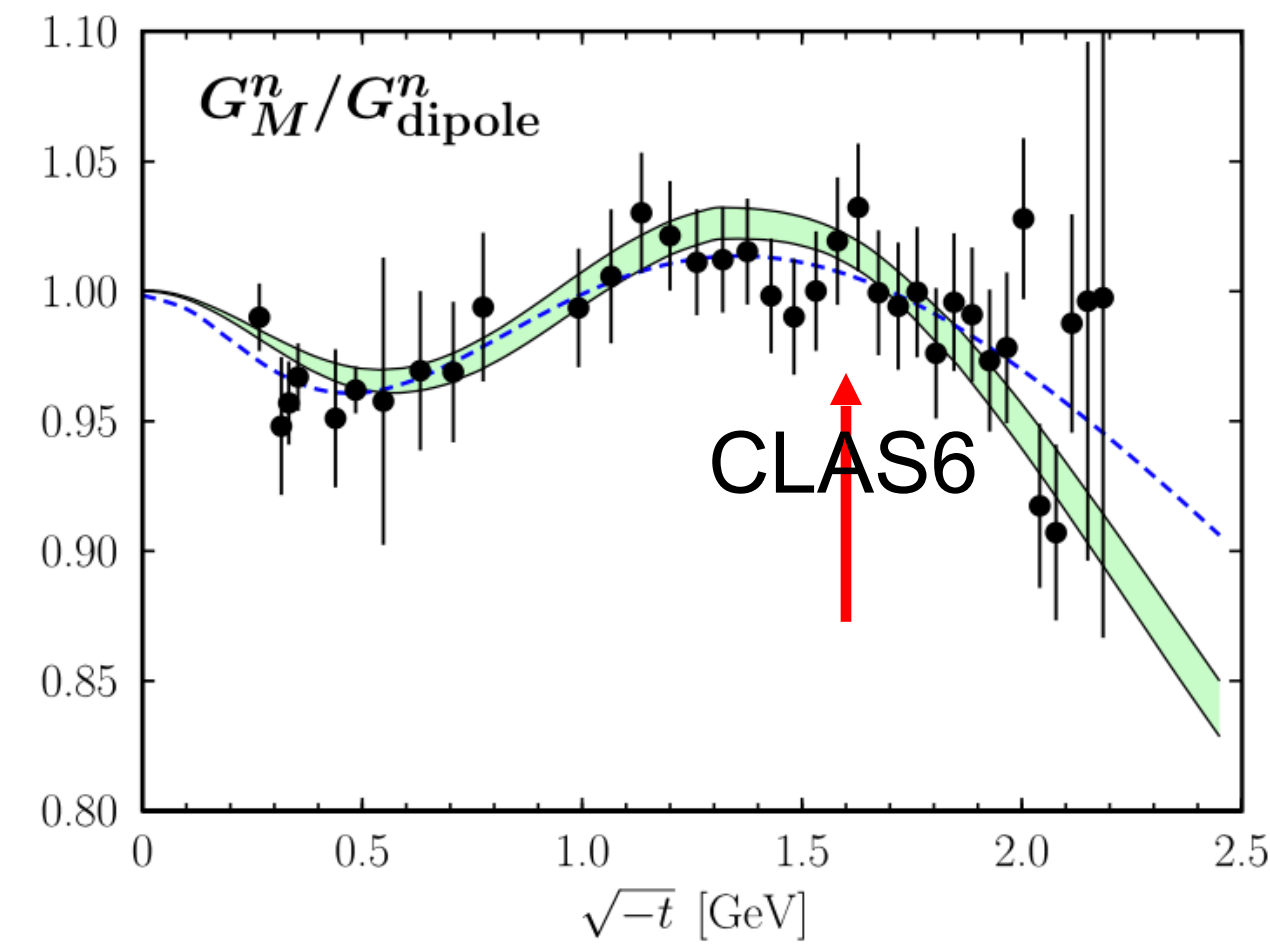
Most sensitive to G_M^p and G_M^n
but these have been well measured

M. Diehl and P. Kroll, 2013



EMFF accuracy at 2.5 GeV²

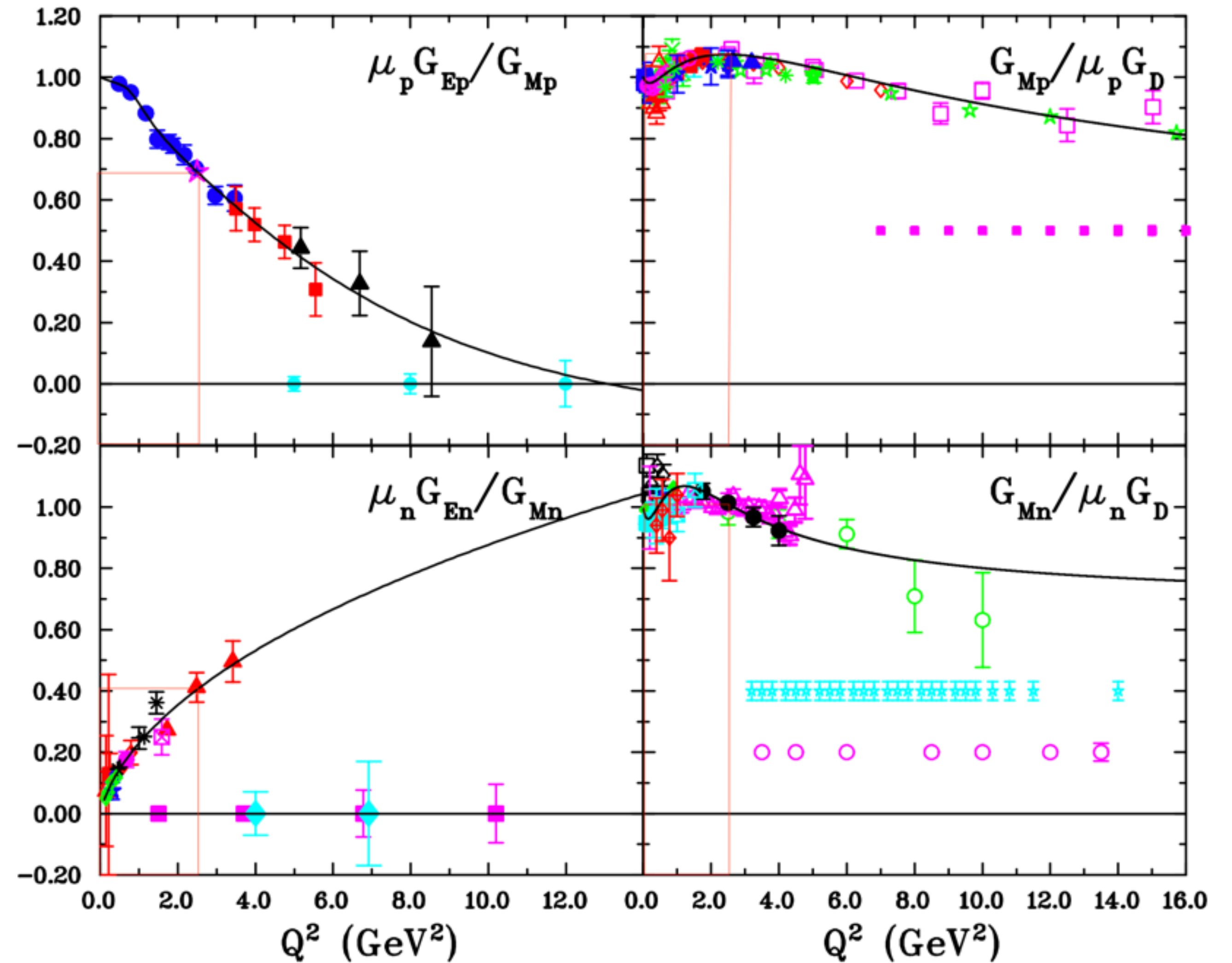
M. Diehl and P. Kroll, 2013



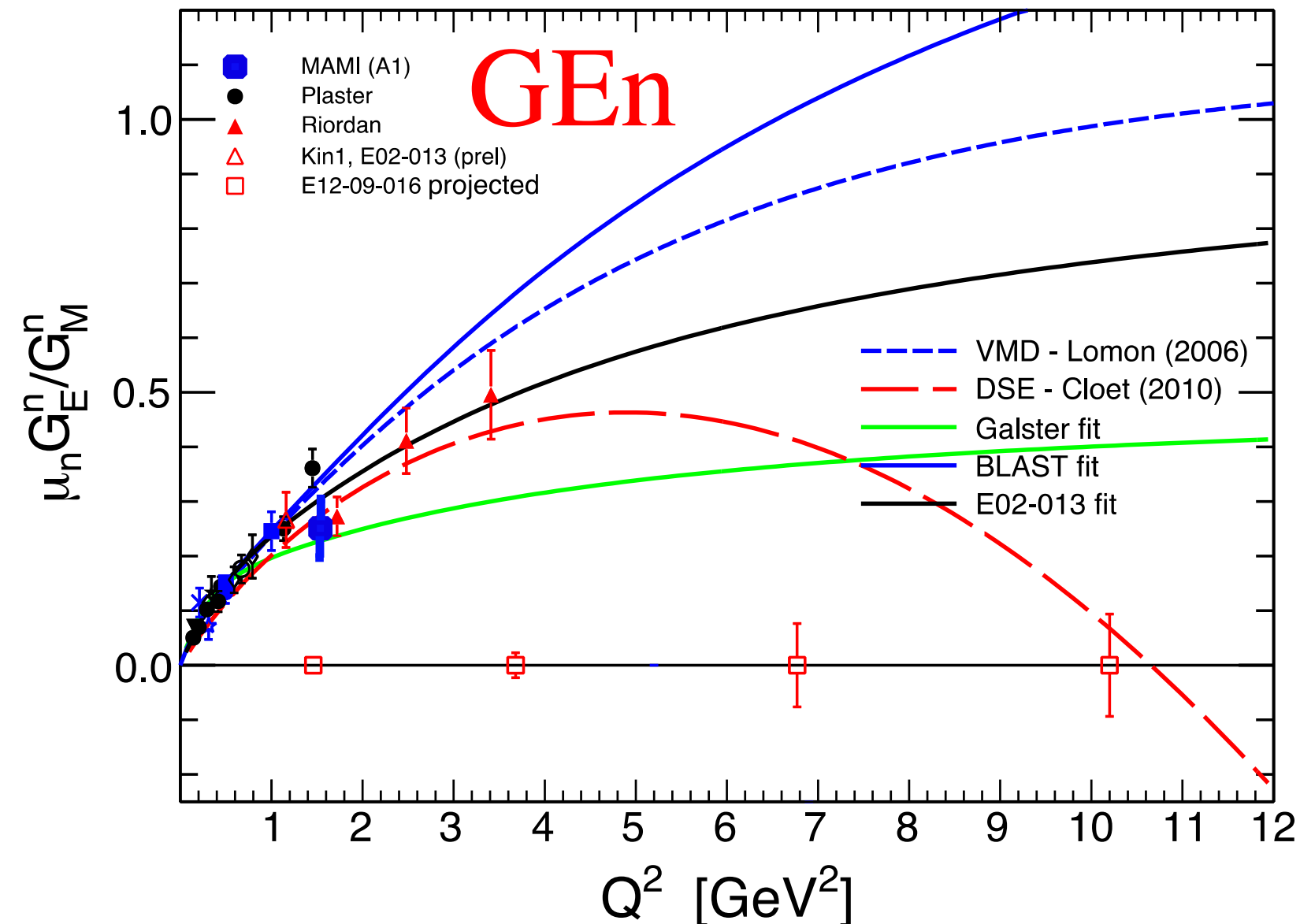
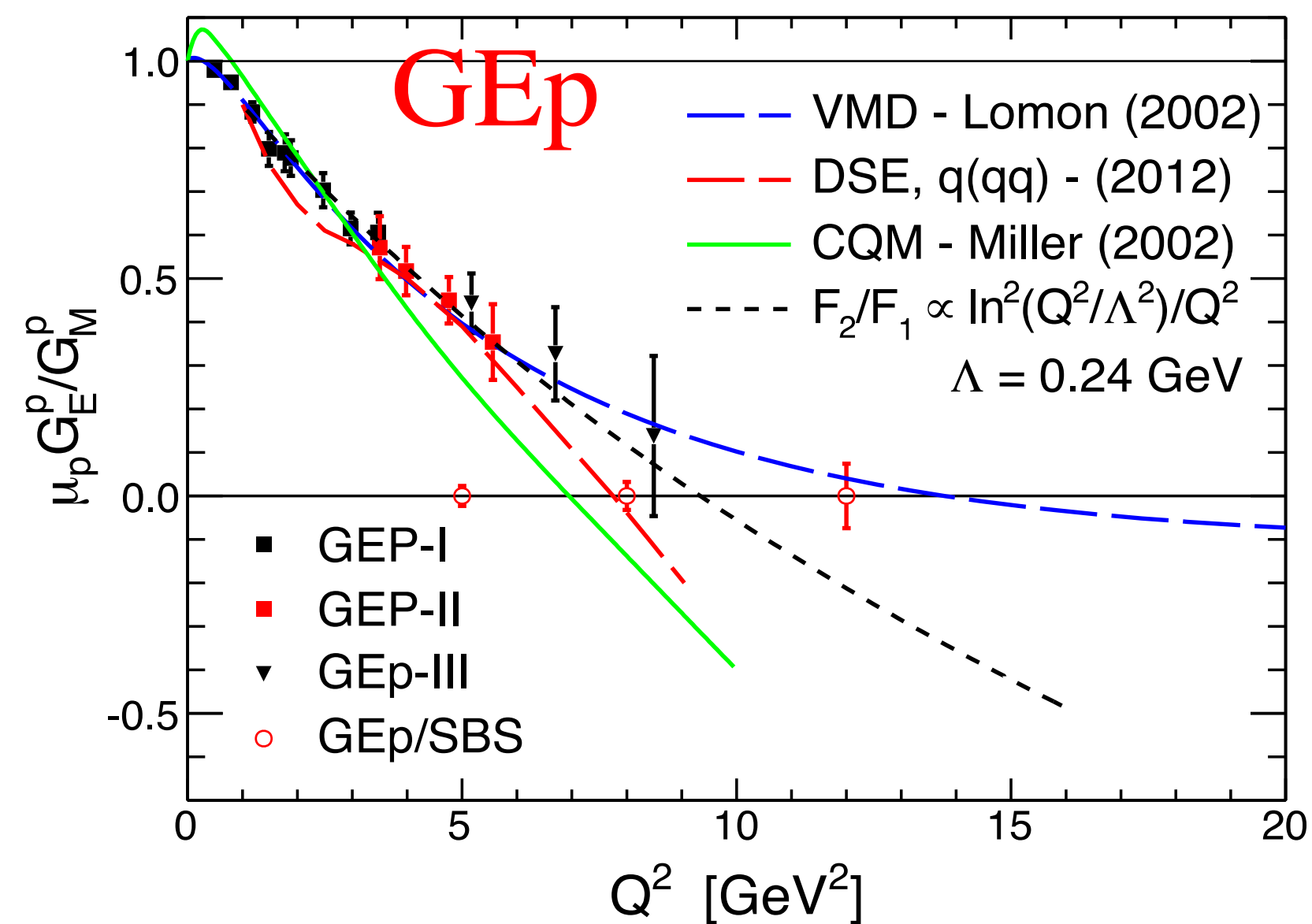
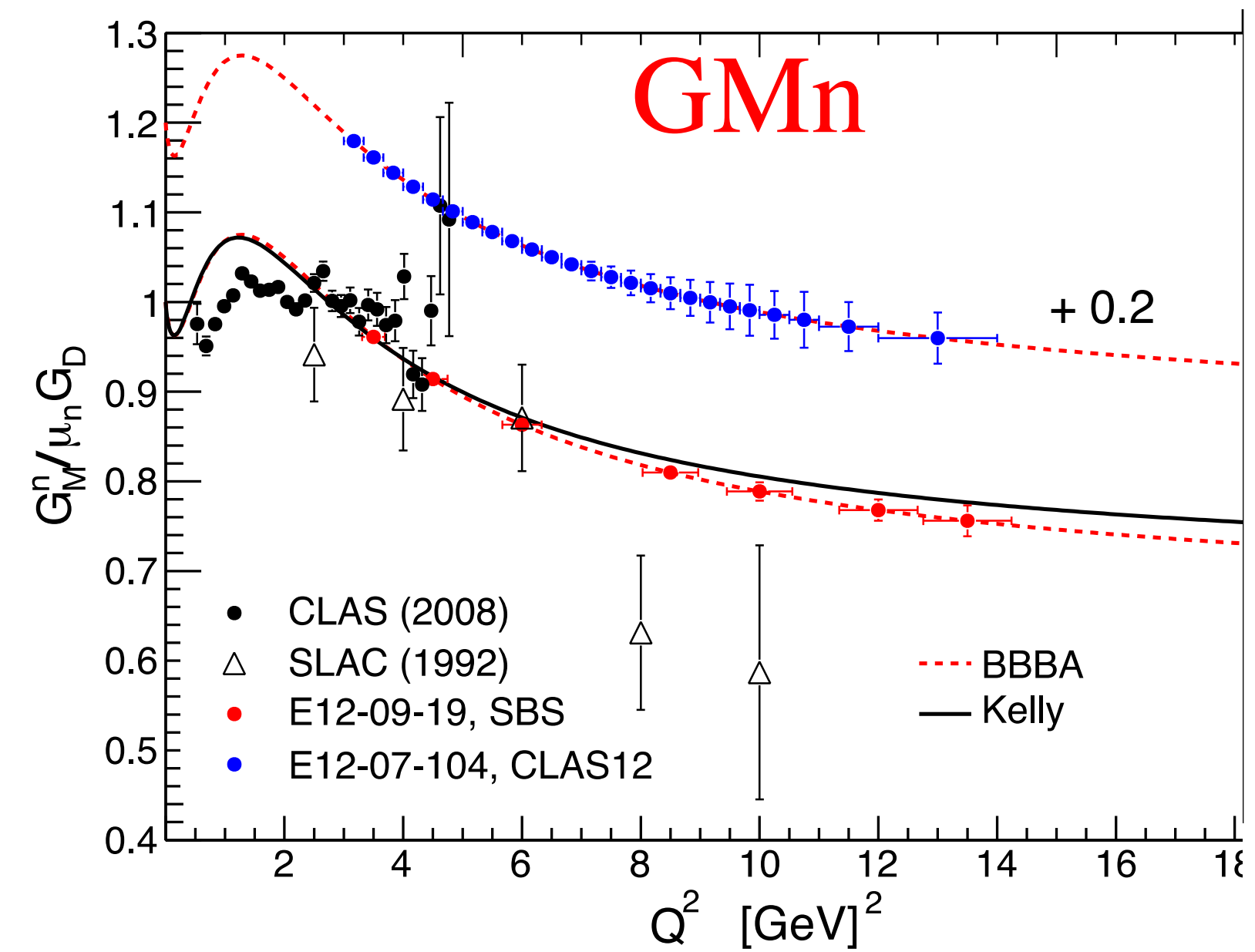
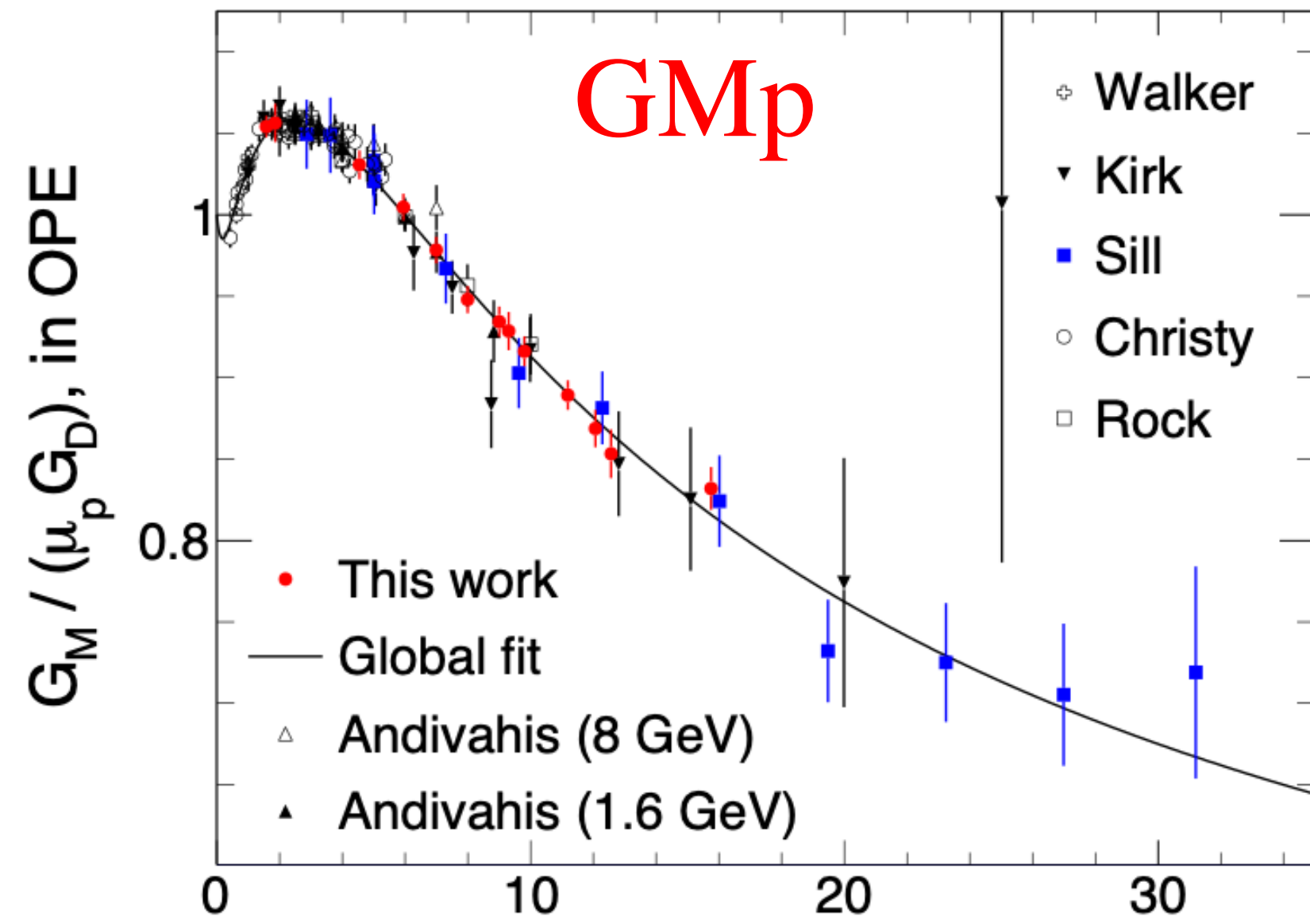
Electromagnetic Form-factors used for this calculation

V. Punjabi, C.F. Perdrisat, M.K. Jones, E.J. Brash, and C.E. Carlson: The Structure of the Nucleon

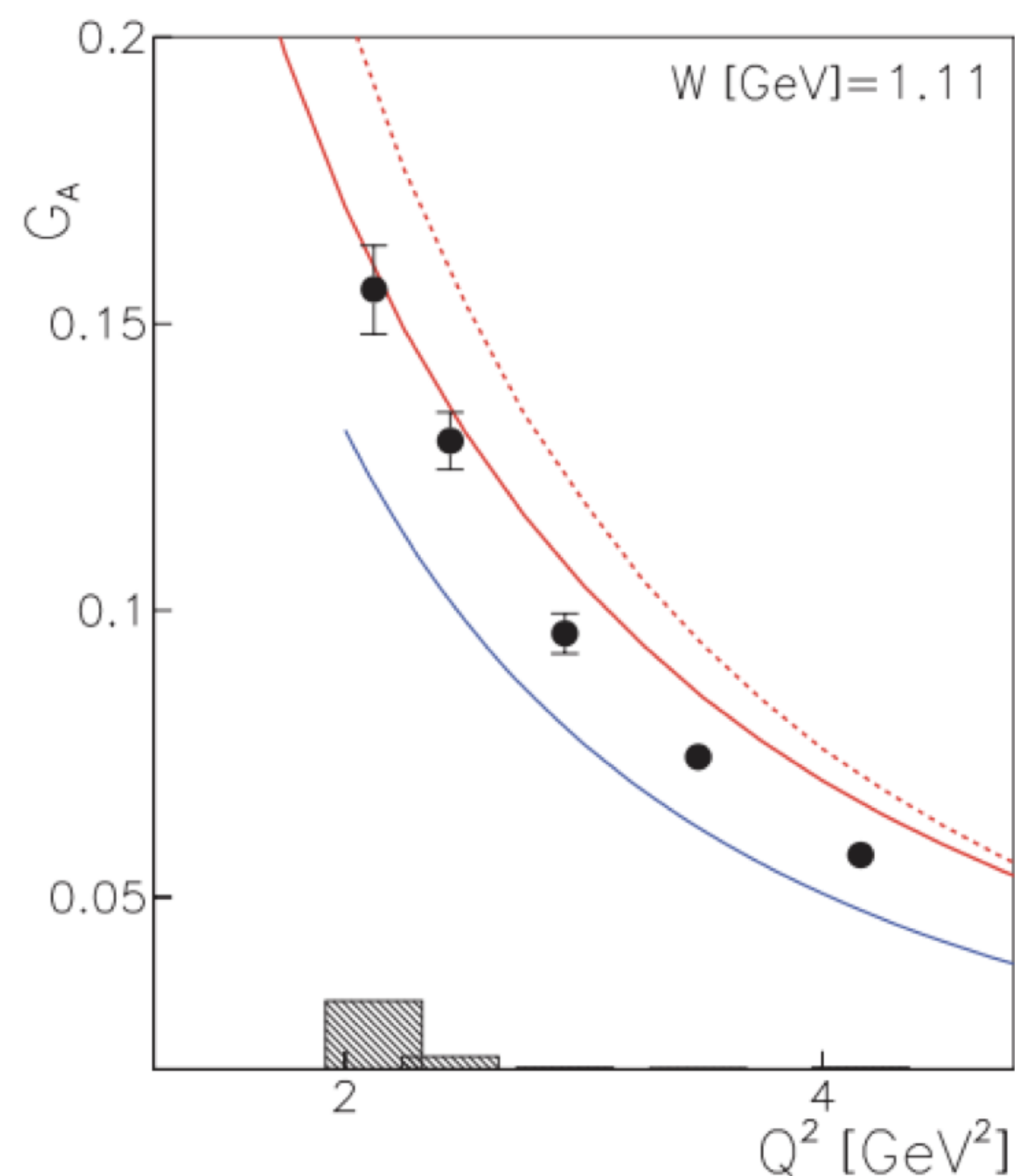
Form Factor	Value at $Q^2 = 2.5 \text{ GeV}^2$
$\mu_p G_{Ep}/G_{Mp}$	0.69
$G_{Mp}/(\mu_p G_D)$	1.08
$\mu_n G_{En}/G_{Mn}$	0.41
$G_{Mn}/(\mu_n G_D)$	1.01



The nucleon electromagnetic form factors



Axial Form Factor



K. Park *et al.* [CLAS Collaboration],
Phys. Rev. C **85**, 035208 (2012).

- Axial form factor parameterization $G_A^p = 0.15$ at $Q^2 = 2.5 \text{ GeV}^2$
 - C. Chen, C. S. Fischer, C. D. Roberts, and J. Segovia, *Form factors of the nucleon axial current*, *Physics Letters B* **815**, 136150 (2021)
- Confirmed with pion photoproduction measurements
 - K. Park *et al.* [CLAS Collaboration], *Phys. Rev. C* **85**, 035208 (2012).
 - (~15% interpretation uncertainty)
 - I.V. Anikin, V.M. Braun, and N. Offen, *Phys.Rev.D* **94** (2016) 3, 034011.
- How uncertain is this measurement because of it?
 - Axial term ~6% of APV
 - ~15% uncertainty, so estimate 1% relative uncertainty on the 4% statistical measurement